Abstract book

14TH BIOMETAL

Symposium on Biodegradable Metals for Biomedical Applications

August 24 – 29, 2022
Hotel Alicante Golf
Alicante
Spain

WELCOME MESSAGE FROM THE CHAIRS

After two difficult years of pandemic, we are proud to introduce and welcome you back to the 14th Symposium on Biodegradable Metals in Alicante, Spain, from Wednesday, August 24th to Monday, August 30th, 2022. This year, a hybrid mode will be applied. Allowing the presenters who cannot be in person to attend the conference and present their works. The symposium will emphasize its academic conference style with an openly discursive format, rather than a lecture and question-answer format. This style will be completed by the traditional discussions and the unconventional daily free-time sessions early in the afternoon. Behind the presentations, this symposium aims to discuss open questions on the session topics, new approaches, background knowledge, and personal views among the participants. Furthermore, discussions at the poster session will focus on specific topics and will encourage the participants to raise critical questions or help each other advance the field of biodegradable metals.

The architectural buildings and the white sand beaches will complete the experience we intend to offer to the attendees. The location was specially selected for bringing the attendees into a new region to explore, know, and be inspired by. We really hope your stay in Alicante will be intellectually rich and exciting and wish you to take a moment to follow the horizon of this Mediterranean city! We are really honored to welcome you to the 14th Biometal 2022 next August!

Symposium Co – chairs:

Diego Mantovani
Laval University, Canada

Yufeng Zheng
Peking University, China

Frank Witte
Berlin Charité, Germany

Mark Staiger
University of Catenbury, New Zeland

UNIVERSITÉ LAVAL

Conferium
Conferences . Events . Service

KeAi
CHINESE ROOTS
GLOBAL IMPACT

CHARITÉ

UC
UNIVERSITY OF CANTERBURY
Te Whare Wānanga o Waitaha
CHRISTCHURCH NEW ZEALAND

PEKING UNIVERSITY 1898

Thursday, August 25, 2022

Workshop

Chairs: Frank Witte & Diego Mantovani
AV support: Masoud & Leticia

9h00 **Introductory remarks (DM, FW)**

9h30 IP1 Plenary Academic Advance: **The invention of tailorable, ultrahigh-purity, lean magnesium alloys for biodegradable implant applications**
Jörg Löffler
ETH Zürich, Switzerland

10h30 IP2 **Update of resorbable metal in dentistry: the NOVAMag® regeneration system**
Svenja Rogge, Ž.P. Kačarević , P. Rider, D. Tadic
Botiss Medical AG, Germany

11h15-11h45 **Break**

11h45 IP3 Geographical Sector Vision: **Update on translational projects in China**
Yufeng Zheng
Peking University, China

12h30 **Lunch & Free Time**

Chairs: Diego Mantovani & Frank Witte
AV support: Souhila & Vinicius

14h00 IP4 Industrial Point of View: **Update and Clinical Results**
Kimmo Lahteenkorva and Christopher Stahle
Bioretec, Finland

14h45 IP5 Regulatory point of view: **Updates on Standardization in Bioabsorbable Metals**
Adam Griebel
Fort Wayne Metals, United States

15h30 IP6 **The challenges and solutions for biodegradable Zinc-based alloys from the aspect of clinical transformation**
Guangyin Yuan
National Engineering Research Center of Light Alloy Net Forming and State Key Laboratory of Metal Matrix Composites, China

16h15-16h45 **Break**

16h45 IP7 **God results - Bad results**
Norbert Hort and P. Maier
Helmholtz-Zentrum Hereon, Germany

17h30 IP8 **20 years of commercializing nanomedicine: From biodegradable metals to selfassembled nanomaterials for fighting COVID-19, inhibiting infection, killing cancer, and regenerating tissues**
Thomas Webster
Hebei University of Technology, China

18h15 **Discussion**

19h00 **End of the UPDATE Workshop at the 14th Biometal 2022**
19h30-21h00 **Dinner**

Friday, August 26, 2022

Session 1 – Metals

Chairs: Norbert Hort & Sandra Cifuentes
AV support: Nguyen & Samira
Assignation Code: K=Keynote; O=Oral presentation; SOP=Short oral presentation

8h20-8h30 **Introductory remarks (DM, FW)**

8h30-9h10 K1 **Nanoindentation to characterize hardness changes by flaring of mini-tubules**
Petra Maier, M. Schmahl, B. Clausius, C. Joy, C. Fleck
University of Applied Sciences Stralsund, Germany

9h10-9h30 O1 **Improving the trackability of biodegradable metals by dual radiopaque bioresorbable coatings and X-Ray filtration**
Samira Ravanbakhsh, C. Paternoster, P. Chevallier, M. Fortin, D. Mantovani
Laval University, Canada

9h30-9h50 O2 **Development of two new Mg-Li-Y alloy wires for application in bioresorbable medical devices**
Kenneth MacLeod, D. Nash, D. Bow
University of Strathclyde, United Kingdom

9h50-10h10 O3 **Multiscale hard-soft structured Zn-Cu-Li alloy with high strength and ductility for biodegradable implants**
Xiyuan Zhang, Z. Gao, J. Niu, G. Yuan

National Engineering Research Center of Light Alloy Net Forming and State Key Laboratory of Metal Matrix Composites, China

10h10-10h15	SOP1	**Effect of processing conditions on mechanical and in vitro degradation behavior of magnesium WE43 alloy wires** Wahaaj Ali, L. Tillmann, T. Mayer, A. Kopp, C. González,J. Llorca *IMDEA Materials, Spain*
10h15-10h20	SOP2 / P1	**Binder Jetting additive manufacturing of the bioresorbable WE43 alloy: Challenges encountered in post-process sintering** Agnieszka Chmielewska, T. Avey, D. Cho, A. Luo, D. Dean *The Ohio State University, United States*
10h20-10h25	SOP 3	**Study on mechanical properties, degradation properties and biocompatibility of Zn-RE binary alloys** S. Du, D.Xia, Yufeng Zheng, X.Xu *Peking University, China*
10h25-10h30	SOP4/P2	**Microstructure and mechanical stability of biodegradable low-alloyed zinc for biomedical applications** Magdalena Wróbel, A Jarzębska, Ł Maj, Ł Rogal, P. Petrzak, M. Kulczyk, M. Bieda *Institute of Metallurgy and Materials Science of Polish Academy of Sciences, Poland*
10h30-10h50	**SOP Discussion**	
10h50-11h20	**Break**	
11h20-11h40	O4	**Effect of groove pressing technique on the degradation rate of pure Mg** Manas Ranjan Sahu, T. S. S. Kumar, U. Chakkingal *Indian Institute of Technology, India*
11h40-12h00	O5	**3D printed Mg-based scaffolds for temporary bone replacement applications** Maria-Dolores Martin-Alonso, G. Dominguez, M. Li, M. Echeverry-Rendon, F. Benn, A. Kopp, J. Llorca, J. Molina-Aldareguia, F. Sket *IMDEA Materials, Spain*
12h00--12h20	O6	**Powder bed fusion of a biodegradable magnesium alloy: the effect of laser scan strategy and build direction on microstructure and mechanical properties** Lisa Larsson, F. D'Elia, C. Persson *Uppsala University, Sweden*
12h20-12h40	O7	**Biodegradation of powder metallurgical (PM) processed Mg ZX10-alloy for biomedical application** Martin Wolff, M. Luczak, H. Helmholz, D. Strerath, T Ebel, R. Willumeit-Römer *Helmholtz-Zentrum Hereon, Germany*
12h40-13h00	O8	**Adjusting mechanical properties of lean Mg alloys via hot extrusion: a wide range of strength and ductility**

Tatiana Akhmetshina, L. Berger, S. Montibeller, R. Schäublin, J.F. Löffler
ETH Zurich,Switzerland

13h00-13h20 O9 **Assessment of extruded magnesium tubing for absorbable stent production**
Adam Griebel, G. Hayes, R. Werkhoven, R. Menze, S. Ahlers, J. Schaffer
Fort Wayne Metals Research Products Corp., United States

13h20-14h50 Lunch & Free Time

Session 2 – Metals

Chairs: Petra Maier & Alberto Coda
AV support: Masoud & Leticia
Assignation Code: K=Keynote; O=Oral presentation; SOP=Short oral presentation

15h00-15h20 O10 **Influence of PEO coating parameters on coating thickness and topography**
Thomas Imwinkelried, A. Walser, L. Berger, W. Rubin, J. F. Löffler
RMS Foundation, Switzerland

15h20-15h40 O11 **Evaluation of bioresorbable squeeze cast Mg-Zn-Ca-Mn alloys**
Dae Hyun Cho, T. Avey, D. Dean, A. A. Luo
The Ohio State Universit, United States

15h40-16h00 O12 **Influence of micro-blasting on biodegradable iron-based stent structures**
Birgit Paul, A. Hofmann, M. Otto, U. Wolff, C. Reeps, J. Hufenbach
Institute for Complex Materials, Germany

16h00-16h20 O13 **Influence of Mn content on the chemical composition, electrochemical behavior, and morphology of oxygen plasma immersion implanted FeMnC alloys**
Leticia Marin de Andrade, C. Paternoster, P. Chevallier, D. Mantovani
Laval University, Canada

16h20-16h40 O14 **Surface modifications of pure Zinc by plasma immersion ion implantation surface oxidation for biomedical applications**
Souhila Ould Mohamed, H. Agbe, C. Paternoster, A. Sarkissian, D. Mantovani
Laval University, Canada

16h40-17h00 O15 **ECAP processing influence on the mechanical properties and the bacterial activity of Zn-2Ag alloys**
Claudia García-Mintegui, I. S. Goncharov, L. Ortiz-Membrado, E. Jimenez-Piqué, M. Vedani, J.L. Cortina, M. Pegueroles
Technical University of Cataloni, Spain

17h00-17h30 Break

17h30-17h50 O16 **Embrittlement of thin magnesium wires during PEO coating**

L. Pricolo, Thomas Imwinkelried
RMS Foundation, Switzerland

17h50-18h10 O17 **Surface modification of a biodegradable Mg-Y-Zn-Mn alloy by oxygen plasma immersion ion implantation**
Masoud Shekargoftar, S. Ravanbakhsh, V.S. Oliveira, C. Paternoster, F. Witte, D. Mantovani

Laval University, Canada

18h10-18h30 O18 **Electrical resistance testing for biodegradable magnesium implants**
Sebastian Meyer, B. Wiese, N. Hort, R. Willumeit-Römer
Helmholtz-Zentrum Hereon, Germany

18h30-18h50 O19 **Electroforming process for Fe-Mn alloy fabrication using deep eutectic solvents**
Vinicius .F. Sales, C. Paternoster, D. Mantovani, G. Kolliopoulos
Laval University, Canada

18h50-19h10 O20 **In situ thermo-mechanical processing in a synchrotron beam of a Mg-2Y-1Zn-1Mn alloy**
Domonkos Tolnai, S. Gavras, A. Stark, M. Bartosch, F. Witte, N. Hort
Helmholtz-Zentrum Hereon, Germany

19h10-19h30 O21 **Coupled growth in Zn-based alloys with Mg additions produced by casting in steel mold of square section**
Luis Angel Domínguez, A. Ramírez, J.S. Flores, J.A. Juárez, C. Paternoster, D. Mantovani
Universidad Nacional Autónoma de México, México

20h-21h30 Dinner

21h30-23h00 Poster Session

21h30-22h15 Poster session 1 (**odd-numbered** posters)

22h15-23h00 Poster session 2 (**even-numbered** posters)

P1 / SOP2 **Binder Jetting additive manufacturing of the bioresorbable WE43 alloy: Challenges encountered in post-process sintering**
Agnieszka Chmielewska, T. Avey, D. Cho, A. Luo, D. Dean
The Ohio State University, United States

P2/SOP4 **Microstructure and mechanical stability of biodegradable low-alloyed zinc for biomedical applications**
Magdalena Wróbel, A Jarzębska, Ł Maj, Ł Rogal, P. Petrzak, M. Kulczyk, M. Bieda
Institute of Metallurgy and Materials Science of Polish Academy of Sciences, Poland

P3 **Influence of alloying and plastic deformation on microstructure and mechanical properties of biodegradable low-alloyed zinc for orthopaedic applications**
Magdalena Bieda, A. Jarzębska, M. Wróbel, Ł. Maj, Ł. Rogal, J. Skiba
Institute of Metallurgy and Materials Science of Polish Academy of Sciences, Poland

P4 **Process development for additive manufacture of zinc-based biomedical substitutes**
Esmat Sheydaeian, A. Marquardt, L. Stepien, E. Lopez, F. Brückner, C. Leyens
Fraunhofer Institute for Material and Beam Technology (IWS), Germany

P5 **Effect of magnetic field on degradation of ferrous alloys in modified Hanks' solution at 37ºC**
Irene Limón, M. Multigner, M. Lieblich, C. Paternoster, D. Mantovani, J. Rams, B. Torres
Universidad Rey Juan Carlos,Spain

P6 **Optimization of attrition milling and Spark Plasma Sintering consolidation of Fe5Mg and its degradation behaviour**
Rafael G. Estrada, M. Multigner, S. C. Cifuentes, B. Torres, J. Rams, M. Lieblich
CENIM-CSIC, Spain

P7 **The study of surface modifications generated by plasma immersion ion implantation on zinc alloys for biomedical applications**
Souhila Ould Mohamed ,*C. Paternoster , D. Mantovani*
Laval University, Canada

P8 **PMMA-coating of biodegradable pure Zinc, pure Magnesium and their alloys through grafting-from technique**
Nicolas Lallemand, F. Mouillard, Alia A. Diaa, N. El-Mahallawy, P. Masson, H. Palkowski, A. Carradò
Université de Strasbourg,France

P9 **Comprehensive study of degradation behaviour of zinc alloys subjected to hybrid plastic deformation**
Anna Jarzębska, H. Helmholz, M. Wróbel, M. Bugajska, A. Bigos, S. Przybysz, R. Willumeit-Römer, M. Bieda
Polish Academy of Sciences, Poland

P10 **Characterisation and assessment of corrosion rate of TiO2 coated WE43 produced by atomic layer deposition**
Clara Grace Hynes, Z. Ghaferi, S. Malinov, A. Flanagan, F. Buchanan
Queen's University Belfast, Ireland

P11 / SOP4 **Effect of Zn/Ca Ratio on Corrosion and Mechanical Properties of Mg-Zn-Ca-Mn Biodegradable Alloys**
Thomas Avey, D. H. Cho, D. Dean, A. A. Luo
The Ohio State Universit, United States

P12 / SOP5 **In vitro and in vivo corrosion behavior and biocompatibility of biodegradable HA coated ZK60 alloy**
L. V. Hai, D.T. H. Hanh, L.e Hanh, V. N. Dinh, Nguyen Viet Nam
Institute of Traumatology and Orthopaedics - Military Central Hospital, Vietnam

P13 Cellular biocompatibility of different calcium phosphate coatings formed on ZK60 magnesium alloy

Le Thi Trang , N. Q. Cao, S.Hiromoto , O. Minho, E. Kobayashi
Tokyo Institute of Technology, Japan

P14 **Characterization of MgF_2conversion coating on Mg-2Y-1Mn-1Zn screws**
S. Gambaro, L. Nascimento, M. Shekargoftar, Samira Ravanbakhsh, V. Oliviera Sales, C. Paternoster,D. Mantovani, M. Bartosch,F. Witte
Laval University

Saturday, 27 August 2022

Session 3 – Corrosion

Chairs: Heinz Palkowski & Marta Multigner
AV support: Vinicius & Souhila
Assignation Code: K=Keynote; O=Oral presentation; SOP=Short oral presentation

8h30-9h10 K2 **Oxygen consumption during Mg alloy biodegradation is alloy and immersion medium dependent**
Berit Zeller-Plumhoff, A.R. Akkineni, H.Helmholz, D. Orlov, M. Mosshammer, M. Kühl, M. Gelinsky, R.Willumeit-Römer
Helmholtz-Zentrum Hereon, Germany

9h10-9h30 O23 **A higher PBF-LB power gives a higher density but a lower corrosion resistance of Mg-Y-Nd-Zr**
H. N. Åhman, C. Wahman, P. Mellin, Cecilia Persson
Uppsala University, Sweden

9h30-9h50 O24 **Microstructural, mechanical and biodegradation properties of as-cast and hot forged Fe-Mn-C alloys**
Martin Otto, A. Gebert, B. Paul, J. Freudenberger, J. Hufenbach
Leibniz IFW Dresden, Germany

9h50-10h10 O25 **Local oxygen concentration above Mg alloys exposed to Hanks' Balanced Salt Solution at 37 °C differs significantly from that at room temperature**
Cheng Wang, M. Zheludkevich, S. Lamaka
Helmholtz-Zentrum Hereon, Germany

10h10-10h30 O26 **Strain distribution in deformed and degraded Mg10Gd using synchrotron radiation based 2D XRD**
Birte Hindenlang, F. Wieland, Domonkos Tolnai, J. Bohlen, R. Willumeit-Römer
Helmholtz-Zentrum Hereon, Germany

10h30-10h50 O27 **The in vitro biodegradation behaviour of as extruded pure Zn, Zn-1.89Mg and PMMA coated Zn-1.89Mg**
A. A. Diaa , N. El-Mahallawy, M. Shoeib, N. Lallemand, P. Masson, Adèle Carradò
Université de Strasbourg, France

10h50-11h10	O28	**Linking geometrical degradation phenomena with the mechanical integrity of rare earth magnesium alloy for implant use** Kerstin van Gaalen, C. Quinn , F. Benn, P. E. McHugh, A. Kopp, T. J. Vaughan *National University of Ireland Galway, Ireland*
11h10-11h40	**Break**	
11h40-12h00	O29	**Investigation of the biodegradation of Mg-based alloys using in situ SRnanoCT** Jan Reimers, H. C. Trinh, S. Flenner, J. Hagemann, H. Cwieka, B. Hindenlang, I. Greving, R. Willumeit-Römer, B. Zeller-Plumhoff *Helmholtz-Zentrum Hereon, Germany*
12h00-12h20	O30	**Local conditions at Zn alloy interface in buffered Hank's Balanced Salt Solution** C. Wang, X. Liu, D. Mei, M. Deng, Y. Zheng, M.L. Zheludkevich, Sviatlana Lamaka *Helmholtz-Zentrum Hereon, German*
12h20-12h40	O31	**Degradation behavior of biodegradable Fe-based alloys in albumin-enriched pseudo-physiological solutions** Quang Nguyen Cao, A. Cherqaoui, P. Mengucci, C. Paternoster, D.Mantovani *Laval University, Canada*
12h40-13h00	O32	**High resolution X-ray imaging of degradation and osseointegration of Mg-5Gd and Mg-10Gd screws implanted in rat tibia** Hanna Ćwieka, B. Zeller-Plumhoff, I. Baltruschat, J. Moosmann, R. Willumeit-Römer *Helmholtz-Zentrum Hereon, Germany*
13h00-13h20	O33	Cellular biocompatibility of different calcium phosphate coatings formed on ZK60 magnesium alloy Le Thi Trang , N. Q. Cao, S.Hiromoto , O. Minho, E. Kobayashi *Tokyo Institute of Technology, Japan*
13h20-13h25	SOP 4 / P11	**Effect of Zn/Ca Ratio on Corrosion and Mechanical Properties of Mg-Zn-Ca-Mn Biodegradable Alloys** Thomas Avey, D. H. Cho, D. Dean, A. A. Luo *The Ohio State Universit, United States*
13h25-13h30	SOP5 / P12	**In vitro and in vivo corrosion behavior and biocompatibility of biodegradable HA coated ZK60 alloy** L. V. Hai, D.T. H. Hanh, L.e Hanh, V. N. Dinh, Nguyen Viet Nam *Institute of Traumatology and Orthopaedics - Military Central Hospital, Vietnam*
13h30-13h50	**SOP Discussion**	
13h50-15h20	**Lunch**	
16h	**Departure by walk to Aloha Sport Beach Club at Playa San Juan**	

17h00-19h30 **Beach & Water Activities**
19h30- 20h30 **Cocktails**
20h30- midnight **Tapas & Drinks on the beach under the stars**

Sunday,28 August 2022

Session 4 – In-vitro

Chairs: Adele Carradò & Joseph Buhagiar
AV support: Masoud & Nguyen
Assignation Code: K=Keynote; O=Oral presentation; SOP=Short oral presentation

8h00-8h40 K3
Magnesium-fiber reinforced bone cement with enhanced mechanical properties
Andrea Rich, R. Deller, B. Helgason, S.J. Ferguson, C. Persson, J.F. Löffler, L. Berger
ETH Zurich, Switzerland

8h40-9h00 O34
Towards the development of a biodegradable metallic ureteral stent: Characterizing the corrosion and encrustation tendency of Mg alloys under in vitro urinary tract conditions
Margarida Pacheco, I.M. Aroso, J.M. Silva, S.V. Lamaka, M. Zheludkevich, J. Bohlen, M. Nienaber, D. Letzig, C.J. Hassila, C. Persson, E. Lima, A.A. Barros, R.L. Reis
University of Minho,Portugal

9h00-9h20 O35
In vitro and in vivo degradation and biocompatibility of Mg-based intermetallic particles
Hongyan Y. Tang, W.T. Lin, Y. Zhao, X.N. Gu, Y.B. Fan
School of Bio-logical Science and Medical Engineering, China

9h20-9h40 O36
Bovine serum albumin additions in Hanks' solutions: Effect on the corrosion mechanism of powder-processed FeMn alloys
Christabelle Tonna, J. Buhagiar
University of Malta, Malta

9h40-9h45 **Switch from In-vitro Session to In-vivo Session**

Session 5 – In vivo

Chairs: Frank Witte & Regine Willumeit-Roemer
Av support: Masoud & Nguyen
Assignation Code: K=Keynote; O=Oral presentation; SOP=Short oral presentation

9h45- 10h25 K4
Comparative tissue performance of Mg alloys in an atherosclerotic in vivo vascular model using multimodal imaging
M. Kwesiga, A. Griebel, Roger J. Guillory II
Michigan Technological University, United States

10h25-10h45 O37
***In-vivo* results of NOVAMag® fixation screw XS performance study**
Patrick Rider, Ž.P. Kačarević, A. Elad, D. Rothamel, G. Sauer, F. Bornert, P. Windisch, D. Hangyási, B. Molnar, B. Hesse, M. Assad, F. Witte, S. Rogge, D. Tadic

Botiss biomaterials, Germany

10h45-11h15 **Break**

11h15-11h35 O38

RF-induced heating of biodegradable magnesium-based implants during MRI

Jonathan Espiritu, M. Berangi, H. Cwieka, K. Iskhakova, A. Kuehne, B. Zeller-Plumhoff, F. Wieland, T. Niendorf, R. Willumeit-Römer, J.M. Seitz

Syntellix AG, Germany

11h35-11h55 O39

Analysis of the bone microarchitecture around biodegradable Mg-10Gd implants

Sandra Sefa, D. C. F. Wieland, R. Willumeit-Römer, J. Espiritu, H. Cwieka, I. Greving, S. Flenner, B. Zeller-Plumhoff

Helmholtz Zentrum Hereon, Germany

11h55-12h15 O40

In vitro and in vivo degradation performance of ZX00 screw for bone implants applications

Diana C. Martinez, A. Dobkowska, R. Marek, J. Jaroszewicz, T. Plocinski, H. Helmholz, R. Willumeit, W. Swieszkowski

Warsaw University of Technology, Poland

12h15-12h35 O41

Long term degradation performance of Mg-Zn-Ca ESIN in a sheep model

Romy Marek, U. Kronsteiner, U. Schwarze, S. Fischerauer, A. M. Weinberg

Medical University of Gra, Austria

12h35-12h55 O42

Bone healing around biodegradable Magnesium implants: Differential response between interfacial and near-implant bone in vivo

Heithem Ben Amara, D.C. Martinez, F.A. Shah, T. Plocinski, W. Swieszkowski, A. Palmquist, O. Omar, P. Thomsen

University of Gothenburg, Sweden

12h55-13h15 O43

Degradable magnesium alloy suture promotes fibrocartilaginous interface regeneration in a rat rotator cuff transosseous repair mode

B. Zhang, W. Zhang, Lili Tan, Q. Zhang, K. Yang

Institute of Metal Research, Chinese Academy of Sciences, China

13h15-13h35 O44

Biocompatibility and Degradation Behavior of Molybdenum in an In Vivo Rat Model

Christian Redlich, A. Schauer, Georg Poehle, V. Adams, P. Quadbeck

Fraunhofer Institute for Manufacturing Technology and Advanced Materials IFA, Germany

13h35-13h55 O45

In vivo comparison of ultrahigh-purified lean Mg alloys and rare-earth-containing WE43

Leopold Berger, S. Dolert, T. Akhmetshina, J.P. Burkhard, M. Tegelkamp, A.M. Rich, W. Rubin, S. Darwiche, G. Kuhn, B. von Rechenberg, B. Schaller, K. Nuss, J.F. Löffler

ETH Zuric, Switzerland

13h55-15h00 Lunch

Session 6 – In-vivo

Chairs: Diana Martinez & Frank Witte
AV support: Samira & Souhila
Assignation Code: K=Keynote; O=Oral presentation; SOP=Short oral presentation

15h00-15h40 K5
In situ reservoir for continuous evolution of H_2 gas to regulate ROS-Warburg Effect Axis for tumor therapy
Qingqing Guan, Z. Yang, J. Tan, G. Yuan, J. Pei, W.Ding
Shanghai Jiao Tong University, China

15h40-16h00 O46
BioMg 250 – Results on in vivo animal model
Tony Melkent, R. Decker, S. Lebeau
nanoMAG,United States

16h00-16h20 O47
In-vivo results of NOVAMag® membrane performance study
P. Rider, Željka P. Kačarević, A. Elad, D. Rothamel, G. Sauer, F. Bornert, P. Windisch, D. Hangyási, B. Molnar, B. Hesse, M. Assad, F. Witte, S. Rogge, D. Tadic
Botiss biomaterials, Germany

16h20-16h40 O48
FeMn and FeMnAg biodegradable alloys: A biological in vitro and in vivo investigation
L. Saliba, K. Sammut, C. Tonna, F. Pavli, V. Valdramidis, Joseph Buhagiar, P. S. Wismayer
University of Malta, Malta

16h40-17h00 O49
Preclinical biocompatibility assessment of high-strength and corrosion-controlled magnesium-based bone implants
C. Billings, M. Abdalla, D. Anderson, Hamdy Ibrahim
University of Tennessee at Knoxville, United States

17h00-17h20 O50
Potential clinical scenarios of bioabsorbable zinc as bone implants
Hongtao Yang, Y. Zheng, B. Jia, X. Qu, K. Dai
Beihang University, China

17h20-17h50 Break

17h50-18h10 O51
In-vivo study of additively manufactured Mg lattices in a large animal model
Felix Benn, R. Smeets, S. Malinov, A. Kopp
Queen's University Belfast, United Kingdom

18h10-18h30 O52
The effect of zinc and calcium on magnesium's biodegradation
Begüm Okutan, U.Y. Schwarze, L. Berger, V. Herber, O. Suljevi1, J.F. Löffler, A.M. Weinberg, N.G. Sommer
Medical University of Graz, Austria

ETH Zuric, Switzerland

18h30-18h50	O53	**Influence of ZX00 implants on the sheep bone ultrastructure** Kamila Iskhakova, D.C.F. Wieland, H. Ćwieka, T Albaraghtheh, B. Zeller-Plumhoff, R. Willumeit-Römer *Helmholtz-Zentrum Hereon, Germany*
18h50-19h00		***Conclusive Remarks***
20h00-20h30		***Cocktail at the Swimming Pool***
20h30-midnight		***BBQ Farewell Party & Swimming Pool Party***

Workshop

Thursday, August 25th, 2022

The invention of tailorable, ultrahigh-purity, lean magnesium alloys for biodegradable implant applications

Jörg F. Löffler[1]

[1] *Laboratory of Metal Physics and Technology, Department of Materials, ETH Zurich, Switzerland.*

INTRODUCTION: This contribution gives an overview of our laboratory's efforts in the development of fine-grained, lean Mg-based alloys with alloying contents below 1 at.%. This development generated the alloys ZX10 (MgZn1.0Ca0.3) [1], ZX20 (MgZn1.5Ca0.25) [2] and ZX00 (Mg0.45Zn0.45Ca) [3] (in wt.%), i.e. $MgZn_{0.37}Ca_{0.18}$, $MgZn_{0.56}Ca_{0.15}$ and $MgZn_{0.17}Ca_{0.27}$ (in at.%), and other more recent rare-earth-free ultrahigh-purified lean Mg alloys (LMg). We show how via optimized hot-extrusion processing we can tune the microstructure and thus the properties of these lean Mg alloys. We also present recent large-animal studies that reveal the advantageous properties of LMg.

RESULTS: Fig. 1 illustrates the possibility of microstructure variation via hot extrusion by changing extrusion parameters such as ratio, temperature and speed. The tensile yield strength (TYS) is strongly governed by the Hall-Petch relationship, $TYS = \sigma_0 + k_y D^{-0.5}$, where $\sigma_0 \approx 47$ MPa and $k_y \approx 240$ MPa $\mu m^{½}$ for ZX10 [4]. The extraordinary high Hall-Petch coefficient allows to achieve strong changes in the TYS by grain-size variations. In fact, for one and the same Mg alloy, we can achieve (i) alloys with bimodal microstructure (submicron grains and elongated non-recrystallized regions, Fig. 1b), revealing a TYS of >400 MPa at ductility >5%, or (ii) alloys with larger grain sizes (Fig. 1c,d), showing a ductility >30% at intermediate strength. The high-strength alloys may be used for orthopaedic screws, while the highly ductile alloy variation may be deployed in biodegradable plates (see insets to Fig. 1b,d).

The LMg alloys were designed to preferentially precipitate Ca-rich Mg_2Ca Laves phase in the form of nanometer-sized intermetallic particles (IMPs) (Figs. 1a,c), which greatly help in the extrusion process to restrict grain size via grain-boundary pinning. These IMPs are, however, less noble than the Mg matrix and can thus act as nanoscale "sacrificial anodes" and dissolve preferentially and completely. As a result, ultrahigh-purified LMg reveals in an *in vivo* sheep study degradation rates of 0.3 mm/year, which is even less than what is obtained in the same animal study for the alloy WE43 [5]. This is an important result because WE43 is a highly corrosion-resistant alloy due to its high rare-earth element content, which may, however, be potentially harmful in biodegradable implant applications [6]. Furthermore, LMg shows significantly increased bone-implant contact (BIC) compared to WE43, presumably resulting from LMg's extremely low degradation rate.

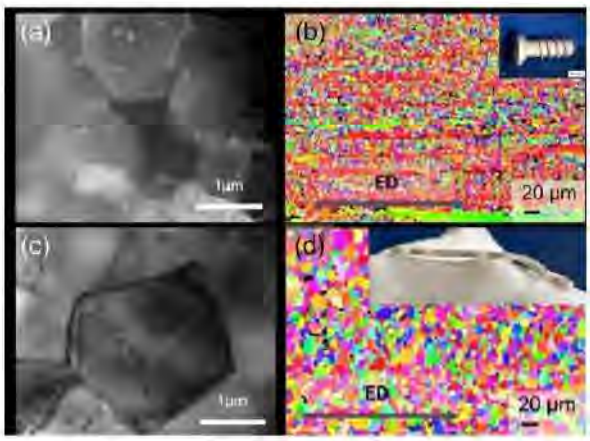

Fig. 1. TEM and EBSD images revealing the potential of microstructure variation via processing. (a, b) Alloy with submicron grains and elongated non-recrystallized regions. (c,d) Alloy with D >2 µm & low texture. Insets: Potential applications in the form of screws and plates.

DISCUSSION & CONCLUSIONS: Via continuous alloy development, we have produced lean Mg alloys (alloying content <1at.%) that show homogeneous degradation rates of 0.3 mm/year, with good biocompatibility and well-tolerated integration into bone tissue (strong BIC). LMg's mechanical properties (strength vs ductility) can be tuned by processing and its degradation rate can be tailored by varying its composition and purity. This alloy family thus appears to be very suitable for a great variety of biodegradable implant applications.

REFERENCES: [1] J. Hofstetter, et al. (2014), *JOM*, **66**:566-572. [2] M. Cihova, et al. (2019), *Acta Biomater*, **100**:398-414. [3] P. Holweg, et al (2020), *Acta Biomater*, **113**:646-659. [4] J. Hofstetter, et al. (2015), *Acta Mater*, **98**:423-432. [5] L. Berger, et al. (2022), same conference. [6] F. Amerstorfer, et al. (2016), *Acta Biomater*, **42**:440.

ACKNOWLEDGEMENTS: The author thanks previous and current LMPT members for various contributions to this work. Support by SNF Sinergia (CRSII5-180367) is gratefully acknowledged.

Update of resorbable metal in dentistry: the NOVAMag® regeneration system

S Rogge[1], ŽP Kačarević[2], P Rider[2], D Tadic[1,2]

[1] botiss medical AG, Berlin, D. [2] botiss biomaterial GmbH, Berlin, D.

LECTURE CONTENT: The NOVAMag® regeneration system has been the first system made of biodegradable magnesium metal that has received CE approval in the dental field. It is a system specifically designed for regenerative procedures in the alveolar jaw, such as GBR and bone block fixation [1], [2].

Guided bone regeneration is a well-established technique that requires the use of a barrier membrane that can be secured in place using devices such as pins or screws to secure bone granules in the augmented area. The membrane and its fixation system can be made from either resorbable or non-resorbable materials, however each choice of material has its own advantages and disadvantages.

Non-resorbable membranes provide the advantage of maintaining their shape and structure for the duration of the treatment yet require a second surgical procedure for their removal. Resorbable membranes can have problems related to their degradative by-products as well as their lack of rigidity and stability[3].

Non-resorbable fixation screws provide a secure fixation of barrier membranes or bone blocks, however, have an unacceptable level of palpability, intraoral exposure, passive migration, particle release as well as distortion of magnetic resonance in diagnostic images [4], [5]. Resorbable polymeric fixation screws have reported issues such as their breakage and the induction of inflammatory or delayed foreign body reactions[6], [7].

Due to the reported complications of both the resorbable and non-resorbable devices, alternative technologies have been explored. Magnesium is a biodegradable metal that is mechanically strong and durable, and is completely resorbed by the human body without toxic residuals, thereby encompassing the benefits of both the resorbable and non-resorbable materials. Magnesium has already been successfully applied in orthopaedic and cardiovascular applications, but only recently clinically applied in regenerative dentistry.

Over the course of the lecture, the NOVAMag® regeneration system and its clinical application will be presented. Key aspects of medical device requirements are covered, including material properties and how these translate into a usable medical device that can be successfully used in the clinic. Recommendations for the introduction onto the market of new resorbable biometal medical devices are also presented.

REFERENCES:

[1] P. Rider *et al.*, "Biodegradable magnesium barrier membrane used for guided bone regeneration in dental surgery," *Bioact. Mater.*, Nov. 2021, doi: 10.1016/j.bioactmat.2021.11.018.

[2] Ž. P. Kačarević *et al.*, "Biodegradable magnesium fixation screw for barrier membranes used in guided bone regeneration," *Bioact. Mater.*, Dec. 2021, doi: 10.1016/j.bioactmat.2021.10.036.

[3] I. Elgali, O. Omar, C. Dahlin, and P. Thomsen, "Guided bone regeneration: materials and biological mechanisms revisited," *European Journal of Oral Sciences*, vol. 125, no. 5. Blackwell Munksgaard, pp. 315–337, Oct. 01, 2017, doi: 10.1111/eos.12364.

[4] E. Willbold *et al.*, "Magnesium alloys: A stony pathway from intensive research to clinical reality. Different test methods and approval-related considerations," *J. Biomed. Mater. Res. - Part A*, vol. 105, no. 1, pp. 329–347, 2017, doi: 10.1002/jbm.a.35893.

[5] L. Yang *et al.*, "Complications of Absorbable Fixation in Maxillofacial Surgery: A Meta-Analysis," *PLoS One*, vol. 8, no. 6, pp. 1–10, 2013, doi: 10.1371/journal.pone.0067449.

[6] K. Tecklenburg, P. Burkart, C. Hoser, M. Rieger, and C. Fink, "Prospective Evaluation of Patellar Tendon Graft Fixation in Anterior Cruciate Ligament Reconstruction Comparing Composite Bioabsorbable and Allograft Interference Screws," *Arthrosc. - J. Arthrosc. Relat. Surg.*, vol. 22, no. 9, pp. 993–999, 2006, doi: 10.1016/j.arthro.2006.05.010.

[7] E. Nkenke *et al.*, "Prospective assessment of complications associated with ultrasound activated resorbable pin osteosynthesis in pediatric craniofacial surgery: preliminary results," *Neurocirugia*, vol. 22, no. 6, pp. 498–506, 2011, doi: 10.1016/s1130-1473(11)70105-1.

ACKNOWLEDGEMENTS: The development of these products have been supported with the expertise provided by Prof. Dr. Frank Witte. Additionally, we would like to thank Dr. Akiva Elad, Dr. Giorgio Tabanella and Univ.-Prof. DDr. Werner Zechner for allowing their clinical cases to be shown.

The challenges and solutions for biodegradable Zinc-based alloys from the aspect of clinical transformation

Guangyin Yuan

National Engineering Research Center of Light Alloy Net Forming and State Key Laboratory of Metal Matrix Composites, Shanghai Jiao Tong University, Shanghai 200240, China

ABSTRACT: Biodegradable zinc alloys are receiving more and more attention as a new type of medical metals in recent years thanks to their suitable degradation rate and acceptable biocompatibility. With the efforts of scientists from all over the world some progresses have been made, including new alloys, new coatings and in vivo evaluations. However, Zinc alloys also face some big challenges for their potential clinical applications because of their intrinsic physical performance, which rarely attract enough attention. These challenges include the following three aspects at least: 1) The value of c/a ≈1.86 is much higher than the ideal value of 1.63 of hexagonal close packed (HCP) metals, resulting in the high tension-compression yield asymmetry (TCYA) which will affect the expansion and compression behavior of Zinc-based vascular stents. 2) The low melting point of 420℃ of Zinc will result in the lower thermal stability, which will lead to the self-aging phenomenon of Zinc-based medical implants. 3) The dynamic recrystallization (DRX) of Zinc will take place at room temperature due to the low melting point, which will lead to the work-softening phenomenon so as to significantly affect the fixation effect and support behavior of Zinc-based vascular stents. In this talk, the underlying reasons why these challenges existed for the biodegradable zinc-based alloys will be analyzed and discussed in detail and the solutions will be proposed on basis of the research work from the author group in the past seven years.

Keywords: biodegradable zinc alloy, vascular stents, challenges, solutions, clinical translation

REFERENCES:

[1] J. Niu, H. Huang, GY Yuan, et al. Mater. Sci. Eng. C 69 (2016) 407-413.

[2] C Chen, H Huang, GY Yuan, et al., Scripta Mater200 (2021) 113922

[3] SH Fan, R Yue, GY Yuan, et al., J. Mater Research 2021,36(7):1475–1486

[4] JM Jian, H Huang, GY Yuan, et al., Scripta Mater, 200 (2021) 113907

[5] C Chen, SH Fan, GY Yuan, et al., Materials & Design 204 (2021) 109676

[6] JM Jian, Y Qian, GY Yuan, et al., Mater Sci Eng C (2022) 112652

[7] Z. Gao, J. Niu, GY Yuan, et al., Mater. Charact. (2022) 111722.

ACKNOWLEDGEMENTS: This work is supported by the National Key Research and Development Program of China (No. 2018YFE0115400), the National Natural Science Foundation of China (No. 51971134 and 52101290), Shanghai International Joint-Innovation Program (No. 20520711700) and Shanghai Jiao Tong University Medial-Engineering Cross Fund (ZH2018ZDA34 and YG2019ZDA02).

Good Results – Bad Results

N. Hort[1,2], P. Maier[3]

[1] *Helmholtz-Zentrum hereon, Geesthacht, Germany*
[2] *Leuphana University Lüneburg, Lüneburg, Germany*
3 University of Applied Sciences Stralsund, Stralsund, Germany

INTRODUCTION: What is a good result? And what makes a result bad? This is a discussion that goes on and on, and it doesn't really make sense.

Whenever a scientific question is to be investigated, one usually starts with an observation. There is something and it seems to follow a certain regularity. One tries to describe this regularity, developing a theory. This also can be seen as the development of a model. A simulation based on this theory/model can already follow here. However, a theory nor a model is reality (but only an incomplete description of a process) and a simulation does not necessarily describe reality. One can use the model to define an experiment. The results of the experiment are then compared with what was previously observed. As a rule, the results are good if they match what is expected and they are bad if they do not match what is expected. You can agree with this, but you don't have to. You can agree with this, but you don't have to. Under certain circumstances, the "bad" results may even lead to surprising new developments.

Figure 1: Sticky Notes

FROM FAILURE TO GLOBAL SUCCESS: Decades ago, S. Silver, an employee of 3M, wanted to develop a "super glue". It did not work. Years later, however, another 3M employee, A. L. Fry, was looking for a way to mark pages in a hymnal. However, he didn't want to insert plain slips of paper because they fell out too often. He also didn't want markings that stuck. And then he remembered the presumed failure of his colleague Silver. An adhesive that stuck but could also be removed without leaving any residue. And thus the sticky note was born. S. Silver's "failure" became a worldwide success!

In general, the corrosion behaviour of magnesium and its alloys prevents in a number of applications. However, unalloyed and low-alloyed steels are also extremely susceptible to corrosion. Here, however, one has solved this problem by adding Cr (> 13 wt%) or by suitable coatings. Coatings can also be applied to Mg and Mg alloys to make them corrosion-resistant. But what if the anodic behaviour was somehow advantageous? All that was needed here was a different angle of vision to turn the disadvantage of corrosion into the advantage of degradation in the case of self-dissolving implants. Here, too, there was a "bad" result that could ultimately be transformed into a "good" result. It depends on the point of view with which one looks at a "problem"!

In many papers one reads the statement that magnesium dissolves too quickly. But what is "too rapid dissolution". If you look at a degradable bone implant for a child, the dissolution may start after several weeks. For a coronary stent, dissolution is only required to start after months. So what is "too fast"? It depends on what the application requires. With suitable alloy elements, suitable process steps, possibly a coating, one has a range of tools available to adapt to the property profile. However, it is necessary to know which properties are actually needed.

SUMMARY If your results do not meet your expectations (theory/model), it may be because they are incomplete or even wrong. It may be because the design of the experiment is wrong or does not represent reality accurately enough. However, if the results of the experiment are reproducible, then the results are also "good" in themselves. One can build on them. Changing the point of view also turns "bad" results into "good" results again. Overall, therefore, results can never be "bad". They are "good" in themselves because they can be used for further decisions. And therefore any results should also be published. They help to reinvent the wheel, save resources and perhaps lay the foundation for new, innovative innovations that change the world.

20 years of commercializing nanomedicine: From biodegradable metals to self-assembled nanomaterials for fighting COVID-19, inhibiting infection, killing cancer, and regenerating tissues

TJ WEBSTER

School of Biomedical Engineering and Health Science, Hebei University of Technology, China

INTRODUCTION: Nanotechnology is now found in almost every aspect in life, from the liposomes that carry vaccines for COVID-19 to coatings placed on floors to reduce wear. Over the past 20 years, the use of nanotechnology in medicine has grown from the unknown to now significantly helping to prevent, diagnosis, and treat numerous diseases. This includes the use of nano biodegradable metals (like Mg) and self-assembled materials that carry metals and are biodegradable. This talk will cover the extensive efforts that have been used to commercialize such efforts to help real human patients as well as present the future directions needed for the field to continue to grow.

METHODS: Numerous biodegradable metal nanoparticles as well as nanotextures have been synthesized[1]. For example, Mg nanoparticles were pressed into model surfaces and soaked in NaOH to create a nanoscale surface roughness. Similarly, self-assembled materials containing biodegradable metals have been synthesized using standard organic chemistry methods (Figure 1)[2]. All materials have been studied for their ability to attach to viruses (such as SARS-CoV-2) to keep the virus from replicating. Further, such materials have been used to fight infection, inhibit cancer cell growth, and improve tissue growth using standard in vivo and in vitro methods[3, 4].

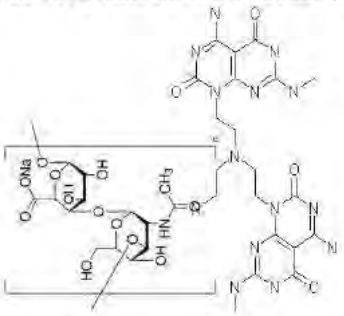

Figure 1: An example of a self-assembled nanomaterial used to reduce aging skin.

RESULTS: Biodegradable Mg with nanoscale roughness was created and was confirmed to increase bone regeneration. Further, nanotextured Mg was shown to reduce the harmful byproducts produced by Mg when it degrades.

For the self-assembled nanomaterials, one type of self-assembled nanomaterial composed of DNA base pairs has been the focus of our efforts to functionalize with specific peptides suitable for attaching to SARS-CoV-2 and all of its known variants. After binding to SARS-CoV-2, the self-assembled molecule inhibits SARS-CoV-2 binding to and entering mammalian cells keeping it from replicating.

Moreover, these unique self-assembled nanomaterials have been functionalized with peptides to attach to and penetrate to kill gram-positive bacteria, gram-negative bacteria, and antibiotic-resistant bacteria. Further, these self-assembled nanomaterials were functionalized with peptides to attach to and kill cancer cells. Lastly, significant effort has been spent to functionalize these self-assembled nanomaterials with peptides to promote bone, cartilage, vascular, skin and other tissue growth.

In vitro and in vivo studies will be presented as well as lessons learned trying to commercialize university-based research into real commercial products.

DISCUSSION & CONCLUSIONS: When created at the nanoscale, biodegradable metals possess significant promise in medicine, from improved disease prevention, detection, and treatment. The results highlighted in this presentation highlight such trends. However, for the use of nano biodegradable metals to reach clinical applications, more attention needs to be paid to toxicity concerns, biodistribution, and reducing the impact of harmful degradation products.

REFERENCES: [1]L. Weng and T.J. Webster (2012), *Nanotechnology* **23(48)**: 485105. [2]A. L. Chun et al. (2005), *Biomaterials* **26**:7304-7309. [3]H. Liu and T.J. Webster (2007), *Biomaterials* **28(2)**: 354-369. [4]J.T. Seil and T.J. Webster, (2012) *International Journal of Nanomedicine* **7**: 2767-2781.

Posters

Friday, August 26th, 2022

Binder Jetting additive manufacturing of the bioresorbable WE43 alloy: Challenges encountered in post-process sintering

Agnieszka Chmielewska [1,2], Thomas Avey[1], Daehyun Cho[1], Alan Luo[1], David Dean[1,3]

[1] The Department of Materials Science and Engineering, The Ohio State University, Columbus, Ohio, USA, [2] Warsaw University of Technology, Faculty of Materials science and Engineering, Warsaw, Poland, [3]Department of Plastic & Reconstructive Surgery, The Ohio State University, Columbus, Ohio, USA,

INTRODUCTION: Recently the additive manufacturing (AM) of biomedically-relevant magnesium alloys has been of great interest in the possibility of fabricating personalized geometries. Due to magnesium's reactivity, flammability, and low melting point temperature, laser and electron beam AM techniques may not be the best three dimensional forming method. Binder Jetting (BJ) is a melt-free technique that utilizes a binding solution to consolidate metal powder. However, BJ rendered parts require curing and sintering to remove the binding agent and solidify the part. This study presents WE43 magnesium alloy (Mg-4Y-3RE-0.5Zr) BJ manufacturing and shows the challenges associated with post-process curing and sintering.

METHODS: WE43 powder was purchased from Luxfer Magtech (Manchester, NJ, USA) with a particle size distribution of 20-63µm. Cubic samples with dimensions of 10 x 10 x 10 mm were rendered with an ExOne Innovent Binder Jetting machine (North Huntingdon, PA, USA). The solvent binder BS004 (ExOne, North Huntingdon, PA, USA) was utilized. After fabrication binder was cured at 150°C for 4h. Sintering temperatures were determined based on CALPHAD calculations and differential scanning calorimetry (DSC) analysis. Sintering was performed in the temperature range of 570-640°C for 5-6h under inert atmosphere. At the specific temperatures of 570 and 590°C, a single step heat treatment, with a heating rate of 10°C/min, was applied. For the sintering temperatures of 620 and 640°C, multiple step heating was performed with a heating rate of 2-10°C /min and a binder-burnout step at 300°C for 30 min was also, subsequently, performed.

RESULTS: It was found that WE43 coupons could be successfully fabricated using a BJ technique (Fig. 1a). CALPHAD calculations showed that the solidus and liquidus temperatures of the WE43 alloy are about 540°C and 635°C, respectively. However, DSC results showed that the melting point of the alloy is, approximately, 640°C. Sintering at 570°C results in binder swelling which caused the samples to crush and then collapse (Fig. 1b). Sintering at 590°C did not result in sample crushing (Fig. 1c), however, the temperature was too low to sinter the powder and the sample fell apart while it was being removed from the furnace (Fig. 1d). Sintering at 620°C resulted in partial sintering of the sample, however the level of sintering was low, and the sample did not remain intact when it was handled after the sintering process (Fig. 1e). Sintering at 640°C showed the best results following the sintering process (Fig. 1f); however, we anticipate that it will be possible to further optimize the sintering parameters to obtain increasingly dense parts.

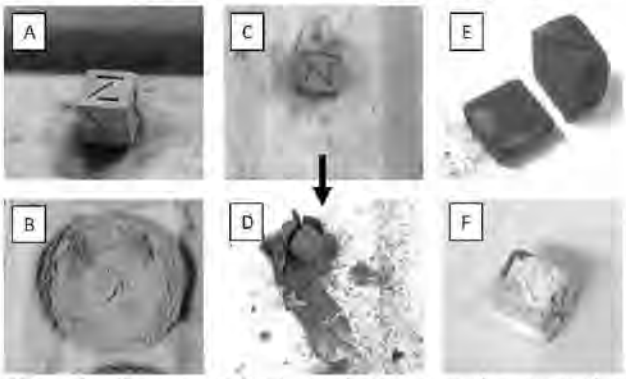

Fig. 1: Images of a) as-built sample; samples sintered at: 570°C; c, d) 590°C; e) 620°C, f) 640°C.

DISCUSSION & CONCLUSIONS: BJ technology is an effective method to fabricate complex parts from magnesium alloy powders. However, due to magnesium's high reactivity with oxygen sintering is a challenging task. Sintering at too low a temperature causes the binder to burn out before the magnesium component can densely sinter. This leads to the sample crushing. Moreover, heating conditions affect the sintering results. This initial success in BJ part rendering will benefit from further optimization of post-process curing and sintering parameters.

ACKNOWLEDGEMENTS: This work has been supported by a Cancer Engineering Fellowship from The Ohio State University, the Biomedical Device Initiative grant from the James Comprehensive Cancer Center, and a State of Ohio "Accelerator" Grant.

Microstructure and mechanical stability of biodegradable low-alloyed zinc for biomedical applications

M Wróbel[1], A Jarzębska[1], Ł Maj[1], Ł Rogal[1], P. Petrzak[1], M Kulczyk[2], M Bieda[1]

[1] *Institute of Metallurgy and Materials Science of Polish Academy of Sciences, Krakow, Poland*
[2] *Institute of High Pressure Physics, Polish Academy of Sciences, Warsaw, Poland*

INTRODUCTION: Specific requirements e.g. high mechanical properties, corrosion resistance, no harmful alloying additives, thermal stability are required for biomaterials. Pure and low alloyed zinc is an excellent material for biodegradable devices like coronary and urinal stent or orthopaedic implants due to its perfect corrosion rate [1]. Moreover it performs important functions in the human body e.g. in the immune systems. However, pure zinc has low recrystallization temperature which is about room temperature, and low mechanical properties. Addition of alloying elements, e.g. magnesium can be beneficial for all these parameters. [2]. It was showed that hydrostatic extrusion and magnesium alloying could positively affects mechanical properties [3]. There is still lack of systematic studied on the microstructural and mechanical thermal stability of zinc and zinc alloys, and this topic is the main aim of presented research [4].

METHODS: Zinc-magnesium alloys (0.6 and 1.2 wg.% Mg) were prepared by gravity casting, followed by hot extrusion, and hydrostatic extrusion in 4 passes. To investigate changes in the microstructure of the final material, ex-situ annealing at temperature range from 37 to 150°C and SEM/EBSD after each step were performed. The samples were additionally immersed in Hanks' solution for 7 and 14 days at 37°C to observe changes in the microstructure under conditions close to those of the human body. In order to examine the mechanical properties, a compression test at room temperature was performed after immersion and annealing.

RESULTS: Microstructure after hydrostatic extrusion consists of the fine α-Zn grains and intermetallic phase Mg_2Zn_{11}. Changes in the microstructure of the investigated material after annealing and immersion tests depend on amount of magnesium addition. Microstructure and mechanical properties are stable in the room temperature and after immersion tests.

DISCUSSION & CONCLUSIONS: The microstructure consists of α-Zn and Mg_2Zn_{11} is crucial not only for the mechanical properties of the alloys but also for its stability. The intermetallic phase inhibits the static recrystallization processes in low temperature. Also worth noticing that amount of alloying elements has an influence on the thermal and microstructural stability during annealing. The higher amount of magnesium the better thermal stability. No significant changes in the microstructure after immersion test in Hanks' solution is promising in the context of the application as a biodegradable biomedical material.

REFERENCES: [1] E. Mostaed, M. Sikora-Jasinska, J.W. Drelich, M. Vedani (2018) *Zinc-based alloys for degradable vascular stent applications,* Acta Biomaterialia, Vol 71, 1-23. [2] X. Zhuo, Y. Wu, J. Ju, H. Liu, J. Jiang, Z. Hu, J. Bai, F. Xue (2022) *Recent progress of novel biodegradable zinc alloys: from the perspective of strengthening and toughening,* Journal of Materials Research and Technology, 244-269. [3] W. Pachla, S. Przybysz, A. Jarzębska, M. Bieda, K. Sztwiertnia, M. Kulczyk, J. Skiba (2021) *Structural and mechanical aspects of hypoeutectic Zn–Mg binary alloys for biodegradable vascular stent applications,* Bioactive Materials, Vol. 6, 26-44, [4] G. Li, H. Yang, Y. Zheng, X.-H. Chen, J.-A. Yang, D. Zhu, L. Ruan, K. Takashima,(2019) *Challenges in the use of zinc and its alloys as biodegradable metals: Perspective from biomechanical compatibility,* Acta Biomaterialia, Vol. 97, 23-45.

ACKNOWLEDGEMENTS: The research was partially co-financed by the National Science Centre Polish UMO-2020/39/O/ST5/02692.

Influence of alloying and plastic deformation on microstructure and mechanical properties of biodegradable low-alloyed zinc for orthopaedic applications

M. Bieda[1], A Jarzębska[1], M Wróbel[1], Ł Maj[1], Ł Rogal[1], J Skiba[2],

[1] *Institute of Metallurgy and Materials Science of Polish Academy of Sciences, Krakow, Poland*
[2] *Institute of High Pressure Physics, Polish Academy of Sciences, Warsaw, Poland*

INTRODUCTION: Besides iron and magnesium alloys, zinc alloys are the most promising materials to be proposed for an application such as cardiovascular and orthopaedic biodegradable implants. Over the last two decades, researchers have been seeking a material that combines mechanical, biocorrosion, and biological properties required for biomedical applications. The main drawbacks of Zn-based materials are insufficient mechanical properties [1-3]. Our previous investigations have shown that subjecting pure zinc and zinc alloyed with magnesium to hydrostatic extrusion (HE) improved their mechanical properties to the level unattainable for other conventional methods [4]. In present investigations two other elements such as Ca and Sr were added to the alloy in order to improve properties.

METHODS: Quaternary alloy composed of zinc with 0.5 % wt. of magnesium and 0.5 wt. % of calcium and 0.5 wt. % of strontium (ZnMgCaSr) for investigation were prepared by gravity casting in argon atmosphere followed by hot extrusion at 250 °C and two-passes of hydrostatic extrusion. Obtained material in the form of 5 mm rods were investigated. Microstructural characterization using SEM, TEM, and XRD phase analysis at each step of processing was performed for as cast, hot extruded, and hydrostatic extrusion material. Crucial for this part of the research is a proper characterization of three possible intermetallic compounds (Mg_2Zn_{11}, $CaZn_{13}$ and $SrZn_{13}$), including their dispersity, area fraction, chemical composition, and grain size. The mechanical properties were examined, including microhardness, static tensile tests, and static uni-axial compression tests. Microstructural and mechanical properties are compared to those obtained for ZnMg and two ternary alloys ZnMgCa and ZnMgSr.

RESULTS: Microstructure of the investigated binary, ternary and quaternary alloy after consists of the α-Zn grains and intermetallic phases Mg_2Zn_{11}, $CaZn_{13}$ and $SrZn_{13}$. It was observed that the dispersity and the size of these phases were changing from the as-cast alloy to material after hydrostatic extrusion. That influenced the mechanical properties of the material after deformation. The highest mechanical properties were obtained for quaternary alloy ZnMgCaSr (UTS= 447MPa, YS=315MPa).

DISCUSSION & CONCLUSIONS: The development of biodegradable implants from Zn alloys is one of the main interest in the new generation of bioabsorbable alloys. From the point of excellent corrosion properties and good biocompatibility in the presented state of the art, the main problem that makes these alloys far from the final products it's their mechanical properties. Thanks to the synergy of the proper alloying (by addition Mg, Ca, and Sr) and using the accurate deformation method (hydrostatic extrusion preceded by hot extrusion), the outstanding properties with UTS above 440 MPa could be reached after two passes of hydrostatic extrusion. Multicomponent zinc alloys positively affect critical aspects of bioabsorbable materials limiting dynamic recrystallization process (DRX) in order to improve the stability of high mechanical properties.

REFERENCES: [1] G. Li, H. Yang, Y. Zheng, X.-H. Chen, J.-A. Yang, D. Zhu, L. Ruan, K. Takashima,(2019*) Challenges in the use of zinc and its alloys as biodegradable metals: Perspective from biomechanical compatibility,* Acta Biomaterialia, Vol. 97, 2019, 23-45, [2] X. Zhuo, Y. Wu, J. Ju, H. Liu, J. Jiang, Z. Hu, J. Bai, F. Xue (2022) *Recent progress of novel biodegradable zinc alloys: from the perspective of strengthening and toughening,* Journal of Materials Research and Technology, 244-269. [3] J. Venezuela, M. S. Dargusch, The influence of alloying and fabrication techniques on the mechanical properties, biodegradability and biocompatibility of zinc: A comprehensive review. *Acta Biomater.* 87, 1–40 (2019). [4] W. Pachla, S. Przybysz, A. Jarzębska, M. Bieda, K. Sztwiertnia, M. Kulczyk, J. Skiba (2021) *Structural and mechanical aspects of hypoeutectic Zn–Mg binary alloys for biodegradable vascular stent applications,* Bioactive Materials, Vol. 6, 26-44,

ACKNOWLEDGEMENTS: This work was supported by Norwegian Financial Mechanism and National Centre for Research and Development (NCBR) - grant NOR/SGS/BioAbsMat/0096/2020

Process development for additive manufacture of zinc-based biomedical substitutes

E Sheydaeian[1], A Marquardt[1, 2], L Stepien[1], E Lopez[1], F Brückner[1, 3], C Leyens[1, 2]

[1] Fraunhofer Institute for Material and Beam Technology (IWS), Dresden, Germany [2] Technische Universität Dresden, Dresden, Germany [3] Luleå University of Technology, Luleå, Sweden

INTRODUCTION: Over the past few decades, biodegradable metals have garnered particular attention due to their superior mechanical performance compared to ceramics and polymers [1-2]. Additive manufacturing (AM) is a method of fabricating objects in a layer-by-layer fashion. The method is revolutionizing the fabrication of biomedical devices by enhancing innovation in both the design and the range of materials in use [3-4]. Among biodegradable metals, zinc (Zn) is an emerging material to be explored more comprehensively. The lower melting and boiling point of Zn, which leads to a small "process window", has been one of the main hurdles on the way of adoption in AM and for the development of high-density and high-performance structures. This research aims to present preliminary results, from an in-progress work, of such structures.

METHODS: The laser powder bed fusion (LPBF) AM method was selected for the development of Zn structures. Pure (99.995%) gas atomized Zn powder with an average particle size of 35 µm was selected. A series of design of experiments was developed in the generation of proper process parameter sets for achieving high-density LPBF-made parts. Next, the powder was loaded on the LPBF system and a series of cylindrical and cubical samples were arranged and next printed on a zinc-based subplate (Fig. 1). The process was performed in an Argon atmosphere. After completion of the process, cylindrical samples were subjected to computed tomography (CT) -6 μm^3 voxel size resolution- for determining their density. The cubical samples were reserved for next step characterizations (in-progress).

Fig. 1: Layout of the printed samples.

RESULTS: Fig. 2 demonstrates the calculated density of the parts from CT scanning with respect to the line energy density (power/speed) applied in the fabrication of parts.

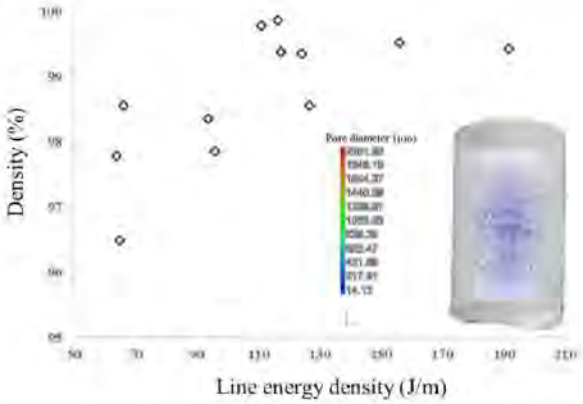

Fig. 2: Density of the samples calculated from CT scanning versus the input line energy density with an example of pores' distribution in one sample.

DISCUSSION & CONCLUSIONS: The initial evaluation of the samples' density demonstrated a volume density of above 99.5% is achievable when energy density ranges from 110 J/m to 130 J/m. The achieved performance is in line with the maximum range of density achievable via the LPBF process. Further analyses are required to identify samples' characteristics and their performance (e.g., mechanical, microstructures, corrosion) for the next steps development of zinc-based biomedical substitutes.

REFERENCES: [1] H. Li, Y. Zheng, and L. Qin 2014 *Progress of biodegradable metals*, Prog. Nat. Sci. Mater. Int. [2] Y. Yun *et al.* 2009 *Revolutionizing biodegradable metals*, Mater. Today. [3] X. Wang *et al.* 2016 *Topological design and additive manufacturing of porous metals for bone scaffolds and orthopedic implants: A review*, Biomaterials. [4] M. P. Chhaya, P. S. Poh, E. R. Balmayor, M. van Griensven, J.-T. Schantz, and D. W. Hutmacher 2015 *Additive manufacturing in biomedical sciences and the need for definitions and norms*, Expert Rev. Med. Devices.

ACKNOWLEDGEMENTS: This work is supported by funds received from Alexander von Humboldt (AvH) Stiftung, High-Performance Center (ATeM) funded by the Fraunhofer-Gesellschaft, and AGENT-3D_Basis_Invest.

Effect of magnetic field on degradation of ferrous alloys in modified Hanks' solution at 37°C

I. Limón[1], M. Multigner[1], M. Lieblich[2], C. Paternoster[3], D. Mantovani[3] J. Rams, B. Torres[1]

[1]Dpto Ciencia e Ingeniería de Materiales, ESCET, Universidad Rey Juan Carlos, c/Tulipán s/n, Móstoles, Madrid 28933, Spain; [2] CENIM-CSIC, Avda. Gregorio del Amo 8, 28040 Madrid, Spain; [3]Laboratory for Biomaterials and Bioengineering, CRC-I, Dept Min-Met-Materials Eng. & CHU de Quebec Research Center, Regenerative Medicine, Laval University, Canada

INTRODUCTION: Iron and its alloys have been proposed as an interesting candidate for biomedical application because of its no toxicity and mechanical properties, but they have a too slow degradation rate for the intended applications. For improving this rate, several methods have been proposed: to add alloying elements[1], surface modification, etc. The corrosion is an electrochemical phenomenon in which an exchange of charges occurs, and it is well known that the behavior of electric charges can be affected by the presence of magnetic fields. Therefore, when a sample is exposed to an aggressive medium in a magnetic field, it is possible to expect an influence on the behavior of the charges present in the medium, and hence on the corrosion rate. The present research is focused on the study of the effect of magnetic field in the corrosion behaviour of ferrous alloys at 37°C in modified Hanks´ solution.

METHODS: Pure ferromagnetic iron (99.8% Fe) rolled and treated 650°C/1h and austenitic steel (12% Mn; 1.5% C) rolled and treated at 800 °C/1 h (paramagnetic) have been selected. Rectangular (14 mm × 7 mm × 1 mm) samples were grinded and polished until 1 µm diamond past. Up to 14 days static *in vitro* tests have been performed in a climatic chamber to control the environment (T=37°C; H=30%) in modified pseudo-physiological Hanks´ solution (pH 7.42) under three different conditions: continuous (H_{DC}), alternate (H_{AC}) magnetic field and no magnetic field applied. Three samples were tested in each condition. Corrosion rate was evaluated through weight loss per area. Surface and corrosion products were characterized by profilometry, scanning electron microscopy, Fourier transform infrared spectroscopy and X-ray diffraction techniques.

RESULTS: The application of an AC or DC magnetic field of 9 mT doubles the degradation rate of the pure ferromagnetic iron after 14 days of immersion, as compared to samples without external magnetic field. The austenitic steel showed increases of 30% and 50% in AC and DC fields, respectively. The oxide products of FeMn samples without external magnetic field detached more easily than in samples exposed to a magnetic field. Due to that, the oxide products would act as a protective layer and, therefore, the weight loss method is not representative. A metrology method provided deeper insight about the corrosion of the samples.

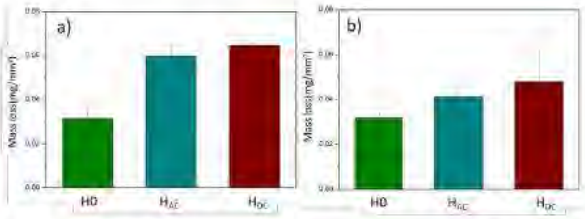

Fig. 1: Weight loss of a) pure iron and b) iron-manganese steel, after 14 days of immersion in modified Hanks' solution.

DISCUSSION & CONCLUSIONS: Both samples, Fe and FeMn, have a different behaviour when a magnetic field is applied. The application of both magnetic fields, AC and DC, causes an increase of the degradation rate of Fe samples. In the case of FeMn, the magnetic fields seem to favour the formation of a corrosion product layer, that are more strongly attached to the base, resulting in a more protective behaviour than for Fe samples.

ACKNOWLEDGEMENTS: This work was partially funded by Comunidad de Madrid Project S2018/NMT-4411, MICINN PID2019-104351GB-C21 and PID2021-123891OB-I00.

[1] B. Liu and Y. F. Zheng, "Effects of alloying elements (Mn, Co, Al, W, Sn, B, C and S) on biodegradability and in vitro biocompatibility of pure iron," *Acta Biomater.*, vol. 7, no. 3, pp. 1407–1420, 2011, doi: 10.1016/j.actbio.2010.11.001.

Optimization of attrition milling and Spark Plasma Sintering consolidation of Fe5Mg and its degradation behaviour

R Estrada[1], M Multigner[2], S C Cifuentes[2], B Torres[2], J Rams[2], M Lieblich[1]

[1]CENIM-CSIC, Madrid 28040, ES, [2]ESCET, Madrid 28933, ES

INTRODUCTION: Fe-Mg alloys have been proposed for temporary medical implants due to their potential to meet suitable degradation rates and mechanical properties [1-4]. In this work, Fe-5% wt Mg (Fe5Mg) powder was obtained by attrition milling in several controlled atmospheres and at different speed rates. In addition, a spark plasma sintering (SPS) study was carried out at different temperatures, pressures and times with the final purpose of obtaining bulk material. Degradation of Fe5Mg SPS samples was studied in Hansks' modified balance salt solution.

METHODS: Fe5Mg powder (Fe: 99.7% purity, dia. ≤74 µm; Mg: 99.8% purity, dia. ≤100 µm) was obtained by attrition milling under nitrogen or air atmosphere at 500, 800 and 1400rpm. SPS trials were carried out in the range of 400-600ºC and 50-150 MPa during 2-10 minutes. In-vitro degradation behaviour of the SPS samples was studied for 3 up to 56 days in Modified Hanks' solution. The milled powders, SPS samples and degraded samples were characterised by X-ray diffraction (XRD) and scanning electron microscopy (SEM).

RESULTS: The milling environment plays a crucial role on the milling process of Fe-Mg. Metallic powders obtained under air atmosphere resulted in Fe powder mixed with periclase (MgO) while the powder obtained in a nitrogen protective atmosphere showed non-oxidized Fe-Mg as can be seen in the XRD patterns, *Figure 1*. In addition, Fe5Mg obtained under protective atmosphere showed increased Mg integration in Fe. Rotating speed plays also an important role in the milling process, Fe5Mg milled at 1400rpm showed a heterogeneous structure compared with lower speeds, where non-milled Fe and Mg particles can be observed.

The parameters that gave rise to the highest density samples were 600 ºC and 80 MPa during 5 minutes. Degradation behaviour of SPS Fe5Mg and Fe samples obtained under mentioned conditions were tested under Hanks' solution from 3 till 56 days. The shape and composition of the degradation products of Fe5Mg samples evolves remarkably (Figure 2) and form an easily detachable layer. SPS Fe degradation products remain at the surface of the sample all along the experiments.

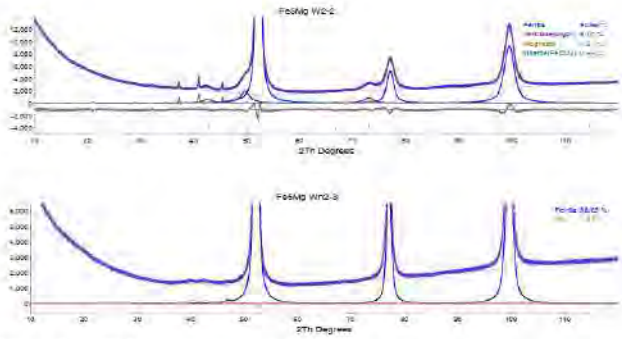

Fig. 1: XRD pattern of Fe5Mg grinded in non-protective atmosphere (top) and in protective nitrogen atmosphere (bottom).

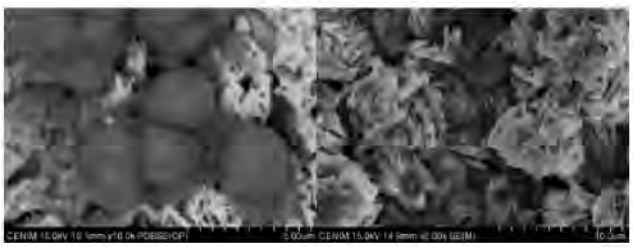

Fig. 2: SEM images of degraded SPS Fe5Mg after 3 days (left) and 14 days (right) immersed for 14 days in Hanks' solution.

DISCUSSION & CONCLUSIONS: Regarding the milling parameters it has been observed, on one side, that the highest milling speed facilitates the integration of Mg inside the Fe structure. On the other side, the continuous nitrogen flow allows to minimize oxidation during processing.

SPS parameters where optimized for achieving a compact material SPS Fe5Mg degradation products detach more easily than those of the SPS Fe.

REFERENCES: [1] Y.Guangyin and N.Jialin, Patent CN103028148A (2012). [2] R Oriňáková, A Oriňák, et al. (2013) *Int J Electrochem Sci* 8:12451. [3] G.Xie, H.Takada, et al. (2016) *Mat Sci Eng A* 671: 48-53. [4] M.Multigner, M.Lieblich et al. (2019) *11th Sym. on Biodegradable Metals*, Met-3.

PMMA-coating of biodegradable pure Zinc, pure Magnesium and their alloys through grafting-from technique

N. Lallemand[1], F. Mouillard[1], Alia A. Diaa[2,3], N. El-Mahallawy[2,3], P. Masson[1], H. Palkowski[4] A. Carradò[1]

[1]*Université de Strasbourg, Institut de Physique et Chimie de Strasbourg, Strasbourg, France.*
[2]*Design and Production Engineering Department, Fac. of Eng., Ain Shams University, Cairo, Egypt.*
[3]*Department of Design and Production Engineering, Fac. of Eng. and Materials Sc., GUC, Cairo, Egypt.*
[4]*Clausthal University of Technology, Institute of Metallurgy (IMET), Clausthal-Zellerfeld, Germany*

INTRODUCTION: Zinc (Zn) and magnesium (Mg) alloys are among the most promising biodegradable metals for medical implants. Their degradation rate can however restrict their field of application, as they tend to degrade too rapidly in the body.
The grafting-from technique is used to coat the alloys with a covalently bonded protective polymer layer, here poly(methyl methacrylate) (PMMA), and thus increase their corrosion resistance and make them better suited for medical applications.

MATERIAL & METHODS: The coating was done on pure Zn, Zn-1Mg (w%), Zn-1.89Mg (w%), pure Mg and Mg-2.37Zn-0.436Sn-0.037Mn (w%).

The grafting-from method is composed of three steps. First the samples are activated through an alkali treatment (NaOH) at 5M at 80 °C for 1 h. They are then functionalized with $C_{15}H_{30}O_5PBr$, which serves as the initiator for the last step, the atomic transfer radical polymerization of MMA to form the covalently bonded PMMA layer on the samples' surface [1].
The surface is characterized using attenuated total reflectance Fourier-transform infrared spectroscopy (ATRP-FTIR) for chemical identification. The surface and cross section are studied through scanning electron microscopy (SEM), and with Energy-dispersive X-ray spectroscopy (EDX) for chemical characterization.

RESULTS: The chemical identification by ATR-FTIR in *Figure 1* indicates that the alloys were successfully coated with a PMMA layer.

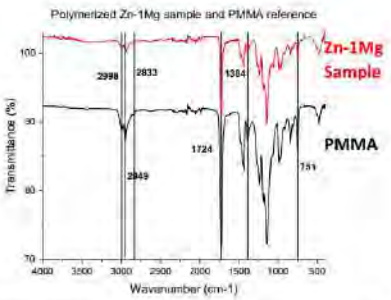

Fig. 1: ATR-FTIR spectra of the coated Zn-1Mg surface compared to PMMA reference.

The SEM surface analysis, *Figure 2,* shows the chemical composition variation on the treated metal's surface. Although the PMMA is concentrated in darker areas, EDX analysis indicates that the polymer is present in the grey areas as well; the layer is therefore considered to be continuous across the surface.

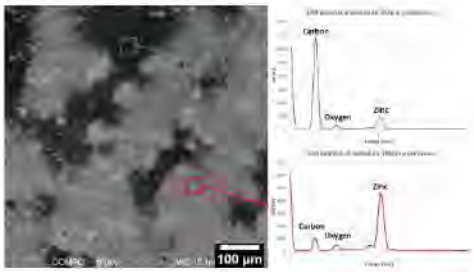

Fig. 2: SEM image of the coated Zn-1Mg surface and EDX analysis of two areas

The cross-section results, *Figure 3,* show that the PMMA layer can reach micrometre thickness and shows no gap at the interface; the metal and PMMA are correctly bonded.

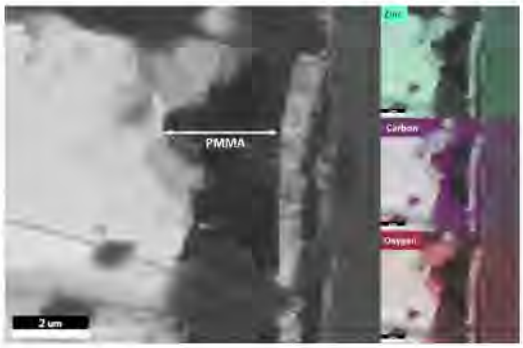

Fig. 3: SEM image and EDX mapping for Zinc, Carbon and Oxygen of the cross section of coated Zn-1Mg

DISCUSSION AND CONCLUSION: Mg and Zn alloys were successfully coated with a continuous PMMA layer, that does not show any breaking point at the interface, using the grafting-from technique. Corrosion tests on all the coated alloys are underway.

REFERENCES : [1] M. Reggente *et al.*, *ACS Appl. Mater. Interfaces*, vol. 10, no. 6, pp. 5967–5977, Feb. 2018.

ACKNOWLEDGEMENTS: We gratefully acknowledge the bilateral financial support provided by: DFG Grant No. PA 837/47-1, ANR Grant No. ANR-18-CE92-0056 and PHC IMHOTEP 2019- Code Projet: 41847QJ.

Comprehensive study of degradation behaviour of zinc alloys subjected to hybrid plastic deformation

A Jarzębska[1], H Helmholz[2], M Wróbel[1], M Bugajska[1], A Bigos[1], S Przybysz[3], R Willumeit-Römer[2], M Bieda[1]

[1] *Institute of Metallurgy and Materials Science, Polish Academy of Sciences, Krakow, Poland*

[2] *Helmholtz Zentrum Hereon, Institute of Metallic Biomaterials, Geesthacht, Germany*

[3] *Institute of High Pressure Physics, Polish Academy of Sciences, Warszawa, Poland*

INTRODUCTION: Studies on biodegradable zinc alloys have been expanding greatly, since their optimal corrosion rates are very promising in terms of future medical applications. The existing challenge of low mechanical properties of pure zinc may be solved by alloying addition supported by plastic deformation. Hydrostatic extrusion (HSE) preceded by hot extrusion (HE) has found to be especially beneficial in improving both strength and plasticity of pure zinc[1] . While being subjected to severe plastic deformation, a material undergoes substantial microstructural changes, such as grain refinement or the development of substructure. These factors can affect the corrosion rate of zinc[2]. Thus, it is of great importance to study degradation behaviour of plastically deformed zinc alloys.

METHODS: In order to study the effect of plastic deformation on degradation rate, pure Zn, Zn-Mg and Zn-Mg-Cu alloys in two different states, after HE and HSE were examined. The prepared samples were immersed for 7 and 14 days in Hanks Balanced Salt Solution (HBSS), HBSS with addition of 10% Fetal Bovine Serum (FBS) and Dulbecco's modified Eagels' medium (DMEM) with 10% of FBS under physiological conditions at 37°C, 5% CO_2 and humidified atmosphere. The determination of corrosion rate of zinc alloys was done based on the measured weight loss. After immersion tests, the identification of phases in the degradation layers was performed by X-ray diffractometer Bruker D8 Discovery. The analysis of corroded surface morphology as well as chemical composition of the layer was carried out by scanning electron microscopy ESEM XL-30. The surface after removal of corrosion products was also examined. Moreover, to better understand the effect of plastic deformation on degradation behaviour, the EBSD measurements were carried out with the aim to describe microstructural features.

RESULTS: The results showed that, regardless of the studied materials, the corrosion rate in HBSS was greater after 14 days than 7 days. The addition of FBS into HBSS led to the opposite trend. In the case of DMEM+FBS, the prolonged immersion time resulted in slower corrosion rate. The sequence of degradation rate was as follows: HBSS>DMEM+FBS>HBSS+FBS. SEM study revealed that depending on medium, different morphology of corrosion products was obtained. The addition of FBS to medium provoked that there were visibly less corrosion products compared to HBSS. The increasing number of alloying addition caused constant increase in degradation rate, regardless of chosen medium or immersion time. After HSE, the corrosion resistance was improved or remained similar as compared to the hot-extruded materials.

DISCUSSION & CONCLUSIONS: The performed studies point out that morphology of corrosion products formed after immersion in HBSS+FBS was more similar to the ones exposed to DMEM+FBS. A contrasting phenomena were obtained while examining corrosion behaviour in HBSS, what indicates strong influence of proteins on corrosion products formation. Moreover, after HSE, for medium enriched with FBS the degradation rate slowed down. This may indicate that grain refinement caused by HSE led to the better adsorption of proteins to the surface acting as a protective layer.

REFERENCES: [1] A. Jarzębska, et al (2020) *Metall Mater Trans A* ***51:****6784-6796.* [2] X Liu, et al (2019) JOM **71**:1414-1425

ACKNOWLEDGEMENTS: This work was financially supported by the National Centre for Research and Development, project no. LIDER/54/0229/L-11/19/NCBR/2020 and NOR/SGS/BioAbsMat/0096/2020.

Characterisation and assessment of corrosion rate of TiO2 coated WE43 produced by atomic layer deposition

CG Hynes[1], Z Ghaferi[2], S Malinov[1], A Flanagan[2], F Buchanan[1]

[1]*School of Mechanical and Aerospace Engineering, Queen's University Belfast, UK.*

[2]*Boston Scientific Ltd., Galway, Ireland*

INTRODUCTION: Atomic Layer Deposition (ALD) is a thin film deposition technique that allows for the development of conformal coatings on high aspect ratio materials, with fine-tuned thickness and composition control[1]. TiO_2 has been investigated as a potential coating material for bio-metallic implants owing to its favorable biocompatibility profile[2]. However, research into its role in controlling the degradation of Mg alloys is limited to a small number of studies[3-5]. This work investigates amorphous TiO_2 produced by ALD as a protective coating to control the degradation rates of WE43 Mg alloy.

METHODS: TiO2 coatings were grown at 150°C by ALD on WE 43 Mg coin components to produce amorphous TiO2 layers with a target thickness of 50nm and 100nm. Coating thickness was confirmed by ellipsometry. XPS was conducted to assess coating composition. STEM studies evaluated the structure and morphology of the coating. Degradation studies were conducted in SBF to measure hydrogen evolution, and optical images were taken before and after immersion.

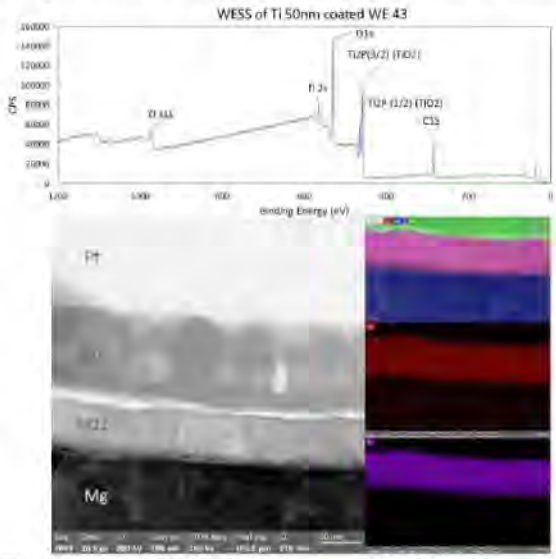

Fig. 1: (top) STEM images of TiO2 50nm coating cross section, (bottom) XPS Wide energy survey scan (WESS) of 50nm TiO2 coated Mg

RESULTS: XPS analysis revealed an atomic concentration of O and Ti at a ratio of 2.5:1 and the wide energy survey scan (Fig. 1) revealed strong peaks at O1S, $Ti2P_{1/2}$ and $Ti2P_{3/2}$ which is in accordance with reported literature[5], indicating an adequate coating process.

STEM images depicted in Fig. 1 revealed a uniform TiO2 coating on the Mg surface with no observed crystallised regions on the material surface. Hydrogen evolution studies shown in Fig. 2 revealed a significantly increased corrosion rate in both the 50nm and 100nm TiO_2 coated Mg as compared to the uncoated control. Images of the 100nm TiO_2 coated Mg demonstrate aggressive localised corrosion on the material surface with substantial material loss after the 5-day immersion period.

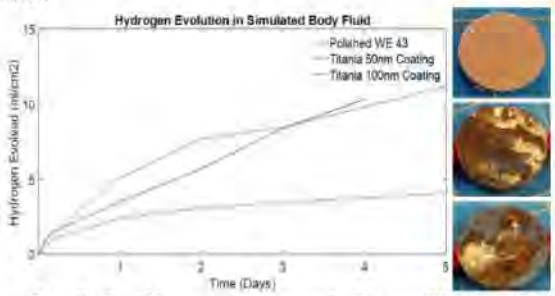

Fig. 2: (left) H_2 evolution of 50nm TiO_2, 100nm TiO_2 and uncoated WE43 in SBF, (right) 100nm TiO2 coated Mg coin before and after immersion in SBF for 5 days.

DISCUSSION & CONCLUSIONS: TiO_2 coatings produced by ALD demonstrated poor performance with respect to the corrosion protection of WE43. The interaction of Ti and Mg when in an electrolyte solution likely resulted in the formation of a galvanic couple leading to aggressive localised corrosion effects.

Characterisation of the coating so far has failed to reveal possible defects in the reaction chemistry or the growth mechanism of the coating that could lead to infiltration of electrolyte medium through the coating to cause this aggressive corrosion.

REFERENCES: [1] Johnson, R. *et al. Materials Today.* **17**, 236-246 (2014). [2] Yang, F. *et al. Int. J. Nanomedicine* **14**, 9955-9970 (2019) [3] Kania, A. *et al. Coatings* **11**, (2021) [4] Peron, M. *et al. J. Magnesium & Alloys* **9**, 1806-1819 (2021) [5] Huang, L. *et al. Rare Metals* **38**, 588-600 (2019)

ACKNOWLEDGEMENTS: This project has received funding from the European Union's Horizon 2020 Research and Innovation Programme under the Marie Skłodowska-Curie grant agreement no 813869. This publication reflects only the author's view.

Effect of Zn/Ca Ratio on Corrosion and Mechanical Properties of Mg-Zn-Ca-Mn Biodegradable Alloys

Thomas Avey[1], Dae Hyun Cho[1], David Dean[1,2], Alan A. Luo[1,3]

[1] Department of Materials Science and Engineering, The Ohio State University, Columbus, OH, 43210, USA, [2] Department of Plastic and Reconstructive Surgery, The Ohio State University, Columbus, OH, 43210, USA, [3] Department of Integrated Systems Engineering, The Ohio State University, Columbus, OH 43210, USA

INTRODUCTION: Among all biodegradable metals, magnesium has an advantage in weight, biocompatibility, and a bone-like modulus.[1] Mg-Zn-Ca alloys, specifically, have demonstrated a good balance of mechanical and corrosion properties. Mg alloys are subjected to micro galvanic corrosion initiation between the matrix and secondary phases. Mg_2Ca, $Ca_2Mg_6Zn_3$, and Mg_2Zn are reported to have stable second phases in the Mg-Zn-Ca system. From a biomedical perspective, a Zn/Ca atomic ratio between 1.2-2.0 has been shown to improve the resulting corrosion and mechanical behaviour. However, exploration of the impact of these phases needs to be better understood to further alloy design and microstructure optimization.

METHODS: Selection of potential alloys was based on CALPHAD calculations performed with Pandat software. Casting of Mg-Zn-Ca-Mn alloys at different Zn/Ca atomic ratios were carried out by SF_6 protected melting of pure Mg and adding master alloys: Mg-25%Ca and Mg-10%Mn with CP-Zn pellets. The resulting composition was measured with OES. Warm rolling was carried out after a solution heat treatment. Microstructure characterization was done by SEM, XRD, and Optical Microscopy. Initial corrosion testing was tracked by weight loss, after immersion in HBSS at 36.5°C. Potentiodynamic testing was also done in HBSS to measure corrosion current. In-depth corrosion measurements were done with Micro-Cell, Scanning Kelvin Probe Force Microscopy (SKPFM), and EIS devices. Mechanical properties were obtained via standard tensile testing.

RESULTS & DISCUSSION: Increasing Zn/Ca atomic ratio shows an expected trend for mechanical properties. The as-rolled samples with higher Zn content exhibited a near-linear increase in yield and ultimate strengths. This is a result of the widely reported solid solution strengthening of Zn in Mg alloys.[1] However, the corrosion rate (Figure 1) shows an initial decrease at 1.5 Zn/Ca and then a sharp increase after 2 Zn/Ca. The total secondary phase fraction increases with Zn/Ca ratio. However, over the investigated range, 1-5 Zn/Ca, there is a transition in the phases that forms with Mg in the eutectic region: Mg_2Ca to $Ca_2Mg_6Zn_3$ to MgZn. However, both Zn and Ca have been shown to modify the formation and protective capability of the corrosion film.[2] Local corrosion testing techniques like SKPFM, and Micro-Capillary Cell with EIS is used here to reveal phase-level corrosion behaviour of Mg-Zn-Ca alloys.

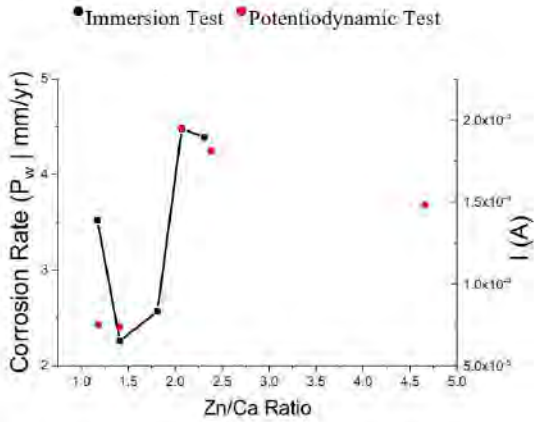

Fig. 1: Corrosion rate measured by weight loss and corrosion current from potentiodynamic testing as a function of Zn/Ca ratio

CONCLUSIONS: Increasing Zn/Ca atomic ratio improves the mechanical properties of Mg-Ca-Zn-Mn alloys but has a more complex effect on the corrosion rate, with the lowest corrosion rate measured between a Zn/Ca ratio of 1.5 to 2. Current micro-scale corrosion tests are being done to understand the mechanism behind this effect.

REFERENCES: [1]H. Ibrahim, A. D. Klarner, et. al: J. Mech. Behav. Biomed. Mater. 69, 203 (2017). [2]M. Deng, L. Wang, et. al:. Mater. Horizons 8(2), 589 (2021).

ACKNOWLEDGEMENTS: Partial support has been provided by the Accelerator Award program at The Ohio State University (OSU) and the Department of Materials Science and Engineering (MSE) at OSU. The authors are grateful to the Fontana Corrosion Center at OSU for providing access to the corrosion testing facility.

In vitro and *in vivo* corrosion behavior and biocompatibility of biodegradable HA coated ZK60 alloy

Le Van Hai[1], Do Thi Hong Hanh[2], Le Hanh[3], Vu Nhat Dinh[1], Nguyen Viet Nam[3,*]

[1] 103 Military Hospital, Military Medical University, Hanoi, Vietnam
[2] School of Materials Science and Engineering, Hanoi University of Science and Technology, Hanoi, Vietnam
[3] Institute of Traumatology and Orthopaedics, 108 Military Central Hospital, Hanoi, Vietnam

INTRODUCTION: Mg alloys demonstrated their great advantages for applications in biomedical devices including good mechanical properties, biodegradability, and biocompatibility [1]. Although these advantages of Mg alloys make their become potential candidates for use as bioabsorbable and biodegradable materials, their clinical application has been hindered due to their fast biodegradation in the physiological environment [2,3]. The aim of this research is to improve the corrosion resistance of Mg ZK60 alloy by Hydroxyapatite (HA) surface coating. The *in vitro* and *in vivo* biological response of the HA coated ZK60 alloy were investigated intensively as well.

METHODS: HA coatings was prepared from ethylenediaminetetraacetic acid calcium disodium salt hydrate ($C_{10}H_{12}CaN_2Na_2O_8$, Ca-EDTA) solution with the concentration of 0.5 mol/L and potassium dihydrogen phosphate (KH_2PO_4) solution with the concentration of 0.5 mol/L. The pH of the treatment solution was adjusted to 7.5 by NaOH. The ZK60 alloy discs were immersed in the treatment solution at 90 °C for 2 h for HA coating. The *in vitro* cell culture tests were carried out using mouse osteoblastic cell line MC3T3-E1 in α-MEM medium supplemented with 10 vol.% fetal bovine serum (α-MEM+FBS) at 37 ± 0.5 °C under a 5% CO_2 atmosphere for 24 h. After the incubation for 24h the samples were retrieved from the medium, and the cells were stained with Giemsa for the observation of cell proliferation and morphology. *In vivo* experiments were carried out on rabbit for 3 months.

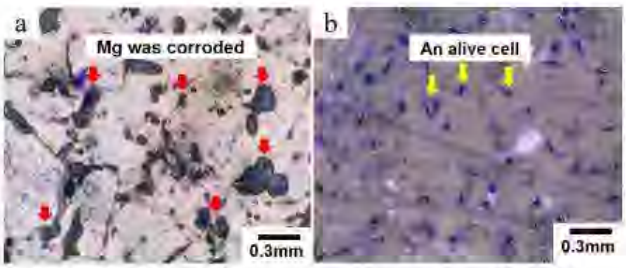

Fig. 1: Optical microscopy images of a: HA coated, and b: non-coated ZK60 specimen after cell culture test for 24 h.

Fig. 2: X-ray images of HA coated ZK60 after implanted on rabbit for a: 1 week, b: 1 month, and c: 3 months.

RESULTS & DISCUSSION: *Fig.1* shows optical microscopy images of HA coated and non-coated ZK60 alloy specimens after cell culture for 24 h. It could be seen that there was almost no cell alive on the surface of non-coated specimen while cell proliferation was on the positive progress on the surface of HA coated specimen. No corrosion occurred on the HA coated specimen, while corrosion occurred severely on the surface of the non-coated specimen.

Fig. 2 shows X ray images of HA coated ZK60 specimen implanted on rabbit after 1 week, 1 month, and 3 months, respectively. After 1 week, the specimen kept original shape without corrosion. After 1 month, corrosion occurred, the specimen was corroded slightly and there was small amount of hydrogen gas accumulated around the specimen. And after 3 months, the specimen was corroded severely and lost the original shape. There was big volume of hydrogen gas accumulated around the specimen; however, the histopathological analysis results indicated that there was no severe inflammation or negative effect due to hydrogen gas after 3 months.

CONCLUSIONS: This research investigated corrosion behavior and biological response of HA coated ZK60 alloy. HA coating layer was effective in improving the corrosion resistance of ZK60 alloy both *in vitro* and *in vivo*. The *in vivo* test results indicated that HA coated ZK60 alloy would be potential material for medical device applications.

REFERENCES: [1] N. Li, et al (2013) *J Mater Sci Technol* **29**;489-502. [2] F. Witte, et al (2005) *Biomaterials* **26**;3557–63. [3] N.T. Kirkland, et al (2010) *Corros Sci* **52**;287–91.

ACKNOWLEDGEMENTS: Center of animal-Vietnam Military Medical University

Cellular biocompatibility of different calcium phosphate coatings formed on ZK60 magnesium alloy

Le Thi Trang[1*], Nguyen Quang Cao[2], Sachiko Hiromoto[3], O Minho[1], Equo Kobayashi[1]

[1]: Department of Materials Science and Engineering, Tokyo Institute of Technology, 2-12-1 Ookayama, Meguro, Tokyo, Japan; [2]: Laboratory for Biomaterials and Bioengineering, Université Laval, 2325 Quebec, G1V 0A6 Canada; [3]: Research Center for Structural Materials, National Institute for Materials Science, 1-2-1 Sengen, Tsukuba, Ibaraki, Japan.

INTRODUCTION: Mg-6mass% Zn-0.5mass% Zr (ZK60) alloy has been attracted as a potential candidate for load-bearing applications because of its high biocompatibility, small mismatch of elastic modulus with human bone and biocompatibility [1]. However, ZK60 alloy exhibits a high degradation rate which limits its application. Calcium phosphate (Ca-P) surface coating is a simple but effective method to reduce corrosion rate while enhancing the biocompatibility of the alloy. Cell response to a Ca-P coated material depends on its surface properties [2]. In our previous work, several Ca-P coatings with different types, morphology and corrosion protection were deposited on ZK60 by changing pH coating condition [3]. Hence, in this study, we investigated the cellular biocompatibility on different Ca-P coatings formed on ZK60 alloy.

METHODS: Extruded ZK60 alloy samples (Osaka Fuji Industry, Japan) with 20 mm in diameter and 2 mm in thickness were ground with SiC papers, cleaned with ethanol. In the chemical conversion method, the samples were coated in a solution containing 0.5 mol/L Ca-EDTA ($C_{10}H_{12}CaN_2Na_2O_8$), 0.5 mol/L KH_2PO_4 and 1 mol/L NaOH solutions at 90^0C for 2h and at three different pH conditions of 6.5, 7.8 and 10.2. In the cell culture test, mouse MC3T3-E1 pre-osteoblasts were prepared through thawing and passaged 4 to 5 times. The culture medium was α-minimum essential medium (α-MEM) supplemented with 10% fetal bovine serum (FBS) and 1% penicillin/streptomycin solution (P/S). The pre-osteoblasts were seeded on the samples (n=3) at a density of $20x10^3$ cells/cm^2 in 3 ml of the culture medium and incubated at 37^0C with 5% CO_2 for 24h and 72h. After the incubation, the cells were stained by Giemsa solution for cell counting and observation. The samples were characterized by optical microscopy (OM), x-ray diffraction (XRD), scanning electron microscopy (SEM) and energy dispersive X-ray spectroscopy (EDS).

RESULTS: The type, surface morphology and corrosion protectiveness of the Ca-P coatings governed the cell morphology, mortality and proliferation. Cell proliferation was the highest on the samples coated at pH 6.5 and 7.8, while showed a decreasing trend on the sample coated at pH 10.2, as shown in Fig. 1. Additionally, the cells showed more elongated morphology with a bigger nucleus on the sample coated at pH 7.8 than on that coated at pH 6.5 but shrunk to death on that coated at pH 10.2.

DISCUSSION & CONCLUSIONS: The cell density on the samples coated at pH 6.5 and 7.8 increased significantly because Ca-P coatings enhanced the absorption protein layer which benefits cell adhesion. The cells showed better morphology on the pH 7.8 coating than the pH 6.5 coating because of both the dense distribution of the outer HAp crystals (which is beneficial for the formation of focal contact) and the higher corrosion protection. The decrease in the cell density on the sample coated at pH 10.2 is attributed to the quick initial corrosion caused by the micro-sized defects of the coating and the nanotopography of the outer dense HAp crystals. Generally, ZK60 coated at pH 7.8 showed the best cellular biocompatibility, suggesting that this sample is the most suitable material to be applied in clinical use.

REFERENCES: [1] M. Niinomi, et al. (2012) *Acta Biomater.* **8**:3888-3903. [2] S. Hiromoto, et al. (2017) *Sci. Technol. Adv. Mater.* **18**:96-109. [3] L.T. Trang, et al. (2022) *Surf. Coat. Technol.* **444**:128639.

ACKNOWLEDGEMENTS: This work is partly supported by NIMS Joint Research Hub Program (ID No. 2020-029) of the National Institute for Materials Science, Ibaraki, Japan.

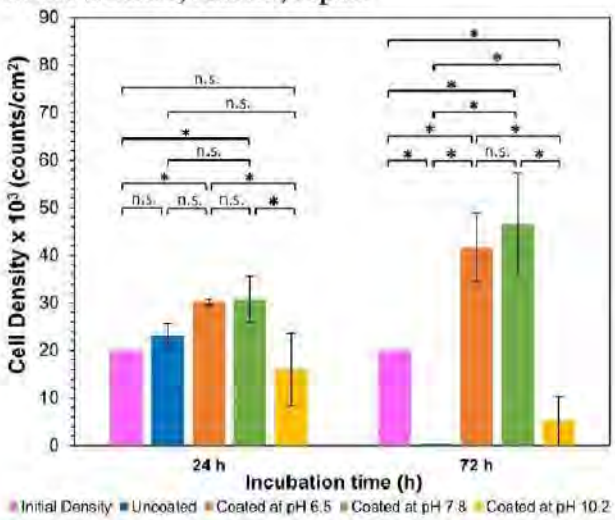

*Fig. 1: Cell proliferation on different types of the cultured samples. n.s.: not significant, *: $p \leq 0.05$.*

Metals

Friday, August 26th, 2022

Nanoindentation to characterize hardness changes by flaring of mini-tubules

P Maier[1], M Schmahl[2], B Clausius[1], C Joy[1], C Fleck[2]

[1] *University of Applied Sciences Stralsund, Stralsund, Germany,* [2] *Technische Universität Berlin, Materials Science & Engineering, Berlin, Germany*

INTRODUCTION: In alloys with heterogeneous microstructure, plastic deformation affects different phases to different extents. Resoloy® consists, depending on the process route, of LPSO phases in lamellar and blocky shape. Resoloy® tends to twin under deformation [1]. The change of hardness after tube flaring, a good method to test the toughness of mini-tubes [2], by nanoindentation is of interest in this study, allowing to identify local changes and supporting alloy development. Pure According to [3] pure Mg has a nanohardness of 0.5 GPa and a plasticity index H/E of 0.0012.

METHODS: A flaring test according to [2] was applied to extruded Resoloy® mini-tubules with a grain size of 7.2 ± 2.9 µm. Notched samples were used and a crack length of several mm was implemented, where 350 µm of length were tested.

RESULTS: Figure 1 shows the microstructure of selected regions and different imaging techniques - the hardness indents are best seen on SEM images. However, features such as blocky LPSO phases and twinned regions agree well. Figure 2 presents the hardness of the Mg-matrix, the blocky LPSO phases (some of them kink under deformation), and the twinned regions. The un-deformed Mg-matrix, before flaring, has a lower hardness. Twinned grains are only seen after flaring, by the average value harder than the Mg-matrix and harder at the crack tip. There is a high scattering seen for the LPSO phases and no clear trend.

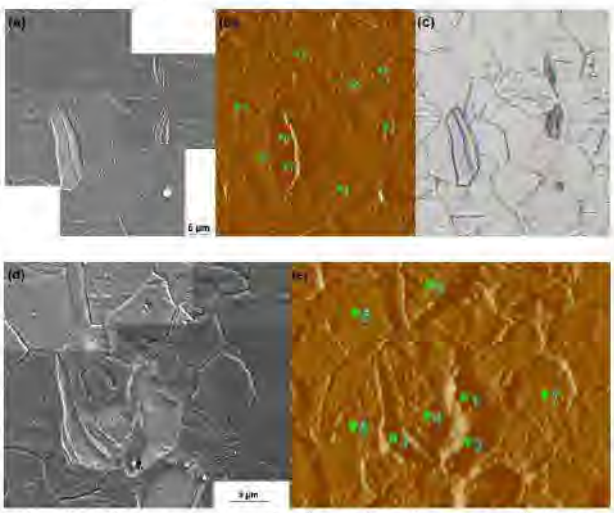

Fig. 1: Microstructure of selected regions: crack tip (a-c) and crack flank (d-e) and imaging methods: SEM (a, d), AFM (b, e) and OM (c)

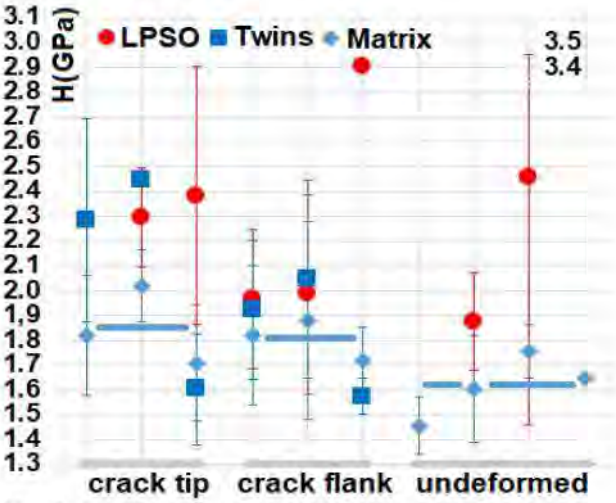

Fig. 2: Hardness at crack and undeformed region

Twinned grains at crack tip and flanks (Table 1) show higher average values for the plasticity index H/E, resistance of the material to elastic deformation, often correlated to work hardening [3], and for H^3/E^2, ability in resisting plastic deformation, compared to untwinned grains (Mg-matrix); highest values are seen for LPSO phases. The differences become more obvious for H^3/E^2.

Table 1. Plasticity index H/E - H^3/E^2 at crack tip region

	Mg-matrix	Twinned grains	LPSO
H/E	0.0399 ± 0.0089	0,0423 ± 0.0074	0,0467 ± 0.0089
H^3/E^2	0.0030 ± 0.0013	0.0036 ± 0.0011	0.0055 ± 0.0027

DISCUSSION & CONCLUSIONS: Individual hardness changes after flaring on Resoloy® mini-tubes could be evaluated by nanoindentation: the hardness of Mg-matrix grains increase up to 113%. Higher values of hardness, H/E and H^3/E^2 for twinned regions are a result of additional defect density by work hardening causing twins, being barriers to dislocation movement. Hardness and H/E values of the LPSO phases depend on their lamellar morphology and direction of indentation.

REFERENCES: [1]P. Maier et al. (2020) Crack Propagation in As-Extruded and Heat-Treated Mg-Dy-Nd-Zn-Zr Alloy Explained by the Effect of LPSO Structures and Their Micro- and Nanohardness, Materials 14(13), 3686. [2]P. Maier et al. (2020) Method to evaluate toughness and crack propagation in metal mini-tubules, Proc. 12th Symp. Biodegradable Metals. [3]M. Haghshenas et al. (2020) Magnesium-samarium oxide nanocomposites: Room-temperature depth-sensing nano-indentation response, Int. J. Lightweight Mater. Manuf. 3, 217.

IMPROVING THE TRACKABILITY OF BIODEGRADABLE METALS BY DUAL RADIOPAQUE BIORESORBABLE COATINGS AND X-RAY FILTRATION

Samira Ravanbakhsh[1,2], Carlo Paternoster[1], Pascale Chevallier[1], Marc-André Fortin[1,2], Diego Mantovani[1*]

[1] Laboratory for Biomaterials and Bioengineering, *CRC-I, Department of Min-Met-Materials Eng., & University Hospital Research Center, Regenerative Medicine, Laval University, QC, Canada*

[2]*Laboratory of Biomaterials for Medical Imaging, Regenerative Medicine Axis, Research center of CHU de Québec, Laval University, Quebec City, Canada*

INTRODUCTION: Biodegradable alloys are the new generation of thin cardiovascular stents. Visualizing and positioning of cardiovascular stents during the surgery have been done with the assistance of X-ray based imaging technique, fluoroscopy. However, the tiny geometry and the fact that biodegradable stents are made of low atomic number (low-Z) materials (ex. Fe, Mg) make the implantation and trace of these devices very challenging[1]. Adding high-Z materials such as tungsten, a degradable radiopaque element, can significantly increase the X-ray attenuation of biodegradable devices and improve their trackability[2]. To enhance the effect of radiopaque elements during the imaging, the X-ray beam in fluoroscopy can be hardened by using filters[3]. A hardened beam can increase the photon-matter interaction at a specific energy range (80kVp). Therefore, in this research work, a dual materials science and medical physics approach was proposed to solve the visibility problem of biodegradable stents by applying a degradable coating on them and altering the medical imaging procedure.

METHODS: First, a magnetron sputtering deposition system was used to cover the stents with a layer (~9 microns) of radiopaque, degradable tungsten-alloy: W-Ta and W-Fe-Mn. The chemical composition and microstructure of coatings were assessed by SEM and XRF. Electrochemical analyses were performed in Hanks' modified solution. Nanoindentation test was carried out to evaluate the mechanical properties of the coatings. The radiopacity of the coatings was assessed using X-ray computed tomography (80 kVp). The fluoroscopy beam was "carved" by using a beam filtration approach based on a combination of tin (Sn), copper (Cu), at max beam energies of 80 kVp. The beam filtration approach was validated by beam calculation tools (SpekCalc) and Monte Carlo (MC) simulation (BEAMnrc).

RESULTS: All the coatings (W-Fe-Mn and W-Ta) showed a columnar structure regardless of the chemical composition. However, the surface morphology was different for W-Ta and W-Fe-Mn (Fig. 1(a) and (b)). The amount of W in the coatings was 60% and 65% for W-Ta and W-Fe-Mn samples. The results of potentiodynamic test (Fig. 1.a) showed that the corrosion rate (CR) was ~100 and 42 µm/year for W-Fe-Mn and W-Ta coatings. The EIS results revealed a modeled circuit consisting of two resistors (R1 and R2) corresponding to electrolyte and charge transfer resistance, respectively, and one constant phase element (Q2). The maximum phase angle of the W-Fe-Mn and W-Ta was 60 and 75°, respectively. Nanoindentation results of coatings showed higher elastic modulus for W-Fe-Mn samples compared to W-Ta ones. Finally, CT-scan results of samples (Fig. 1.b and c) revealed that ~9 µm of W-Fe-Mn and W-Ta coatings resulted in 40% and 60 % of radiopacity improvement, respectively. While in the presence of a filter, the contrast improvement increased to ~80% and 93%.

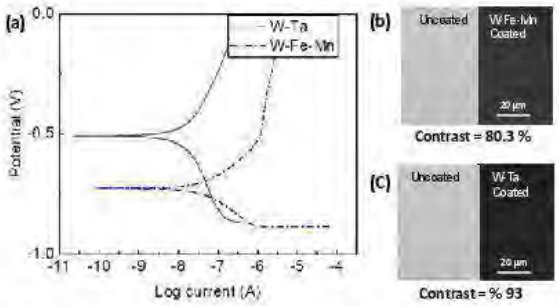

Fig 1: (a) Potentiodynamic results, (b) and (c) contrast evaluation of W-Fe-Mn and W-Ta

DISCUSSION & CONCLUSIONS:

The simulation with SpekCalc and BEAMnrc confirmed that a layer of low-Z filter could shift the X-ray spectrum toward high energy photons which significantly affects the contrast of W-coated samples. Depending on the elements, the coatings could provide long or short term radiopacity. Therefore, beam filtering, combined with a W-based coating, is a promising approach to enhance the visibility of biodegradable stents, with a strong impact for the patient and the clinical team.

REFERENCES: [1]*Park C et al., Surf Coatings Tech. 2016;305:139-145.* [2]*Li H, et al., Mater Sci Eng C. 2016;60:554-559.* [3]*Chabior M, et al. Med Phys. 2011;38(3):1189-1195.*

ACKNOWLEDGEMENTS: This work was supported by NSERC-Canada.

Development of two new Mg-Li-Y alloy wires for application in bioresorbable medical devices

K MacLeod[1], D Nash[1], D Bow[1]

[1] *University of Strathclyde, Department of Mechanical and Aerospace Engineering, Glasgow, UK*

INTRODUCTION: Magnesium (Mg) alloy wires offer attractive properties for application in several bioresorbable medical devices. New Mg alloys with high ductility are required for use in devices that undergo severe plastic deformation such as balloon expandable bioresorbable vascular scaffolds. Alloying with Li and Y can improve the mechanical properties of Mg through increased activation of non-basal slip, solid solution strengthening and texture weakening.[1, 2] Therefore, two new Mg-Li-Y alloy wires have been developed with an aim to maximise ductility. The suitability of each alloy for application in devices that undergo severe plastic deformation is investigated through characterisation of their microstructure and mechanical properties.

METHODS: Mg-4Li-0.5Y (0.5Y) and Mg-4Li-2Y (2Y) alloy wires were provided cold drawn to a diameter of 125µm. A series of annealing protocols were conducted to maximise the ductility of each alloy wire. The microstructure and mechanical properties of the alloys post annealing were characterised through EBSD analysis, tensile, minimum bend diameter, and hardness testing.

RESULTS: An uneven grain size distribution (with refined grains in the centre and larger grains towards the outer diameter) was evolved in the 0.5Y alloy, with a strong basal texture, post annealing for maximum ductility. The 2Y alloy evolved a more homogeneous microstructure with a weaker texture (Figure 1). The 0.5Y and 2Y wires both exhibited relatively high ductility, 20.3±0.4% and 19.7±1.1% respectively (Figure 2).

DISCUSSION & CONCLUSIONS: Both alloys developed a strong basal texture post annealing. The increased Y content in the 2Y alloy, however, promoted texture weakening and recrystallisation of a more homogeneous microstructure. Weaker textures are generally associated with reduced anisotropy and increased ductility though the tensile testing showed both alloys exhibit similar ductility. The increased Y content in the 2Y alloy increased both the yield and ultimate tensile strength by approximately 10MPa. The relatively high ductility of both alloys demonstrates their potential for application in devices that undergo high levels of plastic deformation. The weaker texture of the 2Y alloy may enhance its performance under complex loading, compared to the 0.5Y alloy. Future work will incorporate optimising both alloys for use in the manufacture of a new medical device.

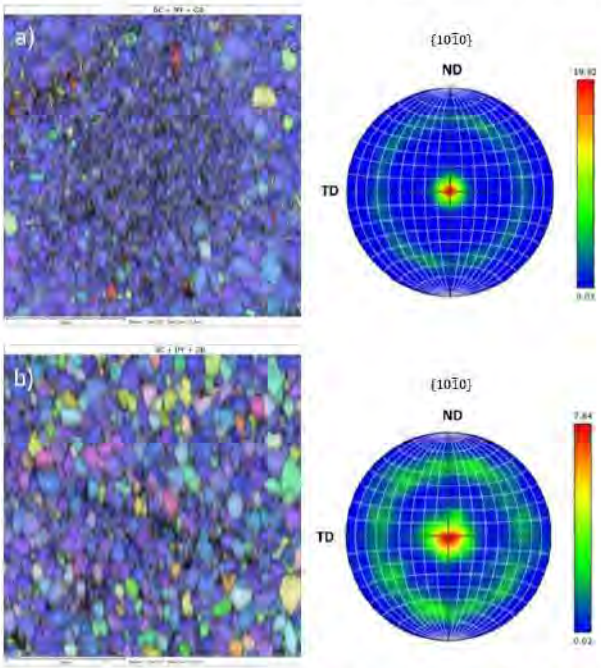

Fig. 1: Inverse pole figures for both annealed alloys and accompanying pole figure a) 0.5Y b) 2Y

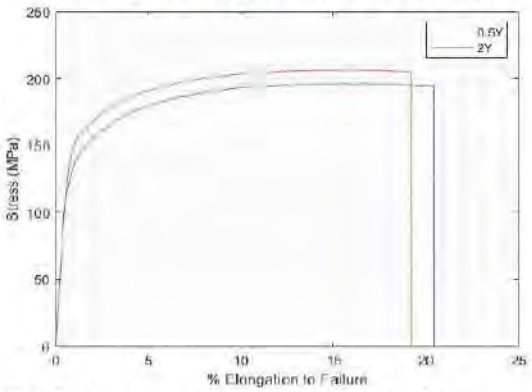

Fig. 2: Tensile curves of annealed wires

REFERENCES: [1]Zeng Y, Jiang B, Yang QR, et al.. *Materials Science and Engineering A*. 2017; 700: 59-65. [2]Gao L,Chen RS and Han EH.. *Journal of Alloys and Compounds*. 2009; 481: 379-84.

ACKNOWLEDGEMENTS: We wish to acknowledge the support of the Henry Royce Institute for advanced materials for (KM) through the Student Equipment Access Scheme enabling access to SEM/EBSD facilities at The Sorby Centre at the University of Sheffield; EPSRC Grant Number EP/R00661X/1

Multiscale hard-soft structured Zn-Cu-Li alloy with high strength and ductility for biodegradable implants

Xiyuan Zhang, Zhiqiang Gao, Jialin Niu *, Guangyin Yuan *

National Engineering Research Center of Light Alloy Net Forming and State Key Laboratory of Metal Matrix Composites, Shanghai Jiao Tong University, Shanghai 200240, China

INTRODUCTION: Zn-Cu alloys have great potential to be employed in biodegradable implants due to their excellent plasticity, anti-aging ability, and antibacterial activity. However, their strength is insufficient to meet broader application requirements. In this study, a new type of Zn-Cu-Li alloy with a unique multiscale hard-soft structure like "brick and mortar" is designed and prepared, which exhibits high strength and ductility, and the corresponding mechanisms are analyzed.

METHODS: The Zn-2Cu-0.8Li alloy was prepared through casting, homogenizing, and extrusion. The microstructure and phase compositions were analyzed through OM, XRD, SEM (equipped with EDS and TOF-SIMS), EBSD, and TEM from the micron, sub-micron scale to the nanoscale. The tensile test and nano-indentation were utilized to obtain the mechanical properties and phases' hardness. Then, the deformation behaviors were characterized by SEM, EBSD, and TEM. Finally, the alloy was fabricated to wires with a diameter of 0.25 mm and 'U type' staples. The in vivo anastomotic ability was also evaluated using beagle dogs.

RESULTS & DISCUSSION: The alloy is matrixed by hard β ($LiZn_4$) intermetallic with micron grain size (~1.64 μm), accomplishing with soft submicron η (Zn) precipitates (~0.60 μm), and hard nano ε ($CuZn_4$) precipitates (length ~42.38 nm, and width ~6.76 nm) (Fig. 1a-b). It exhibits high strength and ductility (with the YS of 426.2 ± 3.4 MPa, the UTS of 472.2 ± 3.5 MPa, and the EL of 63.7 ± 5.9%) (Fig. 1c). The high strength of the alloy is attributed to the hard β ($LiZn_4$) matrix, fine matrix grains, and a high density of coherent nano ε ($CuZn_4$) precipitates. The high ductility is attributed to soft η (Zn) precipitates at the GBs with submicron size, the CDRX behavior (Fig. 1d), and <c+a> slips in β ($LiZn_4$). The alloy shows an appropriate degradation rate and biocompatibility, and the corresponding staples implanted into beagles show excellent anastomotic ability and prognosis.

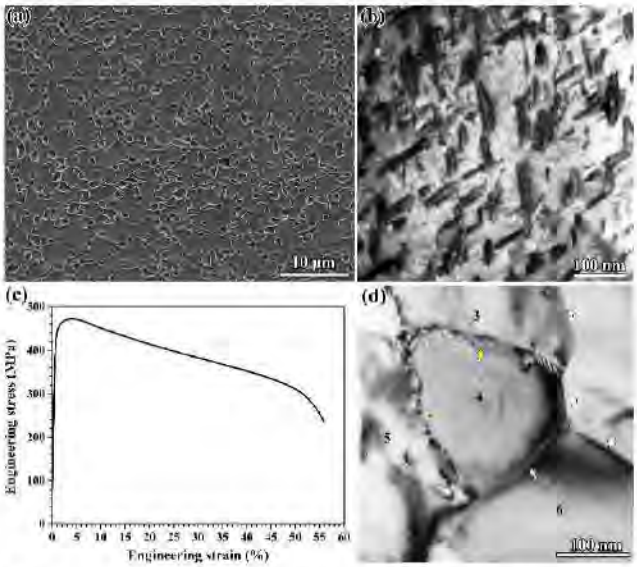

Fig. 1: Microstructure and mechanical properties of Zn-Cu-Li alloy.

CONCLUSIONS: The Zn-Cu-Li alloy shows an excellent strength-ductility synergy thanks to its unique multiscale hard-soft structure. The combined hard-soft phases, coherent precipitates, and CDRX processing in β ($LiZn_4$) are all devoted to it. The new alloy exhibits great prospects for further medical applications.

REFERENCES: [1] J. Niu, H. Huang, G. Yuan, et al. Mater. Sci. Eng. C 69 (2016) 407-413.
[2] Z. Gao, J. Niu, G. Yuan, et al. Mater. Charact. (2022) 111722.

ACKNOWLEDGEMENTS: This work is supported by the National Key Research and Development Program of China (No. 2018YFE0115400), the National Natural Science Foundation of China (No. 51971134 and 52101290), Shanghai International Joint-Innovation Program (No. 20520711700) and Shanghai Jiao Tong University Medial-Engineering Cross Fund (ZH2018ZDA34 and YG2019ZDA02).

Effect of processing conditions on mechanical and *in vitro* degradation behavior of magnesium WE43 alloy wires

Wahaaj Ali[1,2], Leon Tillmann[3], Tim Mayer[3], Alexander Kopp[3], Carlos González[1,4] and Javier LLorca[1,4]

[1]*IMDEA Materials, Spain,* [2]*Departament of Material Science and Engineering, Universidad Carlos III de Madrid, Spain,* [3]*Meotec GmbH, Aachen, Germany,* [4]*Department of Materials Science, Polytechnic University of Madrid, Spain*

INTRODUCTION: Bioresorbable magnesium wires have a broad range of potential biomedical applications such as wound closure, orthopedics, cardiovascular, bioresorbable electronic sensors, tumor treatment, nerve repair etc. However, degradation rate of magnesium is highly sensitive in wire form and controlling it is also a measure challenge because the manufacturing of wires is accomplished by a massive deformation route, from casting, extrusion and then many drawing steps. The manufacturing route not only alters the degradation behavior but also significantly affects the mechanical properties (2). In this study, we manufactured the 0.3 mm diameter wires of Magnesium WE43 alloy by cold drawing process and studied the effect of different processing conditions (Cold Work % and Annealing treatments) on mechanical and degradation behavior.

METHODS: Billets of approximately 51 mm diameter of WE43 MEO Mg alloy were produced by casting, machining, and heat-treatment processes (Meotec GmbH, Aachen) and then converted to 1.5 mm in diameter wire (Meotec GmbH, Aachen and Fort Wayne Metals Research Products Corp., Indiana, USA). This wire of 1.5 mm in diameter wire was used as feedstock for further cold drawing of wire. Total number of 28 passes were performed with intermediate annealing and lubrication to reduce wire diameter to 0.3 mm. Finally, wires were cleaned by passing them continuously through an ethanol ultrasonic bath. Wires with two different cold work percentages i.e., CW-1-34% and CW-2-13% were prepared. The latter was used for annealing treatments at different temperatures (400°C and 450°C) and times (5 s and 10 s). Tensile tests were performed on wire samples with 20 mm gage length. *In vitro* degradation tests in Simulated Body Fluid (SBF) were also performed with recording of hydrogen gas volume with time.

RESULTS: Cold-drawn wires possess the highest tensile strength ~355 MPa with negligible plastic deformation. On the other hand, the heat-treated wires have higher strain-to-failure than cold-drawn wires. The yield and tensile strength decreased with increasing temperature and time, as shown in Fig. 1. The early degradation rate of CW-1-34% was highest while lowest for CW-2-13%. Among heat treated samples, the HT-3 (450°C-5s) had relatively lowest degradation rate.

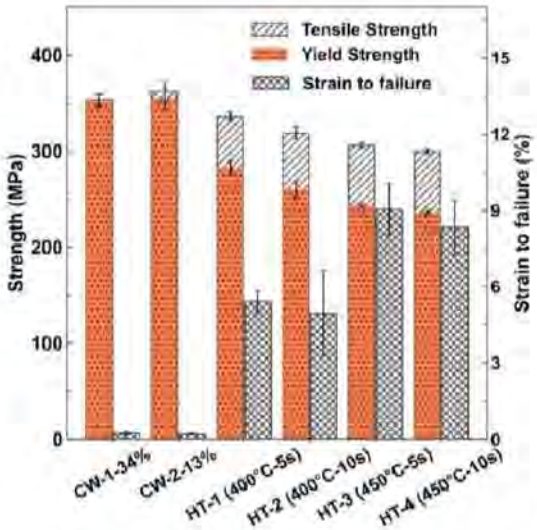

Fig. 1: Tensile properties of Mg WE43 wires after different processing conditions.

DISCUSSION & CONCLUSIONS: Processing conditions on the final workpiece in bioresorbable wire manufacturing offers the potential to tailor mechanical and degradation properties according to the application. For applications where the wire has to bear a load, HT-3 can be a suitable candidate as it has decent strain-to-failure, and degradation is relatively slow and close to best case of CW-2-13%.

ACKNOWLEDGEMENTS: This investigation was supported by the European Union's Horizon 2020 research and innovation programme under the European Training Network BioImpant Marie Skłodowska- Curie grant agreement No 813869.

REFERENCES: *Griebel AJ, Schaffer JE, Hopkins TM, Alghalayini A, Mkorombindo T, Ojo KO, et al. An in vitro and in vivo characterization of fine WE43B magnesium wire with varied thermomechanical processing conditions. J Biomed Mater Res - Part B Appl Biomater. 2018;106(5):1987–97*

Binder Jetting additive manufacturing of the bioresorbable WE43 alloy: Challenges encountered in post-process sintering

Agnieszka Chmielewska [1,2], Thomas Avey[1], Daehyun Cho[1], Alan Luo[1], David Dean[1,3]

[1] The Department of Materials Science and Engineering, The Ohio State University, Columbus, Ohio, USA, [2] Warsaw University of Technology, Faculty of Materials science and Engineering, Warsaw, Poland, [3]Department of Plastic & Reconstructive Surgery, The Ohio State University, Columbus, Ohio, USA,

INTRODUCTION: Recently the additive manufacturing (AM) of biomedically-relevant magnesium alloys has been of great interest in the possibility of fabricating personalized geometries. Due to magnesium's reactivity, flammability, and low melting point temperature, laser and electron beam AM techniques may not be the best three dimensional forming method. Binder Jetting (BJ) is a melt-free technique that utilizes a binding solution to consolidate metal powder. However, BJ rendered parts require curing and sintering to remove the binding agent and solidify the part. This study presents WE43 magnesium alloy (Mg-4Y-3RE-0.5Zr) BJ manufacturing and shows the challenges associated with post-process curing and sintering.

METHODS: WE43 powder was purchased from Luxfer Magtech (Manchester, NJ, USA) with a particle size distribution of 20-63µm. Cubic samples with dimensions of 10 x 10 x 10 mm were rendered with an ExOne Innovent Binder Jetting machine (North Huntingdon, PA, USA). The solvent binder BS004 (ExOne, North Huntingdon, PA, USA) was utilized. After fabrication binder was cured at 150°C for 4h. Sintering temperatures were determined based on CALPHAD calculations and differential scanning calorimetry (DSC) analysis. Sintering was performed in the temperature range of 570-640°C for 5-6h under inert atmosphere. At the specific temperatures of 570 and 590°C, a single step heat treatment, with a heating rate of 10°C/min, was applied. For the sintering temperatures of 620 and 640°C, multiple step heating was performed with a heating rate of 2-10°C /min and a binder-burnout step at 300°C for 30 min was also, subsequently, performed.

RESULTS: It was found that WE43 coupons could be successfully fabricated using a BJ technique (Fig. 1a). CALPHAD calculations showed that the solidus and liquidus temperatures of the WE43 alloy are about 540°C and 635°C, respectively. However, DSC results showed that the melting point of the alloy is, approximately, 640°C. Sintering at 570°C results in binder swelling which caused the samples to crush and then collapse (Fig. 1b). Sintering at 590°C did not result in sample crushing (Fig. 1c), however, the temperature was too low to sinter the powder and the sample fell apart while it was being removed from the furnace (Fig. 1d). Sintering at 620°C resulted in partial sintering of the sample, however the level of sintering was low, and the sample did not remain intact when it was handled after the sintering process (Fig. 1e). Sintering at 640°C showed the best results following the sintering process (Fig. 1f); however, we anticipate that it will be possible to further optimize the sintering parameters to obtain increasingly dense parts.

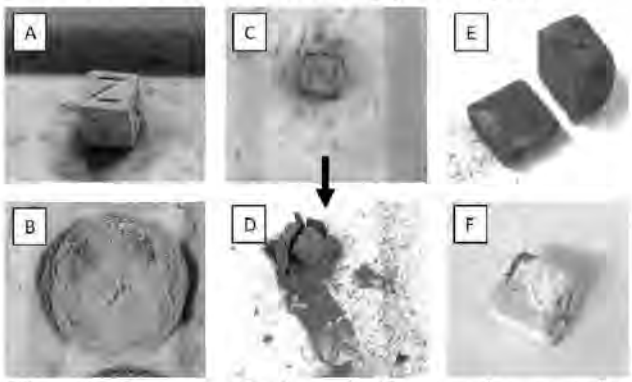

Fig. 1: Images of a) as-built sample; samples sintered at: 570°C; c, d) 590°C; e) 620°C, f) 640°C.

DISCUSSION & CONCLUSIONS: BJ technology is an effective method to fabricate complex parts from magnesium alloy powders. However, due to magnesium's high reactivity with oxygen sintering is a challenging task. Sintering at too low a temperature causes the binder to burn out before the magnesium component can densely sinter. This leads to the sample crushing. Moreover, heating conditions affect the sintering results. This initial success in BJ part rendering will benefit from further optimization of post-process curing and sintering parameters.

ACKNOWLEDGEMENTS: This work has been supported by a Cancer Engineering Fellowship from The Ohio State University, the Biomedical Device Initiative grant from the James Comprehensive Cancer Center, and a State of Ohio "Accelerator" Grant.

Study on mechanical properties, degradation properties and biocompatibility of Zn-RE binary alloys

Shaokang Du[1], Dandan Xia[2], Yufeng Zheng[1, 3], Xiaoxue Xu[4]

[1] Academy for Advanced Interdisciplinary Studies, Peking University, Beijing, China. [2] Department of Dental Materials, Peking University School and Hospital of Stomatology, Beijing, China. [3] School of Materials Science and Engineering, Peking University, Beijing 100871, China. [4] Faculty of Engineering and Information Technology, University of Technology Sydney, Sydney, Australia.

INTRODUCTION: Biodegradable Zn materials exhibit good biocompatibility and good degradation properties, and have promising applications in the clinical field. However, the poor mechanical properties of pure Zn limit its application scope. There have been studies to improve the mechanical properties of Zn and adjust the corrosion rate by alloying [1]. In order to investigate the functionalization of Zn by rare earth elements (REEs), Zn-RE binary alloys were prepared by adding REEs to Zn alloys, and a series of properties of the materials were characterized.

METHODS: A total of 16 REEs (except the radioactive element Pm), La, Ce, Pr, Nd, Sm, Eu, Gd, Tb, Dy, Ho, Er, Tm, Yb, and Lu, were added to Zn, and 16 Zn-RE binary alloy compositions were designed by combining the phase diagram and thermodynamic data of the Zn-RE system [2,3]. The mechanical properties, degradation product composition and in vitro cytocompatibility of the materials were characterized by mechanical tensile tests, immersion experiments and indirect contact method for cell culture.

RESULTS: As shown in Figure 1(a), the ultimate tensile strength and yield strength of the alloyed material are significantly increased, and elements such as Y and Ho can significantly improve the tensile strength of the material. The degradation corrosion morphology of the material (Zn-0.2Gd as an example) under scanning electron microscopy (SEM) is given in Figure 1(b). It can be found that after 1 month of immersion, many corrosion products are deposited on the surface of the material, as shown in the red region in the figure, which is mainly composed of elements such as Zn, O, P, Cl, Ca, etc. Figure 1(c) shows the morphology of human umbilical vein endothelial cells (HUVEC) cultured for 5 days. The experimental group showed a greater cell density and a higher relative survival rate compared to the pure Zn as well as the positive control group.

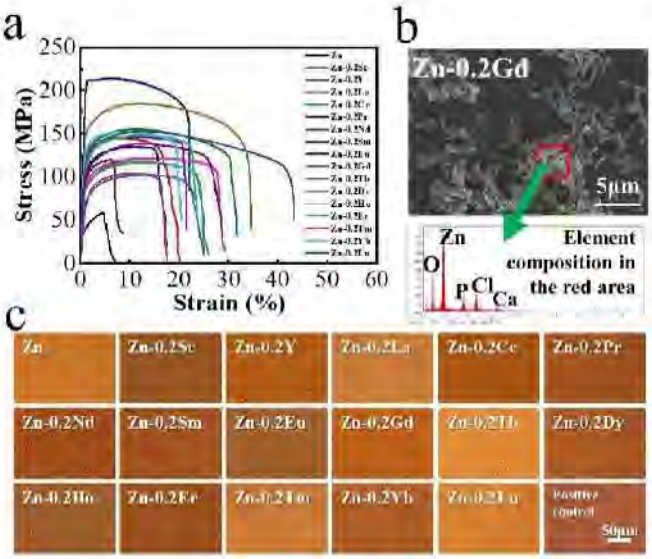

Fig. 1: (a) The stress-strain curves of pure Zn and binary Zn-RE alloys. (b) Elemental analysis of corrosion products of alloy immersed in SBF for one month. (c) HUVEC morphology after 5 days of indirect contact culture.

DISCUSSION & CONCLUSIONS: REEs can improve the properties of Zn. The addition of REEs has different effects on the mechanical and degradation properties of Zn-based materials due to the different element types. The materials are able to promote cell proliferation and have good cytocompatibility. It is shown that the Zn-RE binary alloy has the potential to be used as a biodegradable metal for biomedical purposes.

REFERENCES: [1] Y Zheng, X Gu, F Witte (2014) Materials *Science & Engineering R-Reports* **77**: 34. [2] Z. Zhu, A.D. Pelton (2015) *Journal of Alloys and Compounds* **641**: 249-260. [3] Z. Zhu, A.D. Pelton (2015) *Journal of Alloys and Compounds* **641**: 261-271.

ACKNOWLEDGEMENTS: This work was supported by National Natural Science Foundation of China (Grant No. 51931001).

Effect of groove pressing technique on the degradation rate of pure Mg

Manas Ranjan Sahu, T. S. Sampath Kumar, Uday Chakkingal

Department of Metallurgical and Materials Engineering, Indian Institute of Technology, Madras, Chennai 600036, India

INTRODUCTION: Pure Mg has attracted attention as a biodegradable implant material because of its excellent biocompatibility, good mechanical properties and density and elastic modulus which are similar to that of bone [1-3]. However its high degradation rate in the physiological environment limits its applicability for temporary implants [2]. Therefore, the objective of the present work is to decrease the degradation rate of Pure Mg by thermo-mechanical processing using the technique of groove pressing (GP).

METHODS:

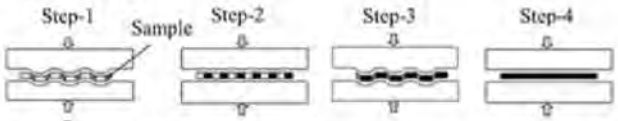

Fig. 1: Schematic representation of the steps involved in a groove pressing cycle [4].

The Pure Mg sample was annealed at 340 °C for 30 min and then groove pressed for one cycle at 340 °C as shown in Figure 1. Optical microscope was used to observe the microstructure of the sample. The weight loss and potentiodynamic polarization (PDP) tests were performed to evaluate the degradation behaviour of the sample in simulated body fluid (SBF) solution and the results compared with that from annealed specimens. The groove pressed and the annealed samples are coded as GP Mg and AN Mg respectively.

RESULTS: The optical micrograph (Figure 2) shows a decreased grain size for GP Mg sample (average size of 30 μm) whereas the AN Mg sample has 300 μm grain size.

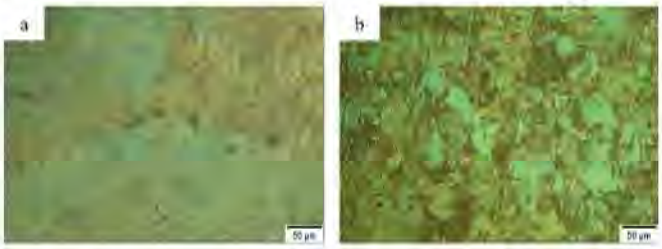

Fig. 2:. The optical microstructure of (a) AN and (b) GP Mg sample.

Figure 3 shows a lower amount of weight loss for GP Mg than AN Mg after immersion for both 25 and 50 h. In Figure 4, the PDP curve shows a higher potential and lower corrosion current density for GP Mg indicating lower degradation rate after groove pressing.

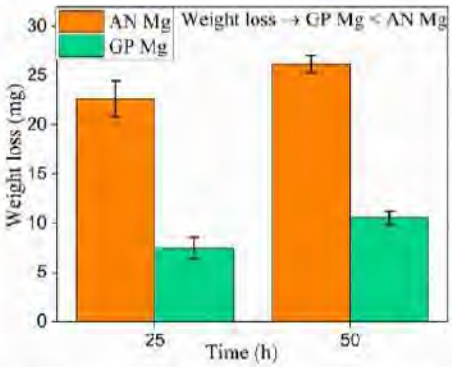

Fig. 3: The weight loss of the sample after immersion in simulated body fluid (SBF) for different time.

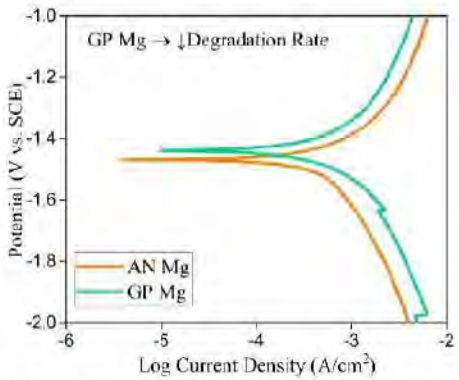

Fig. 4: The potentiodynamic polarization curve using SBF as the electrolyte.

DISCUSSION & CONCLUSIONS: In the present study, finer grained pure Mg obtained after groove pressing provides more grain boundary area which are preferential site for nucleation and adherence of passivating layer. Therefore, lower degradation rates are observed after groove pressing. The weight loss data and PDP curve confirms the lower degradation in GP Mg than in AN Mg. Therefore, groove pressing has the potential to decrease the degradation rate in Pure Mg and make it more suitable for biodegradable implant applications.

REFERENCES: [1] J. Dong *et al.*, (2022) J. Alloys Compd. **908**: 164600. [2] H. Li. *et al.*, (2020) Adv. Eng. Mater. **22**: 2000213. [3] E. Öcal *et al.*, (2019) Mater. Chem. Phys. **241**: 122350. [4] B. Ratna Sunil et al., (2013) Mater. Sci. Eng. C. **33**: 1607-1615.

3D printed Mg-based scaffolds for temporary bone replacement applications

MD Martin-Alonso[1], G Dominguez[1], M Li[1], M Echeverry-Rendon[1], F Benn[2,4], A Kopp[2], J Llorca[1,3], J Molina-Aldareguia[1,3], F Sket[1]

[1] IMDEA Materials Institute, Getafe (Madrid), Spain. [2] Meotec GmbH & Co., Aachen, Germany. [3] Universidad Politécnica de Madrid, Madrid, Spain. [4] Queen's University Belfast, Belfast, United Kingdom

INTRODUCTION: Porous Mg scaffolds manufactured by laser power bed fusion (LPBF) are promising structures for bone regeneration as they allow tissue ingrowth and permit body fluid transportation. Moreover, Mg implants can be fully re-absorbed by the human body and the mechanical properties are similar to those of bone, which prevents stress shielding effects. The application of Mg scaffolds in bone repair applications requires a detailed knowledge of the degradation behaviour and the load bearing capability during degradation. These two properties are investigated in order to obtain sufficient mechanical load bearing strength and controlled degradation, the latter allowing for controlled and sustainable bony ingrowth.

METHODS: Open porous cubic scaffolds of 10x10x10mm^3 of WE43 alloy with different lattice structures (BCC, FCC, TPMS) and average strut diameter of 500 µm were manufactured by LPBF. They were surface modified by plasma electrolytic oxidation to improve the corrosion resistance and biocompatibility [2].

The degradation behaviour was determined in simulated body fluid (SBF) by measuring the hydrogen release. The evolution of corrosion products, and *in situ* hydrogen release, was followed by synchrotron X-ray microtomography (S-XCT) and fast acquisition systems. Additionally, *in situ* S-XCT compression tests were carried out in as-printed scaffolds and after immersion in simulated body fluid for different periods (i.e. 7, 14, 21 days).

RESULTS: When immersing in SBF, scaffolds exhibited an improved degradation behaviour compared with the non-PEO surface modified scaffolds [1]. The corrosion products are located mainly at the inner part of the scaffold, and consequently some holes are created firstly at this part (*Fig. 1*). Hydrogen release at the early stage of immersion, captured by tomographies acquired in 2 seconds intervals, shows how H_2 bubbles are detected at specific sections of the surface. H_2 bubbles interact between them becoming larger with immersion time.

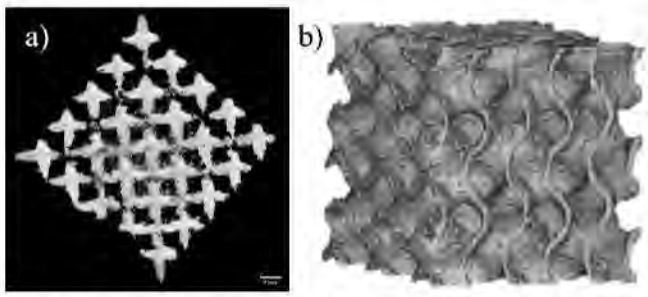

Fig. 1: a) Cross-section of BCC scaffold after 7 days of immersion in SBF and b) 3D XCT TPMS scaffold

The evolution of damage analysed with *in situ* compression tests, reveals the formation of cracks at the joints at different locations depending on topology: between nodes and struts (BCC), in lack-of-fusion defects (TPMS) and in diagonal struts (FCC). Testing of the degraded scaffolds, reveals how degradation time affects not only the compressive mechanical performance, but also the failure mode of the scaffolds.

DISCUSSION & CONCLUSIONS: Following *eq. 1*, the degradation process of Mg results in hydrogen gas, which is directly stoichiometrically connected to the bonding of Mg. It turns meaningful to find where this hydrogen is generated.

$$Mg_{(s)} + 2H_2O_{(aq)} \rightarrow Mg(OH)_{2(s)}\downarrow + H_{2(g)}\uparrow \qquad (1)$$

The detection of H_2 bubbles points out defects on the PEO surface which lead to higher degradation rates and localized corrosion, not desirable for bone replacement applications. This information can help to adjust the degradation rate to the bone regeneration rate.

TPMS scaffolds provides a higher compressive mechanical performance. Also, its great capacity to get compressed could makes it the perfect candidate for bone regeneration implants.

REFERENCES: [1]M. Li, F. Benn, et al (2021) *Materials Science and Engineering*, 119, 111623. [2]A. Kopp, T. Derra, et al (2019) *Acta Biomaterialia*, 98, 23–35, 10th BIOMETAL2018.

ACKNOWLEDGEMENTS: This investigation was supported by the FEDER/ Ministry of Science and Innovation - State Research Agency (TOPOMAG3D - PID2019-109962RB-I00)

Powder bed fusion of a biodegradable magnesium alloy: the effect of laser scan strategy and build direction on microstructure and mechanical properties

L Larsson[1], F D'Elia[1], C Persson[1]

[1]Department of Materials Science and Engineering, Uppsala University, Uppsala, SE.

INTRODUCTION: Magnesium-rare earth alloys show promise for use in biomedical applications. Advancements in 3D-printing techniques, such as powder bed fusion – laser beam (PBF-LB), has further propelled the interest in magnesium alloys for use in patient specific, degradable implants. Work on PBF-LB on various metals has shown that the choice of laser scan strategy during the printing process can heavily affect the final microstructure[1], and thus the properties of the printed part. When developing new alloys for biomedical implants, especially load bearing such, understanding the connection between the printing process and the final mechanical response is of great importance. The aim of this work is therefore to investigate the influence of laser scan strategy and build direction on the microstructure and mechanical properties in a biodegradable magnesium alloy.

METHODS: Samples were printed in an EOS M100 machine with gas-atomized spherical powder (particle size 23-60 µm) of biodegradable rare-earth magnesium alloy WE43 (Mg-4wt%Y-3wt%Nd-0.5wt%Zr, NMD GmbH) The influence of two laser scan strategies and build direction on the final microstructure and mechanical properties of the printed parts was investigated. The scan strategies under study were a 67° rotation and a 90° rotation between consecutive scan layers.

RESULTS: The scan tracks were similar for both scan strategies, and the layer rotation is clearly seen in Light Optical Microscopy images (fig. 1 b)-c)) after etching in 2% Nital solution. Scanning Electron Microscopy using Back Scattered Electrons showed the presence of secondary phases, which in previous works have been shown to consist of Yttrium oxides and various intermettallics[2]. The laser scan strategy and build direction did not induce any significant change in porosity in the samples (all >99%). The tensile data (fig 1a)) show that the build direction has a large impact on both the UTS and yield strength of the built material. The influence of the scan strategy is less pronounced, however, using a 90° scan strategy led to slightly higher ductility.

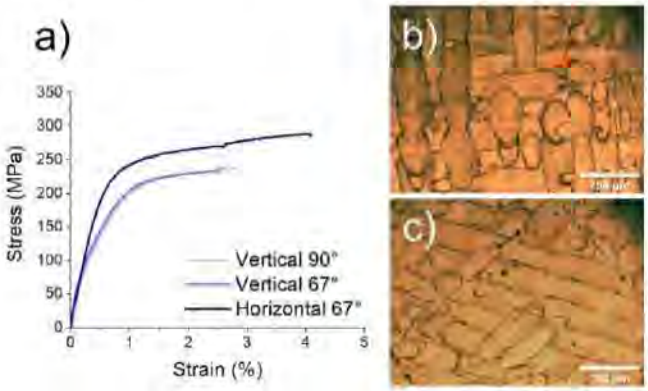

Fig. 1: a) Representatie tensile curves for the samples under study. a) Light optical microscopy images of the cross section of the 90° scan strategy and b) 67° scan strategy.

DISCUSSION & CONCLUSIONS: The results of SEM suggest that laser scan strategy does alter alloy microstructure, but only a minor effect on the mechanical response of the Mg-parts was observed. In contrast, for materials such as 316 SS[1], the laser scan strategy has been shown to significantly impact the mechanical response. This was attributed to the growth of intergranular cellular structures being affected by the choice of scan strategy. Here, the build direction did have a larger impact on the mechanical properties of the final WE43 alloy specimens. This was likely due to differences in the resulting grain orientations and texture in the direction of loading. Further research will seek to confirm this hypothesis through texture analysis of the as-printed materials.

REFERENCES: [1]J. J. Marattukalam et al., Materials & design, vol. 193, 2020. [2] H. Nilsson-Åhman (2022), Materials, vol. 15.

ACKNOWLEDGEMENTS: The authors would like to thank the Swedish Foundation for Strategic Research (SSF) within the Swedish national graduate school in neutron scattering (SwedNess), and VINNOVA's Competence Centre in Additive Manufacturing for the Life Sciences AM4Life (2019-00029) for providing financial support to this project. The authors are also grateful to Fanny Sandblad and Fanny Saarela for their contributions.

Biodegradation of powder metallurgical (PM) processed Mg ZX10-alloy for biomedical application

M Wolff, M. Luczak, H Helmholz, D. Strerath, T Ebel, R Willumeit-Römer

Helmholtz-Zentrum hereon GmbH, Germany.

INTRODUCTION: Due to absence of potentially harmful alloying elements Mg-0.52Zn-0.5Ca (ZX10) alloy obtain high potential for biomedical application [1]. In this study, ZX10 powder material was investigated with regard to its general biodegradation performance towards further binder based additive manufacturing (AM) and metal injection moulding (MIM) processing.

METHODS: ZX10 material was produced by casting. The cast ingots were extruded into rods on the one hand and gas atomised into spherical powder (SFM, Martigny, schwitzerland) on the other hand. The ZX10 powder was friction compacted into a cylinder, obtaining no residual porosity (see Figure 1, right side). Spark-wire-erosion, cutting and grinding were applied onto the friction compacted powder material (see Figure 1, left side) , as well as onto the as cast reference and as extruded reference material for manufacturing of biodegradation test specimens of 10 mm in diameter and 1.5 mm in height.

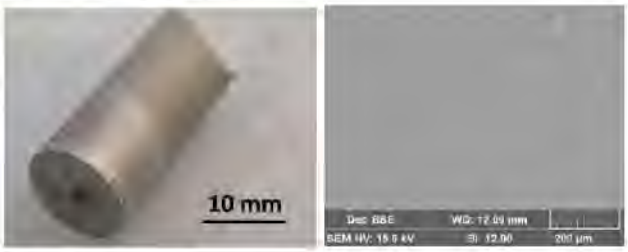

Fig. 1: Friction compacted and spark wire eroded ZX10 cylinder (left) and SEM-BSE-image of corresponding microstructure (right)

Biodegradation tests were done using DMEM+10%FBS under physiological conditions [2]. Impurity levels of the as atomised powder (Fe, Cu, Ni) were measured using ICP-OES (Spectro-Ametek, Acros II FHX22) and AAS (Agilent, 240FS AA) to assess the general suitability of the as atomised powder for biomedical applications. Microstructure was investigated by means of SEM equipped with EDS (Tescan Vega3, Czech Republic)

RESULTS: ICP-OES and AAS measurements pointed out a Fe-impurity level of 66 ppm and 36 ppm, respectively. The results of the biodegradation test setup are shown in Table 1.

Table 1. Results of the biodegradation test setup

ZX10 material-route	Mean degradation rate (MDR) [mm/a]
as cast	0.202 ± 0.03
as extruded	0.319 ± 0.10
friction compacted	0.318 ± 0.08

It can be seen that the as cast reference material obtained the best mean degradation rate (MDR). The as extruded reference material, as well as the friction compacted powder material achieve very good mean degradation rate of below 0.32 mm/a.

DISCUSSION & CONCLUSIONS: ICP-OEC and AAS pointed out that general suitability of the powder material for acceptable or even good biodegradation performance was given in view of its impurity level. Typically, additional processing steps involve the risk of additional impurity uptake. This might explain the minor increase of MDR of the as extruded and the friction compacted powder material. Because this work focusses on later MIM and 3D-printing activities, a closer lock in view of Fe-impurity uptake has to be taken onto the multiple processing steps of MIM and AM to keep the good biodegradation performance of the ZX10 powder material. Hence iron free handling tools, crucibles, as well as bending-, granulation- and extrusion equipment has to be established to enable even good biodegradation results using MIM and AM production routes.

REFERENCES: [1] J. Hofstetter et al (2014) *High-Strength Low-Alloy (HSLA) Mg–Zn–Ca Alloys with Excellent Biodegradation Performance*, JOM: the journal of the Minerals, Metals & Materials Society, DOI: 10.1007/s11837-014-0875-5. [2] N. Ahmad Agha et al, *Materials Science and Engineering: C* **58** (2016) 817-825, https://doi.org/10.1016/j.msec.2015.09.067 [3]

ACKNOWLEDGEMENT: To our partners at the AIT Austrian Institute of Technology in the framework of the project WST3-F-5030665/004-2017 MgAnOkk for providing ZX10-material, founded by: NÖ Wirtschafts- und Tourismusfonds. Also many thanks to Lars Rath and Hendrik Buresch for friction compaction of the ZX10 powder.

Adjusting mechanical properties of lean Mg alloys via hot extrusion: a wide range of strength and ductility

T Akhmetshina[1], L Berger[1], S Montibeller[1], R Schäublin[1], JF Löffler[1]

[1]*Laboratory of Metal Physics and Technology, Department of Materials, ETH Zurich, CH*

INTRODUCTION: Magnesium (Mg) alloys are excellent candidates for biodegradable medical implants. However, they should have appropriate strength and ductility to be safely used in medicine, and it is still challenging to produce such a material. Thus, Mg is often alloyed with significant amounts of other elements to improve mechanical properties, which can lead to excessive corrosion rates or reduced biocompatibility[1]. In this work we show how hot extrusion can tailor the mechanical properties of lean Mg alloys, i.e. Mg alloys with less than 1 wt.% of alloying elements, to make them suitable for various implant applications.

METHODS: In a first step, alloying range and promising candidates for extrusion parameters were determined by thermodynamic calculations with Pandat[2]. The extrusion speed was varied from 0.05 mm/sec to 8 mm/sec. Tensile tests were conducted on the extruded rods using a uniaxial testing machine at a strain rate of 10^{-3} s^{-1}. Hardness was measured using a Vickers hardness tester with a 1 kg load for 10 s. Microstructural analysis was performed via light and electron microscopy (SEM and TEM).

RESULTS: Fig. 1 shows the ultimate tensile stress (UTS), elongation at fracture and Vickers hardness (HV) of differently extruded alloys. The mechanical properties depend strongly on the extrusion parameters whereas the detailed composition determines the optimal extrusion parameters for each case.

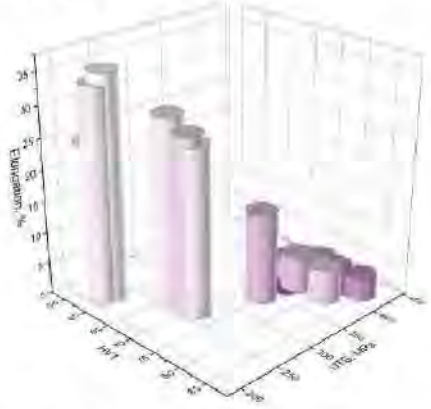

Fig. 1: Mechanical properties as measured (z-axis: elongation, y-axis: UTS, and x-axis: HV).

Microstructural analysis shows that the grain size varies from submicron to 60 µm in diameter depending on the extrusion parameters. The most ductile sample revealed 36% of elongation at fracture. SEM EBSD combined with TEM reveals, apart from a weak texture, the activation of <*c*+*a*> pyramidal slip in the alloy (Fig.2).

Fig. 2: Bright-field TEM micrograph with diffraction vector (0002) of a sample revealing 36% of deformation. Colored segments indicate the dislocation-line direction by type. The material exhibits a high density of pyramidal dislocations, which is highlighted by dotted lines in inset.

DISCUSSION & CONCLUSIONS: This work has demonstrated that lean Mg alloys can reach tensile strengths of more than 400 MPa or, alternatively, high ductility with elongation at fracture of up to 36%. Small alloying element additions to magnesium can significantly improve texture and activate non-basal slip.

REFERENCES: [1]M. Song, R. Zeng Y. Ding, et al. (2019) *J. Mater. Sci. and Techn.* **35**:535–544. [2]W. Cao et al. (2009) *CALPHAD* **33**:328–342.

ACKNOWLEDGEMENTS: The authors gratefully acknowledge financial support from the Sinergia program of the Swiss National Science Foundation (Grant No. CRSII5-180367).

Assessment of extruded magnesium tubing for absorbable stent production

Adam Griebel[1], Gregory Hayes[2], Robert Werkhoven[2], Roman Menze[3], Sandra Ahlers[3], Jeremy Schaffer[1]
[1]Fort Wayne Metals Research Products Corp., Fort Wayne, IN, USA
[2]Complex Materials, Eindhoven, Netherlands [3]MeKo Manufacturing e.K., Sarstedt, Germany

INTRODUCTION: Precision tubing is vital to many stent designs, and absorbable stents are no exception. This study aims to demonstrate a commercially viable manufacturing route and compare performance of two lean alloys to WE43.

METHODS: ZX10 and LZ21 [1] alloys were vacuum induction melted and cast into 50 mm diameter ingots at Fort Wayne Metals. These ingots were directly extruded at 300°C to 15 mm diameter bars for an extrusion ratio of 11. These 15 mm bars were used as input to the tube extrusion process. WE43 was included as a reference. ZX10, LZ21, and WE43 rods were extruded into 1.8 mm OD and 0.15 mm wall thickness tubing through a proprietary process at Complex Materials. No heat treatment was applied after extrusion. Extruded tubing was tensile tested to assess strength. Extruded tubing was then laser-cut into representative stent scaffolds (strut width and thickness of 140 and 130 µm, respectively) and electropolished at MeKo. Scaffolds were then crimped to 1 mm, expanded to 3.3 mm, and radial force tested.

RESULTS: ZX10, LZ21, and WE43 tubes were successfully manufactured (Fig.1) Grains were relatively fine at ~5µm for each alloy. Tensile results are displayed in Fig. 2. After crimping, crossing profiles were 1.26, 1.19, and 1.26 mm for ZX10, LZ21, and WE43, respectively (Fig. 3 top). Radial force and recoil of scaffolds tested in both PBS and air are shown in Fig. 4.

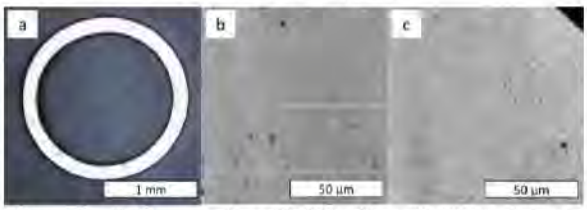

Figure 1. A) Cross-section of ZX10 tubing. B) ZX10 microstructure. C) LZ21 microstructure.

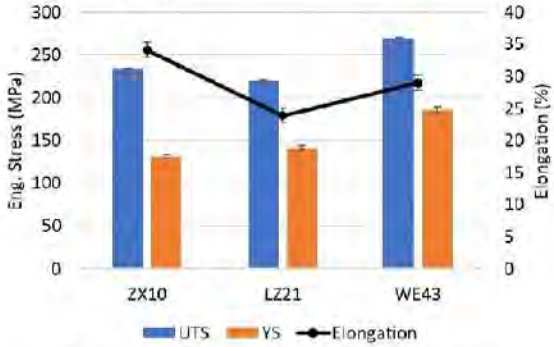

Figure 2. Tensile properties of extruded tubing.

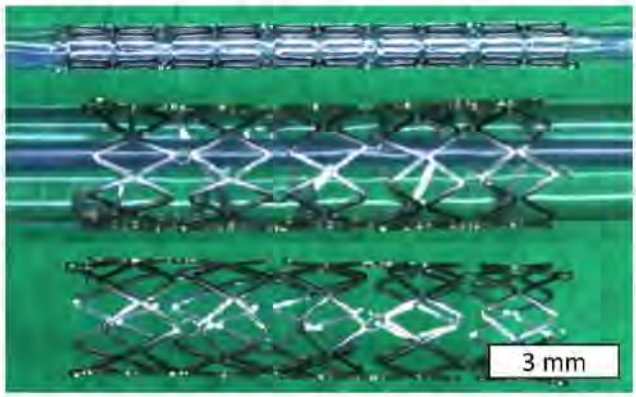

Figure 3. Scaffolds were first crimped to 1 mm diameter (top), then inflated with a balloon to ~3.3 mm (middle), followed by balloon deflation and removal (bottom).

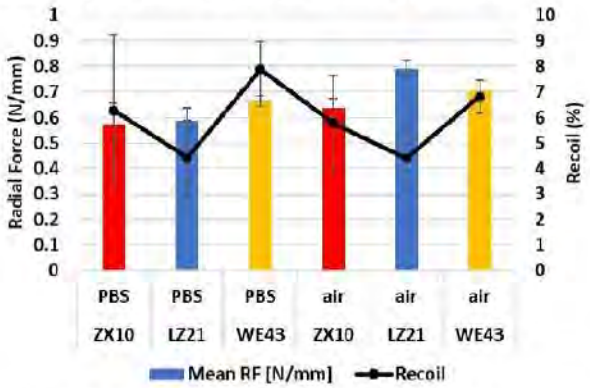

Figure 4. Radial force (bar chart) and recoil (line chart) values are shown for the 3 alloys expanded in both PBS (left) and air (right).

DISCUSSION & CONCLUSIONS: This work has demonstrated a commercially viable melt-to-scaffold manufacturing process suitable for a range of magnesium alloys. Having established the general process flow and capabilities will facilitate future development of new absorbable magnesium devices, where alloy composition and processing parameters can be fine-tuned on a case-by-case basis. Strengths of ZX10 and LZ21 tubing were expectedly less than WE43, but the surprising combination of high radial force and low recoil in the LZ21 alloy is potentially attractive. Future work may incorporate extrusion modification, coating application [2] and corrosion testing.

REFERENCES: [1] A. Griebel and J. Schaffer, "Magnesium-based absorbable alloys". WO Patent 2020/247383 A1, 3 June 2019. [2] R. Menze and E. Wittchow, "In vitro and in vivo evaluation of a novel bioresorbable magnesium scaffold with different surface modifications," Journal of Biomedical Materials Research Part B, vol. 109, no. 9, pp. 1292-1302, 2021.

Influence of PEO coating parameters on coating thickness and topography

T Imwinkelried[1], A. Walser[2], L. Berger[2], W. Rubin[2], J. F. Löffler[2]

[1] RMS Foundation, Bettlach, Switzerland, [2] Laboratory of Metal Physics and Technology, Department of Materials, ETH Zurich

INTRODUCTION: The coating of magnesium implants should delay initial gas release, avoid premature failure by stress corrosion cracking and enhance tissue integration.

METHODS: Lean magnesium X alloys were coated by plasmaelectrolytic oxidation (PEO) using direct current in three different electrolytes: phosphate[1], boron acid[2] and KOH based[3]. Coating parameters were varied from 250 – 460 V and from 7 – 28 mA/cm^2. Coating thicknesses were determined by mass gain and with eddy current measurements. The topographies of the rectangular samples (35 x 8 x 0.3 mm) were measured using white light interferometry (S neox, Sensofar, Spain). In-vitro degradation of the coated plates was tested by immersion in simulated body fluid.

RESULTS: Coating thicknesses mainly depended on the applied voltage (Figure 1) for all three electrolytes. At 250 V, the initial surface structure was still visible (Figure 2).

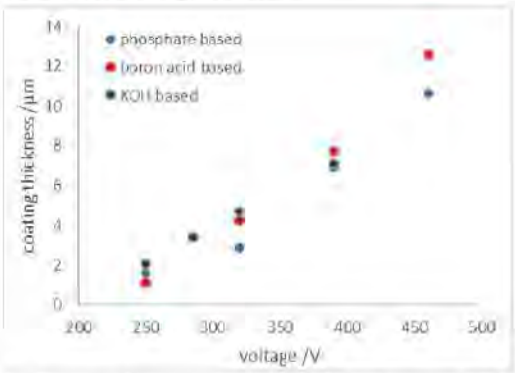

Fig. 1: Dependence of coating thickness of PEO coated magnesium plates on the applied voltage as measured by eddy current.

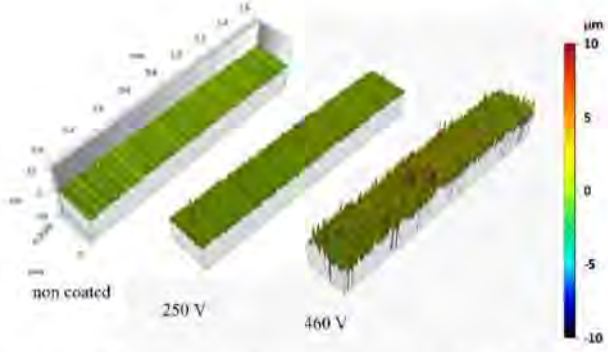

Fig. 2: 3D topography of non-coated and coated Mg plates for the boron acid based electrolyte.

At higher coating voltages, the initial surface topography vanished and was replaced by a much rougher topography with characteristic peaks and craters (Figure 3).

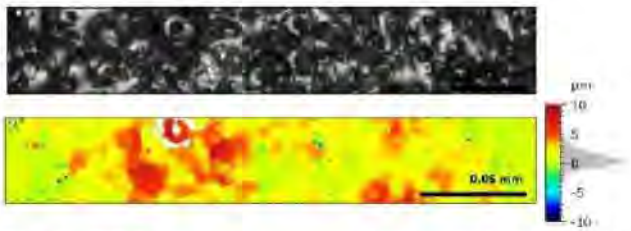

Fig. 3: PEO surface topography for a plate coated at 460 V with boron acid based electrolyte.

The roughness Ra of the non-coated plate was compared to the values for the coated plates (Table 1). The in-vitro degradation tests showed a delay of initial gas release for all three coating types compared to the non-coated plate.

Table 1. Comparison of the roughness values Ra for non-coated and PEO coated magnesium

Electrolyte	*Non-coated*	Phosphate based	Boron acid b.	KOH based
Voltage	*µm*	µm	µm	µm
250	*0.24*	0.45	0.37	1.05
320		1.44	0.88	1.32
390		1.29	1.41	1.13
460		1.05	1.23	n.a.

DISCUSSION & CONCLUSIONS: The influence of PEO coating parameters on the coating thickness and on surface topography of magnesium plates was tested for three different electrolytes. The coating thickness linearly increased with the applied voltage. Roughness values Ra of the coated plates were higher than for the non-coated plate and reached a maximum at intermediate voltages. Further in-vitro tests with tensioned samples are recommended to choose the best suited coatings for clinical applications.

REFERENCES: [1]Patent WO 2013/070669A1. [2]Patent EP 2 189 170 A1. [3]PB Srinivasan et al. (2010) J Mater Sci 45 (5), 1406–1410.

Evaluation of bioresorbable squeeze cast Mg-Zn-Ca-Mn alloys

Dae Hyun Cho[1], Thomas Avey[1], David Dean[1,2], Alan A. Luo[1,3]

[1] Department of Materials Science and Engineering, The Ohio State University, Columbus, OH, 43210, USA, [2] Department of Plastic and Reconstructive Surgery, The Ohio State University, Columbus, OH, 43210, USA, [3] Department of Integrated Systems Engineering, The Ohio State University, Columbus, OH 43210, USA

INTRODUCTION: The major merits of bioresorbable Mg alloys are their natural ability to biodegrade in aqueous solution and their remarkable biocompatibility. Furthermore, the modulus and density of Mg alloys studied to date are close to that of natural bone, thereby reducing the risk of stress shielding bone or other adjacent tissues and subsequent reoperation if those tissues fail. Mg-Zn-Ca-Mn based alloys are promising bioresorbable owing to the possibility of desirable biomechanical properties and bio-corrosion resistance. Squeeze casting is a process intended to improve mechanical properties and corrosion performance of Mg alloys. The aim of this study is to evaluate the mechanical and corrosion properties of squeeze cast Mg-Zn-Ca-Mn alloys in *in vitro* and *in vivo* conditions.

METHODS: Mg-4.0Zn-0.5Zn-xMn alloys were manufactured using a squeeze casting process. The microstructure of these alloys was characterized by optical microscopy (OM) and scanning electron microscopy (SEM). Tensile and corrosion tests were conducted. To test the *in vitro* cytocompatibility, live/dead cell viability, and indirect MTT assays were performed using the MC3T3-E mouse osteoblast cell line. Finally, *in vivo* assays were employed to investigate the immune response and biocompatibility utilizing a local lymph node assay, hematological indices, and gross findings following implantation in mice.

RESULTS & DISCUSSION: With increasing Mn addition to squeeze cast Mg-4Zn-0.5Ca alloys, the mechanical properties and corrosion resistance were increased, respectively (Fig. 1). Also, uniform biodegradation was observed during electrochemical corrosion test and immersion test in Hank's solution at 36.5 °C. The proliferation of MC3T3-E (mouse osteoblast) cells test was studied with increasing Mn addition. Further, theses alloys demonstrated good biocompatibility through the murine local lymph node assay, hematological evaluation, and tissue analysis during *in-vivo* testing. We observed initial swelling at the implantation site of as-cast specimens. In contrast, swelling was not evident in Mn-containing squeeze-cast Mg-4Zn-0.5Ca-xMn alloys.

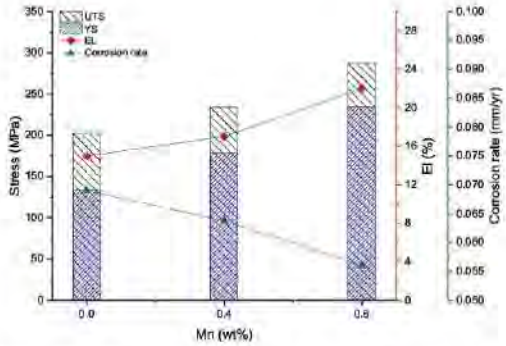

Fig. 1: Mechanical properties and corrosion rate of squeeze cast Mg-4Zn-0.5Ca-xMn alloys (x = 0.0. 0.4, and 0.8).

CONCLUSIONS: Up to 0.8 wt.% Mn addition to a squeeze cast Mg-4Zn-0.5Ca alloy can improve its mechanical properties and corrosion properties due to grain refinement and stable corrosion protective film. According to *in-vitro* and *in-vivo* tests, while squeeze cast Mg-4Zn-0.5Ca-xMn alloys have good biocompatibility, the direct impanation to Sprague Dawley rats showed swelling an implanted site of Mn-free Mg-4Zn-0.5Ca alloy. This result indicates that Mn addition to a squeeze-cast Mg-4Zn-0.5Ca alloy may improve mechanical properties, corrosion properties, and biocompatibility.

REFERENCES: [1]F. Witte, The history of biodegradable magnesium implants: A review, Acta Biomater. 6 (2010) 1680–1692. [2] D.H. Cho, B.W. Lee, J.Y. Park, K.M. Cho, I.M. Park, Effect of Mn addition on corrosion properties of biodegradable Mg-4Zn-0.5Ca-xMn alloys, J. Alloys Compd. 695 (2017) 1166–1174.

ACKNOWLEDGEMENTS: Partial support has also been provided by the Department of Materials Science and Engineering at The Ohio State University. The authors are grateful to Profs. Kyoung Hyup Nam and Ik Min Park for their contributions. Daehyun Cho was at Pusan National University for the early phase of this study.

Influence of micro-blasting on biodegradable iron-based stent structures

B Paul[1], A Hofmann[2], M Otto[1], U Wolff[3], C Reeps[2], J Hufenbach[1,4]

[1] Institute for Complex Materials, Leibniz IFW Dresden, Dresden, Germany, [2] Division of Vascular and Endovascular Surgery Department for Visceral-, Thoracic and Vascular Surgery, Medical Faculty Carl Gustav Carus and University Hospital Carl Gustav Carus Dresden, Technische Universität Dresden, Dresden, Germany, [3]Institute for Metallic Materials, Leibniz IFW Dresden, Dresden, Germany, [4]Institute of Materials Science, Technische Universität Bergakademie Freiberg, Freiberg, Germany

INTRODUCTION: Laser powder bed fusion (LPBF), the dominating metal additive manufacturing process based on a layer-by-layer technique, is very attractive for Fe-based alloys to fabricate customized implants with complex geometries and to tailor materials' properties. [1] It is well known that LPBF-processed surfaces exhibit a process-immanent high roughness due to partially molten particles. One main challenge presents the surface treatment for such biodegradable materials. In this study, as-built Fe-30Mn-1C-0.02S generic stent structures were sandblasted by glass beads and corundum particles to reduce the roughness. The influence of the surface topography on smooth muscle cells was investigated.

METHODS: Spherical powders of Fe-30Mn-1C-0.02S (in wt%, FeMnCS) were processed with a SLM 250 HL device (SLM Solutions Group AG) to fabricate generic stent structures [2]. Stent surfaces were treated by micro-blasting using glass beads or corundum. Microstructural characteristics were investigated by SEM combined with EBSD, as well as by micro-computed tomography analysis. Compositional elements were measured with EDX. Surface topographies were analyzed by AFM and light microscope. Smooth muscle cells were cultured on those different surfaces for 24 h.

RESULTS: Stent surfaces were clearly smoothened at the macrolevel by micro-blasting with spherical glass beads as well as with irregular corundum particles (Fig. 1). At the nano level, a slightly different pattern emerged. Due to the irregular shape of the corundum particles, Rq (159.9 nm) of those stent surfaces was much higher compared to Rq of the surfaces treated by micro-blasting with glass beads (88.5 nm). Residuals of the main components were found at the surface of the stent, the oxides of Si, Na and Ca on surfaces micro-blasted with glass beads and Al_2O_3 on the surfaces micro-blasted with corundum. The influence of the different roughness was also visible in cell adhesion.

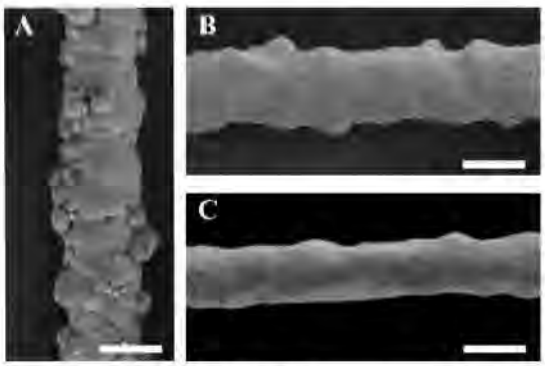

Fig. 1: SEM images of FeMnCS stent struts: (A) as built and after micro-blasting with (B) glass beads and (C) corundum particles (scale bars equal 100 µm).

DISCUSSION & CONCLUSIONS: For clinical application of LPBF-processed stents, a rather smooth surface is essential for e.g. placing the stent by a catheter without harming the vessel. One method for surface smoothing is the mechanical process of micro-blasting, which was applied. The reduction of roughness due to partially molten particles is clearly visible. At the nano level, the higher roughness of micro-blasted surfaces with corundum is of high interest, since endothelial cells favour a certain roughness. As shown for endothelial cells [3], also smooth muscle cells seem to adhere on the as-built stent surface. However, the two different micro-blasted stent surfaces generated a difference in cell adhesion, which will be investigated in more details.

REFERENCES: [1] A.A. Zadpoor (2019) *J. Mater. Chem. B* **7**:4088-4117. [2] J. Hufenbach, J. Sander, F. Kochta, S. Pilz, A. Voß, U. Kühn, A. Gebert (2020) *Adv Eng Mater* 2000182. [3] B. Paul, A. Lode, J. Hufenbach et al. (2022) *ACS Appl Mater Interfaces* **14**:439-451.

ACKNOWLEDGEMENTS: Funding of this work by Leibniz IFW Dresden is gratefully acknowledged.

Influence of Mn content on the chemical composition, electrochemical behavior, and morphology of oxygen plasma immersion implanted FeMnC alloys

LM Andrade[1], C Paternoster[1], P Chevallier[1], D Mantovani[1]

[1] Laboratory for Biomaterials and Bioengineering, CRC-I, Department of Min-Met-Materials Eng., & University Hospital Research Center, Regenerative Medicine, Laval University, QC City, Canada

INTRODUCTION: In the past two decades, FeMnC-based alloys have been investigated as promised biodegradable implant materials for cardiovascular and orthopedic applications[1]. Many strategies were developed to control the ambivalent progress achieved in the past years: outstanding mechanical properties and a slow degradation rate compared to Zn and Mg-based alloys[2]. In addition, it was demonstrated that Mn-oxides could hinder cell attachment for the first 1-7 days in contact with the body[3]. In contrast, Fe-oxides, mainly Fe-O, suggested an enhancement in cell viability for the same period[4]. Plasma techniques can effectively be used for surface modification; oxygen plasma immersion ion implantation (O-PIII) was already implemented, allowing the tuning of the surface properties of several alloys. The present work analyzed the chemical composition, surface morphology, and corrosion behavior of pure iron (Fe), Fe-5Mn-0.4C (Fe-5Mn), and Fe-13Mn-1.2C (Fe-13Mn), after an O-PIII treatment. Due to space reasons, just the influence of oxygen on Fe and Fe13Mn substrates is presented herein.

METHODS: 1 cm^2 substrates were mechanically polished and oxidized by a PBII-300 plasma system (Plasmionique, Varennes, QC, Canada) consisting of a radio frequency inductively coupled plasma reactor connected to a pulsed negative high voltage switch. Pure O_2 (99.995% pure, Linde Gas, Canada) was used as implantation gas with a feeding flow of 10 sccm. The substrates were implanted with a pulsed bias of $U_{bias} = -10$ kV. The chemical composition of the modified surfaces was assessed by X-ray Photoelectron Spectroscopy (XPS). In addition, electrochemical impedance spectroscopy (EIS) measurements were carried out for implanted samples in modified Hanks' solution at 37°C. Impedance spectra were collected from 100 kHz to 0.1 Hz with 5mV perturbation amplitude. The surface features were also investigated by SEM and EDS, to put in evidence the specific morphology of the materials before and after implantation.

RESULTS: Fig 1. a shows the chemical composition assessed by EDS line scan for Fe condition after EIS analysis. A distinguished interface can be observed at the distance point of 1500 µm. A higher amount of oxygen (47.6 ± 1.5 at.%) was detected in the corroded area (III). Other elements such as Cl, P, and F were found as well for this region. For the area analyzed between 1500 – 2225 µm, less O and more Fe were found, as expected, for a pure Fe concentration. XPS surveys of oxygen implanted samples showed a higher oxygen content for Fe13Mn than for Fe (52.2 ± 1.5 at.% and 47.6 ± 1.3 at.%, respectively). Surveys also revealed the appearance of C (4.5 ± 1.4 at.%) for O-Fe. Fig. 1b showed a phase angle higher than 55 ° for low frequencies, in the case of untreated conditions, Fe and Fe13Mn, while a phase angle lower than 30° for high frequencies was measured for O-Fe13Mn. Contrarily, O-Fe presented a plateau at 80° for low frequencies.

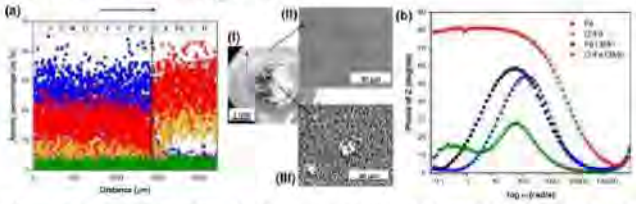

Fig 1: (a) Surface chemical composition (b) and Bode plots for untreated and treated Fe and Fe13Mn analyzed in Hanks' modified solution at 37 °C.

DISCUSSION & CONCLUSIONS: Mechanically polished conditions showed a similar behavior when tested in Hanks' modified solution. However, after oxygen plasma implantation, two different specific trends were observed: a more capacitive behavior, evidenced by a larger phase angle, as it was observed for O-Fe which suggests the formation of a more stable and denser oxide layer, confirming an improved corrosion resistance. In contrast, O-Fe13Mn demonstrated a lower resis-tance to the electrolyte penetration compared to all the other considered conditions. Indeed, the Mn content facilitates the formation of Fe and Mn oxides, at the same time that led to a less dense and resistant surface.

REFERENCES: [1]H. Han et al. (2018) Mater. Today. 23 pp. 57–71. [2] F. Witte, A. Eliezer (2012) Degrad. Implant Mater, pp.93–109. [3]S. Loffredo et al. (2021) Bioact. Mater. [4]N. Zhu et a. (2009) Surf. Coat. Technol. 203 pp 1523-1529.

ACKNOWLEDGEMENTS: DM was and is supported by NSERC-Canada and holds a Canada Research Chair Tier I.

Surface modifications of pure Zinc by plasma immersion ion implantation surface oxidation for biomedical applications

S Ould Mohamed[1], H Agbe[1], C Paternoster[1], A Sarkissian[2], D Mantovani[1]

[1]*Lab Biomaterials and Bioengineering, CRC Tier I, Dept Min-Met-Materials Engineering & CHU de Québec Research Center, Division of Regenerative Medicine, Laval University, Quebec City, Canada;*[2] *Plasmionique Inc., Varennes, QC, Canada*

INTRODUCTION: The development of zinc and its alloy as bioresorbable metals for biomedical applications has attracted significant interest in recent times. Although their biological behavior meets the minimum requirements for implant device applications [1], their corrosion behavior leaves much to be desired [2]. To modify corrosion and surface properties, plasma immersion ion implantation (PIII) surface modification appears interestingly attractive, for example with the use of oxygen. This surface modification technique is currently used for many applications [3], and it finds practical use in the treatment of alloys for biomedical applications, to modify corrosion rates, surface properties, element release, etc. [4, 5]. The aim of this exploratory work is to study the effect of ion implantation energy and time (in oxygen atmosphere) on the morphology, surface properties and corrosion behavior of pure zinc. In the present study, the relationship between the implantation parameters and the final surface features are studied, trough different complementary characterization techniques.

METHODS: Pure cold rolled Zinc was used to produce 10 mm x 10 mm x 1 mm samples. Specimens were then mechanically polished, followed by a treatment in an oxygen PIII system. An antenna power of 300 W was used, as well as a pulse repetition rate of 1000 Hz and a feeding rate of 10 sccm.The PIII surface modification was performed for two different implantation times (30 min and 60 min) and three different potentials (-1, -5 and -10 kV). The chemical composition and morphological features, before and after PIII treatment, were characterized using scanning electron microscopy (SEM), X-ray electron photo-spectroscopy (XPS), and contact angle (CA). Corrosion behavior was subsequently performed using potentiodynamic polarization (PDP) and electrochemical impedance spectroscopy (EIS) techniques in a three-electrode system and modified Hanks' balanced salt solution.

RESULTS: Figures 1(a)-(b) show the SEM surface morphologies of treated zinc. Compared to the pure Zn, oxide layer forms with different morphologies. The CA value generally decreased after treatment (from ~100° to ~ 65°); this behavior was attributed to the change in the chemical composition of the surface and to the roughness modification. XPS profiling and high-resolution analyses evidenced a C removal from the surface after treatment, and the formation of Zn oxides and hydroxides. For 30 min-10 kV treated samples, uniform and homogeneous oxide layer was observed (shown in fig.1 (b)). On the other hand, clusters of isolated crystalline zinc oxides, were noticed for 10 kV- 60 min samples. Also, preliminary results from both PDP and EIS suggest a higher corrosion rate for PIII treated Zn compared to pure Zn for certain implantation conditions. A higher degradation rate has been achieved for some PIII conditions compared to pure Zn.

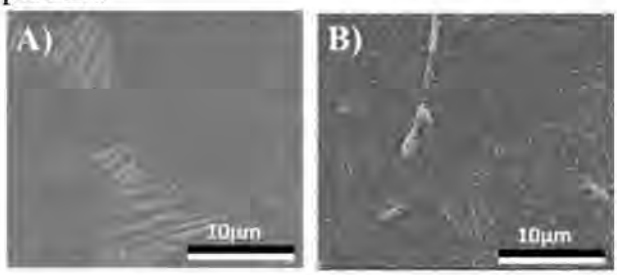

Fig. 1: Surface morphology: (a) Pure zinc; (b) PIII-30min-10kV.

DISCUSSION & CONCLUSIONS: The surface properties of oxygen implanted pure Zn changed in a considerable way as a function of the implantation parameters. As Zn shows a lower sputtering yield compared to other metals used in biomedical applications, the effects of surface re-sputtering and gas penetration played a relevant role in the morphological surface change.

REFERENCES: [1] P. K. Bowen *et al*, *Adv. Healthc. Mater 2016* (5)112. [2] C. Díaz, J. W *et al. Surf. Coat. Technol 2014* (256) 59. [3] C C Bortolan *et al, Biointerphases* 2020 (15) 0410. [4] V. M. C. A. Oliveira *et al.* ,2017 (109) 157 [5] Panel R. C. Shivamurthy & al, *Woodhead Publ. Ser. Met. Surf. Eng.*, pp.177–287,2012

ACKNOWLEDGEMENTS: DM was and is supported by NSERC-Canada and holds a Canada Research Chair Tier I.

ECAP processing influence on the mechanical properties and the bacterial activity of Zn-2Ag alloys

C. García-Mintegui[1], I. S. Goncharov[2], L. Ortiz-Membrado[1], E. Jimenez-Piqué[1], M. Vedani[2], J.L. Cortina[1], M. Pegueroles[1]

Dept. of Materials Science and Engineering, UPC, Barcelona, Spain

[1] *Dept. of Materials Science and Engineering, UPC, Barcelona, Spain.* [2] *Dept. of Mechanical Engineering, Politecnico di Milano, Milan, Italy.*

INTRODUCTION: Zinc (Zn) alloys are potential candidates for biodegradable implants. However, mechanical anisotropy and bacterial infection are risks factors for implant failure [1,2]. In this work, equal-channel angular pressing (ECAP) was performed on Zn-2Ag alloy and the mechanical isotropy and antibacterial activity were evaluated.

METHODS: Cold-rolled Zn-2Ag (2 wt.% Ag) bar (GoodFellow, UK) underwent one (E1) and two (E2) ECAP cycles. ECAP was performed with a 90º internal angle via route B_C at RT. The microstructure was observed by FEG-SEM, XRD, and EBSD. Mechanical characterization was carried out by tensile tests, Vickers hardness, and nanoindentation. Electrochemical behaviour was evaluated by PDP and immersion tests in Hanks' solution (37 ºC; pH 7.4). The antibacterial effect was assessed after 2 h of *S. Aureus* adhesion.

RESULTS: The microstructure of the alloys consisted of a Zn matrix and an $AgZn_3$ secondary phase. EBSD confirmed the grain refinement after ECAP (Fig. 1a). UTS and YS decreased from 125 ±1 MPa and 100 ± 7 MPa to 81 ± 3 MPa and 52 ± 4.2 MPa, respectively, after 2 ECAP cycles; and superplasticity was reported. Similar micro-hardness in transversal (46.7 ± 0.7 HV) and longitudinal (45.5 ± 0.8 HV) sections of the E2 suggested isotropic behaviour, also confirmed by the nanoindentation results, with a homogeneous hardness distribution after ECAP cycles (Fig. 1b).

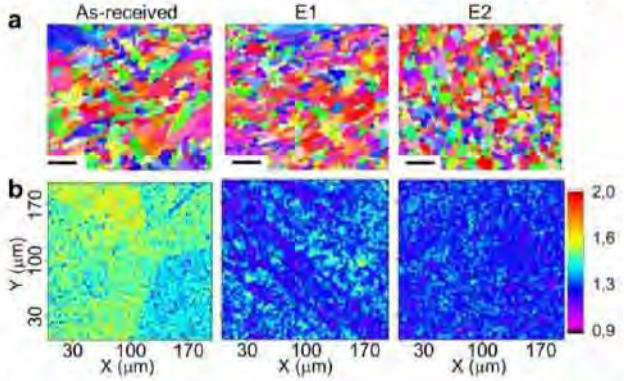

Fig. 1: (a) EBSD-IPF maps (bar: 5 µm) and (b) maps of hardness of the samples (bar: GPa).

Similar degradation behaviour was observed from PDP and immersion tests in Hanks' solution, with a calculated corrosion rate by weight difference of approximately 90 µm/yr. Bacterial assay, Fig. 2, showed a decrease of adhered *S. Aureus* onto the Ag-containing alloys' surfaces compared with inert Ti or pure Zn. The E2 samples showed an excellent antibacterial effect.

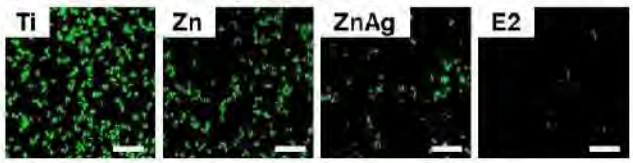

Fig. 2: Live-dead staining of S. Aureus after 2h of adhesion on the different surfaces. Scale bar: 20 µm.

DISCUSSION & CONCLUSIONS: The high formability of Zn-2Ag alloy allowed to perform ECAP at RT without recrystallization of Zn grains. The decrease in tensile properties may be due to the activation of non-slip deformation mechanisms of Zn-2Ag alloy [3]. Therefore, E2 would not be suitable for load-bearing implants but still meets the criteria for other wound-closure applications. The excellent formability provides proper knot security for wires. Mechanical isotropy was achieved after ECAP processing, fundamental to the performance of the final implant. Even though no significant corrosion behavior was observed in Hanks' solution, Zn-2Ag and E2 samples had different responses in contact with bacteria. *S. Aureus* adhered to the degradation products of Zn-2Ag, whereas no bacteria agglomeration was observed on E2. Overall, the high formability, mechanical isotropy, and outstanding antibacterial activity make E2 alloy interesting for suture applications.

REFERENCES: [1] M. Motoyoshi, et al (2009) *Int J Oral Maxillofac Surg* **38(9)**:972-977. [2] B. Aslam et al (2018) *Infect Drug Resis* 11:1645-1658. [3] W. Bednarczyk, et al (2019) *Mater. Sci. Eng. A.* **748**:357-366.

ACKNOWLEDGEMENTS: Financial support was received from, MINECO/FEDER, (Grant No. RTI2018-098075-B-C21) C.G.-M. thanks AGAUR for FI Scholarship.

Embrittlement of thin magnesium wires during PEO coating

L Pricolo[1], T Imwinkelried[1]

[1] RMS Foundation, Bettlach, Switzerland

INTRODUCTION: Magnesium meshes might be used to reinforce calcium phosphate cements and to extend their application range in osteosynthesis.

METHODS: Magnesium alloy LZ 11[1] wires were prepared by vacuum induction melting, extrusion and conventional wire drawing by Fort Wayne Metals. Two lots were provided: Ø 0.45 mm annealed wire and Ø 0.2 mm cold worked wire. The wires were coated with magnesium phosphate by plasma-electrolytical oxidation (PEO) as a single wire and as a woven mesh using direct current[2].

In-vitro degradation tests[3] were carried out in simulated body fluid (SBF) with the wires under tension and with non-loaded meshes. Topographies of non-coated and of coated wires were measured using white light interferometry (S neox, Sensofar).

RESULTS: Both wire diameters could be coated in a batch process. The Ø 0.45 mm wire could be knotted before and after the coating process (Figure 1). The Ø 0.2 mm thick wire showed signs of embrittlement after the coating and could no longer be used for knotting or weaving.

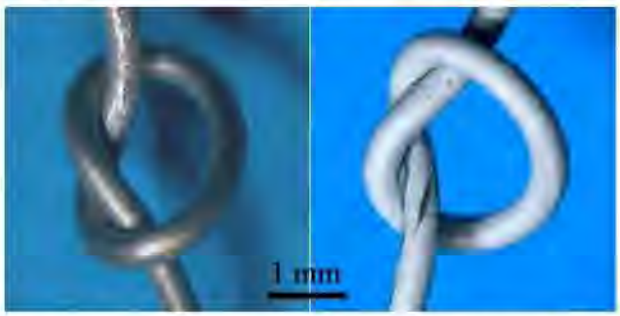

Fig. 1: Knotting of a Ø 0.45 mm magnesium wire without (left) and with PEO coating (right).

Witness plates (WP) at the end of a 2 m long wire, contacted and suspended by a single wire (Figure 2) were used to check the coating thickness. For the thicker wire, the coating thickness stayed at about 11 µm. At the end of the thin wire, the coating thickness was reduced to 3.5 µm as the electrical resistivity increased by several orders of magnitude.

The *in-vitro* degradation of the wires wrapped around a floating holder showed failure of all wires within 5 days of immersion in SBF (presumably 5 - 10 times faster than *in-vivo*). Time to failure of the coated wires was slightly delayed compared to the non-coated wires.

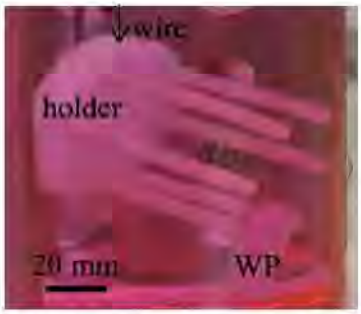

Fig. 2: PEO-bath with a suspended holder (arrow) and witness plate (WP) at the end of 2 m of wire.

The topography measurements revealed a significant increase of the roughness for witness plates and wires with a coating (Table 1).

Table 1. Roughness parameter Ra of non-coated and coated magnesium samples

Sample	Non coated	coated
Witness plate	0.01 µm	3.0 µm
Wire Ø 0.45 mm	0.07 µm	0.4 µm

DISCUSSION & CONCLUSIONS: The PEO coating of magnesium wires led to an increase in surface roughness and to an embrittlement of the thinner wire when using the same coating parameters as for thicker, machined parts. Those parameters need to be adjusted in order to obtain thinner and smoother coatings.

The coating of thin single wires was different from more massive parts as electrical resistance became a limiting factor. These findings also need to be taken into account when coating woven meshes.

REFERENCES: [1]Patent WO 2020/247382A1 – Magnesium based absorbable alloy. [2]Patent WO 2013/070669A1 - Lean electrolyte for biocompatible coatings on magnesium implant materials. [3]T. Imwinkelried (2015) in ISBN 978-1-78242-077-4, 311-329.

ACKNOWLEDGEMENTS: Fort Wayne Metals, Fort Wayne, IN 46809, USA is acknowledged for providing the wire material for this study.

Surface modification of a biodegradable Mg-Y-Zn-Mn alloy by oxygen plasma immersion ion implantation

M Shekargoftar[1], S Ravanbakhsh[1], VS Oliveira[1], C Paternoster[1], F Witte[2] and D Mantovani[1]

[1] Laboratory for Biomaterials and Bioengineering, *CRC-I, Department of Min-Met-Materials Eng., & University Hospital Research Center, Regenerative Medicine, Laval University, QC, Canada*

[2] *Department of Prosthodontics, Geriatric Dentistry and Craniomandibular Disorders, Charité Universitätsmedizin, Berlin, Germany.*

INTRODUCTION: Mg alloys are considered as promising biodegradable and osteoconductive biomaterials. In clinical applications, Mg-based alloys have to show appropriate surface properties and corrosion behavior[1]. In addition, degradation of Mg alloys comes with producing hydrogen gas which needs to be minimized[2]. Recently, several surface modification strategies have been used for Mg-based alloys[3]. A promising strategy proposed for the modification of Mg alloys is based on plasma. Plasma contains highly energetic and mostly reactive species (ions, electrons radicals, etc), many of which induce physiochemical changes upon collision with a surface[4]. Over time, different plasma sources have been developed and one of the most promising ones is plasma immersion ion implantation (PIII). In this study, Mg-2Y-1Zn-1Mn (MWZN211) was treated by PIII in an oxygen environment. The purpose of this work was to study the effects of PIII treatment on the surface properties as well as the corrosion behavior of the Mg-alloys after treatment.

METHODS: PIII treatments were carried out on mechanically polished substrates to study the effects of different parameters. The chemical composition, morphology, and microstructure of the samples were analyzed by using x-ray photoelectron spectroscopy (XPS), scanning electron microscopy (SEM), energy-dispersive x-ray spectroscopy (EDS), and X-ray diffraction (XRD). The electrochemical properties of the samples were evaluated using a Mini-cell System (MCS). The Mini-cell was filled with 3 mL of Hanks' buffered saline solution (HBSS) from Gibco. Open circuit potential was registered during the initial and then potential was kept at this value for linear scan voltammetry (LSV).

RESULTS: Figure 1 presents the results of LSV curves along with an inserted table of electrochemical parameters of the MWZN211. It was noticed that after PIII the spectrum shifted to positive potential values compared to the untreated sample. In addition, O-PIII treatment resulted in a lower corrosion current density. The polarization resistance (R_p) values were measured from the extrapolation of the LSV. It was observed that the R_p decreased from ~ 1432 ohm cm^2 corresponding to the untreated sample to ~ 4334 ohm.cm^2 for the O-PIII-treated sample. The calculated corrosion rate (Crate) showed in the inserted table. The Crate values for untreated and O-PIII treated were ~0.23 mm/y and ~ 0.07 mm/y, respectively. The formation of a rich Y oxide layer after PIII was evidenced by XRD; the surface O enrichment, which is also detected by EDS and XPS, was attributed to the formation of amorphous MgO. The different plasma treatments modifed not only the chemical composition of the syrface, but also their roughness, which was generally increased by the implantation process.

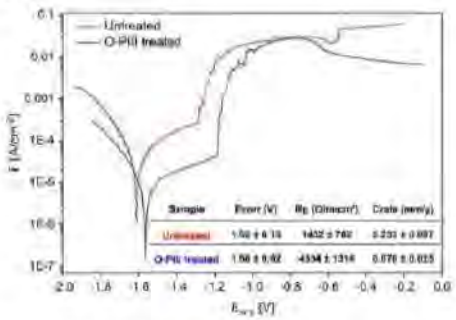

Fig 1: Typical LSV and electrochemical parameters of Mg alloys before and after an O-PIII treatment.

DISCUSSION & CONCLUSIONS: The higher corrosion resistance improvement was attributed to the formation of an oxide layer on the surface. The PIII treatment, in spite of the different applied parameters, were responsible for the segregation of some elements on the samples surfaces, expecially Y. A limited set of treatment parameters, modified the corrosion pattern of the studied alloy due to the formation of new phases.

REFERENCES: [1.] Bonithon R et al.. *Acta Biomater.* 2021;127:338-352. [2.] De Braga et al. *Surf Coat Technol.* 2022;433:128078. [3.] Zheng YF et al. *Mater Sci Eng R Reports.* 2014;77:1-34. [4.] Baranov O et al. *Mater Horizons.* 2018;5:765-798.

ACKNOWLEDGEMENTS: This work was supported by NSERC-Canada-Alliance and Prima-Quebec- partnership funds. DM holds a Canada Research Chair Tier I.

Electrical resistance testing for biodegradable magnesium implants

S. Meyer, B. Wiese, N. Hort, R. Willumeit-Römer
Institute of Metallic Biomaterials, Helmholtz-Zentrum Hereon, Max-Planck-Str. 1, Geesthacht 21502, Germany

INTRODUCTION: Electrical resistance testing offers a fast and non-destructive method, which is very sensitive to crystal defects and microstructural features. Mechanically introduced strain leads to work hardening and modified properties. Monitoring these properties can ensure safe use in quality control of implants.

METHODS: Pure Mg (99.98%) with addition of 0.45, 0.91 and 1.42 at.% Ag (99.99%) were cast into billets and extruded into 1 mm wire. Cold drawing was applied to reduce the wire diameter down to a final of 0.65 mm (0.48 mm for Mg-0.45Ag). Drawn wires were annealed at 425 °C for 30 s [1].

The 4-point probes method enables the compensation of the contact resistance between probes and sample. A model 6221 source and Model 2182 Nanovoltmeter from Keithley (Tektronix GmbH, Solon, USA) was used to measure the resistance over a length of 100 mm. An alternating current of 10 mA was used to minimize ohmic heating and resulting resistance increase.

RESULTS: The true strain is calculated for one or several drawing passes by the initial A_0 and final wire cross section A_1:

$$\varepsilon = ln(A_0/A_1) \quad (1)$$

The resistivity of the annealed state for each silver concentration is subtracted from the measured resistivity after wire drawing. In Figure 1 the resistivity increase above the annealing state is shown. The resistivity of the four strain states and of three Ag concentration, but same strain state were fitted and are displayed in Table 1.

Table 1. Fitted linear Resistivity increase by silver content and unit strain.

	Ag content [nΩm/at.%]	Strain [nΩm/1]
Mg wire	6.58 ± 0.06	8.96 ± 0.17

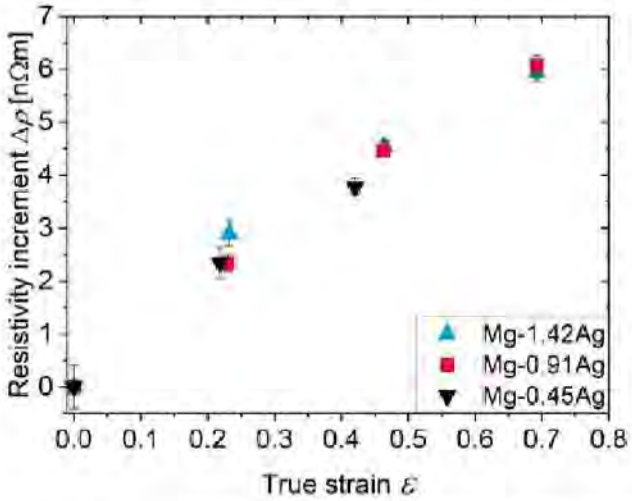

Fig. 1: Resistivity increase from the annealed state with increasing true strain.

DISCUSSION & CONCLUSIONS: The Ag atoms perturbate the lattice of the Mg matrix due to their modified valence band. Following Nordheims rule the resistivity increase is linear with solid solution content. The proportionality displayed in Table 1 is a bit lower than the value of 7.5 nΩm/at.% reported previously [2].

The mechanical strain introduced by wire drawing forces the formation of crystal defects like dislocations that interrupt the periodicity of the line potentials. The increase in resistivity is proportional to the true strain by the factor of 8.96 nΩm per unit strain, regardless of silver content. This indicates equal work hardening behaviour due to dislocation density and makes the magnitude of the effect potentially transferable to other alloy systems [1].

The measuring principle is fast, non-destructive and allows to allocate Mg wires to alloy systems, as well as deformation states.

REFERENCES: [1] S. Meyer, B. Wiese, N. Hort, and R. Willumeit-Römer (2022) *Characterization of the Deformation State of Magnesium by Electrical Resistance* Scr. Mat. 215: 114712. [2] E. I. Salkovitz, and A. I. Schindler (1955) *Resistivity of Dilute Magnesium Alloys* Phys. Rev. 98, 2: 543–44.

Electroforming process for Fe-Mn alloy fabrication using deep eutectic solvents

V.F. Sales[1,2], C. Paternoster[1,2], D. Mantovani[1,2], G. Kolliopoulos[2]

[1] *Lab Biomaterials and Bioengineering, CRC-I, Dept Min-Met-Mater Eng. & CHU de Quebec Research Center, Division of Regenerative Medicine, Laval University.*

[2] *Department of Mining, Metallurgical and Materials Engineering, Université Laval, Quebec City, G1V 0A6, Canada.*

INTRODUCTION: Reabsorbable alloys are raising the interest of the scientific and technological community for the production of biomedical implants, such as coronary stents and intraosseous screws [1]. Current processing routes for biomedical alloys foresee the casting of the initial alloy, a series of plastic deformation steps and often some thermo-mechanical processes [2]. This scheme can be replaced with other production techniques, especially when materials or devices with advanced features are needed [3]. Electroforming is a well-established technique for Fe-based alloy thin component production; in this case, the mainly used solvent is water. Nevertheless, the deposition of certain metals (i.e., Mn, Al, and Mg) from aqueous solutions is not an optimal process, because their reduction potential is lower than the reduction potential of the solvent. Recently, deep eutectic solvents (DESs) have been proposed as a promising alternative solvent for electrochemical processes. The present work proposes the uses of three deep eutectic solvents for the deposition of Fe-Mn alloys; the relationship between the solvent chemical and physical properties and the obtained deposited films are studied.

METHODS: In 1:2 molar ratio mixtures of choline chloride and ethylene glycol (ChCl/EG), choline chloride and glycerol (ChCl/Gly), and choline chloride and urea (ChCl/Urea) 0.1M $FeCl_2$ and 0.05M $MnCl_2$ were added. Electrodeposition was carried out on mechanically polished titanium substrates. Cyclic voltammetry experiments were carried out in a range of temperatures; a potential range from +2.0 V to -2.0 V was scanned at 20 mV/s. Viscosity, solvent chemical stability, and conductivity in the range 20 – 80°C were studied, with different amounts of diluted salts. Scanning electron microscopy (SEM) and energy dispersive x-ray spectrometry (EDX) were used for the analyses of the deposited alloys.

RESULTS: Cyclic voltammetry tests were performed to identify the reduction potential of Fe and Mn for each DES. The conductivity of the considered solvents was affected by temperature, reaching a maximum in the range 5 – 10 mS/cm for T=80°C. The viscosity for T=80°C was in the range 10 to 100 mPa·s, depending on the salts in solution. Figure 1 shows the obtained Fe-Mn deposits after electrodeposition. Table 1 shows the atomic percentage of Fe and Mn in the deposit.

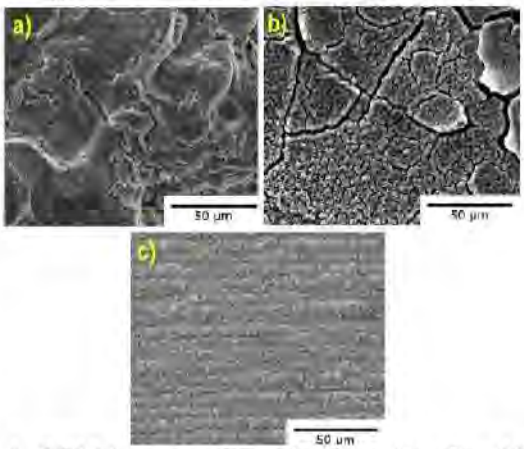

Fig. 1: SEM images of Fe-Mn deposits after 30 min deposition at 80°C in ChCl/EG (b) ChCl/Gly, and (c) ChCl/Urea with dissolved Fe and Mn salts

Table 1. Atomic percent of Fe and Mn of the electrodeposited Fe-Mn alloys obtained with EDX

DES	Fe (at%)	Mn (at%)
ChCl/EG	87.17 ±1.52	12.83 ±1.52
ChCl/Gly/	81.27 ± 5.95	18.73 ± 5.95
ChCl/Urea	50.29 ± 3.11	49.71 ± 3.11

DISCUSSION & CONCLUSIONS: The use of ChCl/Urea allowed the formation of coatings with and homogeneous distribution of Fe and Mn and a good adhesion to the substrate. The system presented a large potential window, allowing the deposition under a relatively large potential interval. Further development to optimize the deposition condition for higher thicknesses and higher deposition rates are needed.

REFERENCES: [1]M. Schinhammer, *Mater. Sci. Eng. C*, vol. 33, no. 4, pp. 1882–1893, 2013. [2]B. D. Ratner, *An Introduction to Materials in Medicine*, 2004th ed. Boston, MT, USA: Elsevier Academic. [3]M. Moravej and D. Mantovani, *Int. J. Mol. Sci.*, vol. 12, no. 7, pp. 4250–4270, 2011.

ACKNOWLEDGEMENTS: D.M. was supported by NSERC-Canada and holds a Canada Research Chair Tier I.

In situ thermo-mechanical processing in a synchrotron beam of a Mg-2Y-1Zn-1Mn alloy

D. Tolnai*[,1], S. Gavras[1], A. Stark[2], M. Bartosch[3], F. Witte[4], N. Hort[1,5]
[1] Institute of Metallic Biomaterials, Helmholtz-Zentrum Hereon, Geesthacht, Germany [2]Institute of Materials Physics, Helmholtz-Zentrum Hereon, Geesthacht, Germany [3]Biotrics bioimplants AG, Berlin, Germany [4]Department of Prosthodontics, Geriatric Dentistry and Craniomandibular Disorders, Berlin, Germany [5]Institute of Product & Process Innovation, Leuphana University Lüneburg, Lüneburg, Germany

INTRODUCTION: Due to its biodegradability and suitable mechanical properties Mg is used as a metallic biomaterial in implant applications.[1] The addition of Y and Zn as alloying elements is an efficient solution to set the mechanical property profile for this application. The aim of this study is to characterize the thermo-mechanical response of an extruded WZM211 alloy with minor additions of Ca under tensile and compressive load at room and elevated temperatures with in situ synchrotron radiation diffraction, thus show the potential of this technique as an aid in materials processing.[2]

METHODS: Pure elements were mixed to cast the alloys. The ingots were subsequently extruded from the initial diameter of 150 mm to 12 mm. The samples for the metallographic investigations were ground, then polished and etched using a picric and acetic acid solution. The in situ synchrotron radiation experiments were performed on cylindrical samples of 5 mm and length of 10 mm for compression and on planar samples of dog bone shape geometry with the thickness of 3 mm for tension, respectively. The diffraction was performed at the P07 beamline of PETRA III, DESY. A monochromatic beam with the energy of 100 keV and with a cross section of 1×1 mm^2 was used. Diffraction patterns were recorded with a PerkinElmer 1621 flat panel detector that was placed at a sample-to-detector distance of 1652 mm from the specimen for the compression tests and 1554 mm for the tensile tests. The acquisition time for each image was 0.1 s. The specimens were tested with a DIL 805A/D dilatometer and deformed with an initial strain rate of 10^{-3} s^{-1} at RT, at 200 °C and at 350 °C, respectively. The Debye-Scherrer rings were analysed using the Fit2D® software.

RESULTS: The results of the mechanical test (Fig. 1) show a higher UCS than UTS at every test temperatures. On the compression curves at RT and 200 °C an inflection can be observed, that can be attributed to twin formation. The diffraction results show a simultaneous change in the intensities of the 10.0 and 00.2 peaks that confirms the twin formation during compression.

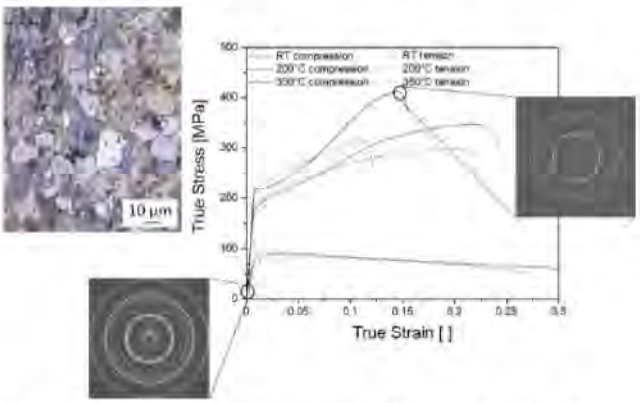

Fig. 1: Deformation curves under tension and compression at different temperatures, with corresponding examples of diffraction patterns.

At 350 °C no pronounced twinning could be observed but the diffraction results indicate that grain rotation and sub-grain formation takes place during the deformation.

DISCUSSION & CONCLUSIONS: The microstructure of the material consists of fine Mg grains after extrusion, while the alloying elements are dissolved in the matrix. The mechanical tests and diffraction show a different deformation behaviour in tension and compression, whereas twinning takes place in compression at RT and 200°C because the grains are oriented in a preferential manner. In tension dislocation slip is the main deformation mechanism at these temperatures. At 350°C in both cases dynamic recrystallization takes place.

REFERENCES: [1] T.A. Grünewald, A. Ogier, M. Meischel et al (2016) *Acta Biomat* 31 448-457. [2] D. Tolnai, M-A. Dupont, S. Gavras et al (2019) *Materials* **12** 10.3390/ma122333935.

ACKNOWLEDGEMENTS: The authors acknowledge the DESY for the provision of beamline facilities and the Biotrics bioimplants AG for the provision of the material.

Coupled growth in Zn-based alloys with Mg additions produced by casting in steel mold of square section.

LA Domínguez[1,2], AL Ramírez[2], JS Flores[2], JA Juárez[1], C Paternoster[3], D Mantovani[3].

[1] *Instituto de Investigaciones en Materiales*, [2] *Facultad de Química, Universidad Nacional Autónoma de México, Ciudad de México, México.* [3] *Lab. for Biomaterials & Bioengineering (CRC – I), Laval University, Quebec City, Canada*

INTRODUCTION: Peritectic alloys have an important role in several engineering fields [1], such as Zn-Ag system, which has been demonstrated to be a potential candidate for biomedical applications in recent years [2]. Zn-Ag alloys have been studied previously under non-equilibrium conditions by rapid solidification [3], in addition to ε-$AgZn_3$ and η-Zn phases, it was observed a coupled growth forming a eutectic-like structure. This work studied the effect of Mg addition on the microstructure of Zn-Ag alloy.

METHODS: For the fabrication of the Zn-10.0Ag-1.0Mg (wt.%) alloy, the starting materials (Zn, Ag and Mg with 99.99% purity) were melted in a vacuum induction furnace in alumina crucibles under the protection of Ar atmosphere. For the solidification experiments, the alloy was casted into a steel mold to obtain a plate of 10cm × 10cm × 1cm. The microstructure was observed by scanning electron microscopy (JEOL 7600f) and all microanalyses were carried out with an EDS coupled system.

RESULTS: The microstructure and EDS results are shown in Fig. 1, Table 1, confirming that the microstructure is conformed by the peritectic η-Zn with the presence of a eutectic-like structure rich in Mg, instead of the typical structure formed by ε-$AgZn_3$ dendrites in the peritectic η-Zn phase.

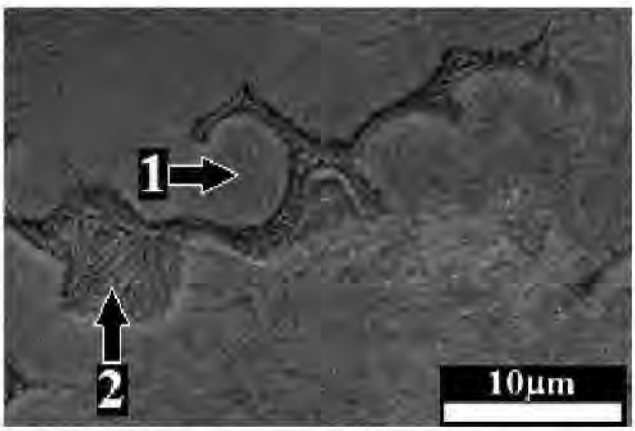

Fig. 1: SEM micrograph obtained from the transversal section of the Zn-10.0Ag-1.0Mg plate.

Table 1. EDS microanalysis from the points marked in Fig. 1 for the alloy under study.

Point	Zn (wt. %)	Ag (wt. %)	Mg (wt.%)	Total
1	90.32	9.68	0.00	100.0
2	92.10	7.28	0.62	100.0

DISCUSSION & CONCLUSIONS: The presence of a eutectic-like structure has been reported previously in a binary alloy with the same composition of silver: Zn-6.3 at. (10 wt.) % Ag as a result of rapid solidification by melt-spinning [4]. Nevertheless, in the present study, the formation of eutectic-like structure is attributed to the following effects: (1) the convection flux during the casting of the system, since it has been established that convection has a strong influence on the development of eutectic-like coupled growth in peritectic systems [5]. (2) the Mg addition to the system Zn-Ag can help to assist the nucleation of the η-Zn phase at multiple sites, when the spacing between nuclei falls inside the stable range of coupled growth spacing, forming a eutectic-like structure. The above agrees with other reports regarding peritectic systems [6]. Thus, the present work, is a contribution to the understanding of the solidification behaviour of peritectic Zn-based alloys, in order to improve the biodegradable materials performance by controlling their casting conditions.

REFERENCES: [1] H.W. Kerr and W. Kurz (1996) *Int Mater Rev* **41**:129-164. [2] A.L Ramírez-Ledesma, L.A. Domínguez-Contreras, J.A. Juárez-Islas et al (2020) *Mat Lett* **279**:128504. [3] W. Xu, Y.P. Feng, Y. Li et al (2002) *Acta Mater* **50**:183-193. [4] W. Xu, D. Ma, Y. Li et al (2002) *Scripta Mater* **44**:631-636. [5] W. Kurz, M. Rappaz, R. Trivedi, (2020) *Inter Mater Rev* **66**:30-76. [6] T.S. Lo, S. Dobler, M. Plapp et al (2003) *Acta Mater* **51**:599

ACKNOWLEDGEMENTS: This work was supported by Programa de Apoyo a Proyectos de Investigación e Innovación Tecnológica (PAPIIT – TA100222) and the Natural Science and Engineering Research Council of Canada.

Microstructure and mechanical stability of biodegradable low-alloyed zinc for biomedical applications

M Wróbel[1], A Jarzębska[1], Ł Maj[1], Ł Rogal[1], P. Petrzak[1], M Kulczyk[2], M Bieda[1]

[1] *Institute of Metallurgy and Materials Science of Polish Academy of Sciences, Krakow, Poland*
[2] *Institute of High Pressure Physics, Polish Academy of Sciences, Warsaw, Poland*

INTRODUCTION: Specific requirements e.g. high mechanical properties, corrosion resistance, no harmful alloying additives, thermal stability are required for biomaterials. Pure and low alloyed zinc is an excellent material for biodegradable devices like coronary and urinal stent or orthopaedic implants due to its perfect corrosion rate [1]. Moreover it performs important functions in the human body e.g. in the immune systems. However, pure zinc has low recrystallization temperature which is about room temperature, and low mechanical properties. Addition of alloying elements, e.g. magnesium can be beneficial for all these parameters. [2]. It was showed that hydrostatic extrusion and magnesium alloying could positively affects mechanical properties [3]. There is still lack of systematic studied on the microstructural and mechanical thermal stability of zinc and zinc alloys, and this topic is the main aim of presented research [4].

METHODS: Zinc-magnesium alloys (0.6 and 1.2 wg.% Mg) were prepared by gravity casting, followed by hot extrusion, and hydrostatic extrusion in 4 passes. To investigate changes in the microstructure of the final material, ex-situ annealing at temperature range from 37 to 150°C and SEM/EBSD after each step were performed. The samples were additionally immersed in Hanks' solution for 7 and 14 days at 37°C to observe changes in the microstructure under conditions close to those of the human body. In order to examine the mechanical properties, a compression test at room temperature was performed after immersion and annealing.

RESULTS: Microstructure after hydrostatic extrusion consists of the fine α-Zn grains and intermetallic phase Mg_2Zn_{11}. Changes in the microstructure of the investigated material after annealing and immersion tests depend on amount of magnesium addition. Microstructure and mechanical properties are stable in the room temperature and after immersion tests.

DISCUSSION & CONCLUSIONS: The microstructure consists of α-Zn and Mg_2Zn_{11} is crucial not only for the mechanical properties of the alloys but also for its stability. The intermetallic phase inhibits the static recrystallization processes in low temperature. Also worth noticing that amount of alloying elements has an influence on the thermal and microstructural stability during annealing. The higher amount of magnesium the better thermal stability. No significant changes in the microstructure after immersion test in Hanks' solution is promising in the context of the application as a biodegradable biomedical material.

REFERENCES: [1] E. Mostaed, M. Sikora-Jasinska, J.W. Drelich, M. Vedani (2018) *Zinc-based alloys for degradable vascular stent applications,* Acta Biomaterialia, Vol 71, 1-23. [2] X. Zhuo, Y. Wu, J. Ju, H. Liu, J. Jiang, Z. Hu, J. Bai, F. Xue (2022) *Recent progress of novel biodegradable zinc alloys: from the perspective of strengthening and toughening,* Journal of Materials Research and Technology, 244-269. [3] W. Pachla, S. Przybysz, A. Jarzębska, M. Bieda, K. Sztwiertnia, M. Kulczyk, J. Skiba (2021) *Structural and mechanical aspects of hypoeutectic Zn–Mg binary alloys for biodegradable vascular stent applications,* Bioactive Materials, Vol. 6, 26-44, [4] G. Li, H. Yang, Y. Zheng, X.-H. Chen, J.-A. Yang, D. Zhu, L. Ruan, K. Takashima,(2019) *Challenges in the use of zinc and its alloys as biodegradable metals: Perspective from biomechanical compatibility,* Acta Biomaterialia, Vol. 97, 23-45.

ACKNOWLEDGEMENTS: The research was partially co-financed by the National Science Centre Polish UMO-2020/39/O/ST5/02692.

Corrosion

Saturday, August 27th 2022

Oxygen consumption during Mg alloy biodegradation is alloy and immersion medium dependent

Berit Zeller-Plumhoff[1,2], Ashwini Rahul Akkineni[3], Heike Helmholz[1], Dmytro Orlov[4], Maria Mosshammer[5], Michael Kühl[5], Michael Gelinsky[3], Regine-Willumeit-Römer[1]

[1] Institute of Metallic Biomaterials, Helmholtz-Zentrum Hereon, Geesthacht, Germany [2] Kiel Nano, Surface and Interface Science KiNSIS, Kiel University, Germany [3] Centre for Translational Bone, Joint and Soft Tissue Research, University Hospital Carl Gustav Carus and Faculty of Medicine of Technische Universität Dresden, Germany [4] Division of Materials Engineering LTH, Lund University, Lund, Sweden [5] Marine Biology Section, Department of Biology, University of Copenhagen, Denmark

INTRODUCTION: Biodegradable magnesium (Mg) alloys are investigated heavily for the application as temporary bone implants. To be able to predict and tailor the degradation behaviour of new alloys, it is pivotal to understand the mechanisms of the biodegradation itself. While the hydrogen evolution equation has long been considered the main cathodic reaction, recent studies have shown that the oxygen reduction reaction can also play a significant role in Mg biodegradation [1,2]. To understand this role in more detail is critical, as prolonged consumption of oxygen following implantation of Mg alloys could maintain a locally hypoxic environment and therefore have a significant impact on tissue healing *in vivo*. In this study we present the evaluation of oxygen concentration during the *in vitro* degradation of three Mg-based alloys in two different immersion media at early time points. Hydrogen evolution was measured for comparison.

METHODS: Discs (Ø 9 mm, height 1.5 mm) of pure Mg, Mg-5Gd and Mg-6Ag were used in this study (n=3). Oxygen-sensitive nanoparticles were mixed into Hank's balanced salt solution (HBSS) and Dulbecco's modified Eagles medium (DMEM). For the degradation experiment 20 µL of the respective medium was placed on each disc and covered by a cover slip, followed by image acquisition for two hours. A ratiometric analysis of the acquired images provided the oxygen concentration distribution on the disc surface over time. The image data was evaluated in Matlab 2020a (The Mathworks Inc., USA) to obtain mean values for the concentration and fit the linear increase over time. In a separate experiment, hydrogen evolution was measured by immersion of the discs in the media for comparison.

RESULTS: Fig. 1 displays the mean oxygen concentration obtained for one disc per alloy and medium, respectively. There are distinct differences in the increase of oxygen concentration over time between the alloys. Apparently, Mg-6Ag consumes more oxygen during degradation than pure Mg and Mg-5Gd, and more so in HBSS. Mg-5Gd shows an intermittent decline during the overall increase in oxygen concentration. At the same time, the hydrogen evolution in Mg-6Ag in DMEM was lowest, yet optical microscopy revealed it to have the strongest surface attack. The hydrogen evolution in Mg-5Gd and pure Mg in DMEM was similar, while it was higher in HBSS for Mg-5Gd than for pure Mg.

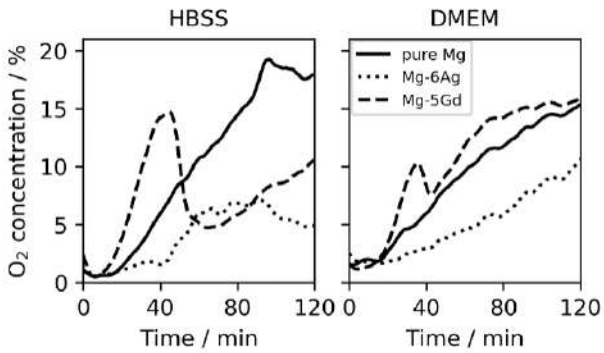

Fig. 1: Mean oxygen concentration for pure Mg, Mg-6Ag and Mg-5Gd in HBSS and DMEM measured using oxygen-sensitive nanoparticles.

DISCUSSION & CONCLUSIONS: Our measurements confirm that the oxygen consumption during Mg alloy biodegradation may be a substantial degradation mechanism, especially for some alloys such as Mg-6Ag. Future studies need to address the oxygen consumption in the longer term and its effect *in vivo*.

REFERENCES:. [1] E.L. Silva *et al.*, ChemistryOpen. (2018). [2] C. Wang, *et al.*, Npj Mater. Degrad (2020).

ACKNOWLEDGEMENTS: We thank Dr. Björn Wiese and Sofie Jakobsen for supporting the preparation of the materials used in this study. BZP acknowledges funding by the Priority Research Area KiNSIS. MK acknowledges funding from the Independent Research Fund Denmark (DFF-8022-00301B).

A higher PBF-LB power gives a higher density but a lower corrosion resistance of Mg-Y-Nd-Zr

Hanna Nilsson Åhman[1,2], Clarence Wahman[1], Pelle Mellin[2], Cecilia Persson[1]
[1]*Department of Materials Science and Engineering, Uppsala University, Uppsala, Sweden*
[2]*Swerim AB, Kista, Sweden*

INTRODUCTION: Large bone defects are extremely challenging to repair, and the drawbacks of auto- and allografts in terms of load-bearing capacity, lack of availability and risk of donor site morbidity calls for further development of the available graft materials[1]. Magnesium (Mg) alloys have shown a lot of promise to this end. In particular, powder extruded Mg-Y-Nd-Zr alloys have successfully been implemented for orthopedic fixtures since 2013, but larger, more complex implants have yet to be developed[2].

Powder Bed Fusion – Laser Beam (PBF-LB) allows for the production of complex structures, designed for increased bone ingrowth, as well as fitting perfectly the patient's defect. Nevertheless, the corrosion rates of Mg alloys processed by PBF-LB remains too high[3]. This study aimed to gain a greater understanding of the influence of the process parameter laser power, on the corrosion behavior of Mg-$Y_{3.9wt\%}$-$Nd_{3.0wt\%}$-$Zr_{0.49wt\%}$.

METHODS: Cylindrical samples (5 mm diameter, 10 mm height) were produced by PBF-LB (EOS M100, EOS, Germany), processing Mg-$Y_{3.9wt\%}$-$Nd_{3.0wt\%}$-$Zr_{0.49wt\%}$ powder (NMD, Germany) of a particle size of 23-64µm. Three sample groups with different laser powers (60W, 80W, 90W) were printed. The other parameters were kept constant (20µm layer height, laser scanning speed 1100 mm/s, and 50µm hatch distance). The surface roughness was measured using an optical system (Alicona Infinity Focus SL, Bruker, U.S.), and the microstructure and composition was evaluated with optical microscopy (OM) (Leica DM, Leica Microsystems, Germany), scanning electron microscopy (SEM) (Sigma 300, Zeiss, Germany), electron diffraction spectroscopy (EDS) (Oxford Instruments, UK) and X-ray diffraction (XRD) (Bruker D8 Discover, Bruker, U.S.).

The corrosion properties were evaluated on as-built samples by immersion in Dulbecco's Phosphate Buffered Saline solution (DPBS D8123, Sigma-Aldrich, U.S.), over a period of 28 days, investigating the volumetric hydrogen evolution, mass change as well as the change in ion concentration in the corrosion media.

RESULTS: The sample printed with 60W exhibited the largest surface roughness (Fig. 1 a). The 60 W samples also contained internal pores >100 µm. The Mg- rare earth intermetallic particles and Y_2O_3 flakes previously observed in Mg-Y-Nd-Zr processed by PBF-LB[3], were present in all samples. However, no difference with regards to their amount, size nor distribution could be established between the samples.

The results from the hydrogen evolution are presented in Fig. 1b), showing an increased hydrogen evolution, and thus an increased corrosion rate, with higher laser power. The ion release and mass change showed a similar trend.

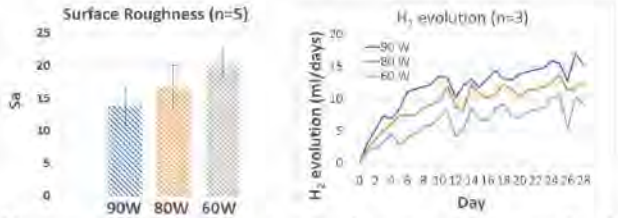

Figure 1: a) Surface roughness of the as-built samples. b) Hydrogen evolution for the as-built samples.

DISCUSSION & CONCLUSIONS: The increased corrosion rates with the higher laser power were unexpected, as larger surface roughness and higher porosity typically leads to higher degradation rates. The higher degradation rates of the 90W samples could be derived from the increased Mg evaporation in these samples, as a result of the higher laser power. This would lead to an increase in the relative amount of intermetallic particles. The higher energy input could also have resulted in growth of the precipitates, increasing their cathodic activity and consequently the corrosion rate of the material. In conclusion, a higher laser power gave a higher degradation rate of the Mg-$Y_{3.9wt\%}$-$Nd_{3.0wt\%}$-$Zr_{0.49wt\%}$ alloy, despite also resulting in lower surface roughness and a denser bulk material.

REFERENCES: [1] Valtanen, R. *et al.* Injury 52, 2021. [2] www.syntellix.de/en/ [3] Suchý, J. *et al.* J. Manuf. Process. 69, 2021.

ACKNOWLEDGEMENTS: Assistance by Lena Thorsson (Exmet AB), and financial support from the Swedish Foundation for Strategic Research (FID17-0028), and Vinnova (2019-05259 and 2019-00029), are gratefully acknowledged.

Microstructural, mechanical and biodegradation properties of as-cast and hot forged Fe-Mn-C alloys

M Otto[1], A Gebert[1], B Paul[1], J Freudenberger[1,2] and J Hufenbach[1,2]

[1] Institute for Complex Materials, Leibniz IFW Dresden, Dresden, Germany. [2] Institute of Materials Science, Technische Universität Bergakademie Freiberg, Freiberg, Germany

INTRODUCTION: For clinical treatment of a variety of soft and hard tissue injuries and diseases the need for bioresorbable metallic materials rises. This can be traced back to their benefit of avoiding revision surgeries or long-term complications effects owing to the materials progressive degradation after giving temporary mechanical support during the tissue healing process. Besides magnesium- and zinc-based systems, iron-based alloys are attractive candidates for such temporary implants [1]. For the latter, Fe-Mn-C alloys present promising materials because of their suitable mechanical properties and excellent processability, especially for vascular implants. An in-depth understanding of the interrelation of the processing route, microstructure and resulting properties flattens the path to tune mechanical properties as well as corrosion behaviour in body fluids. This is of great importance for successful application of the material.

METHODS: Fe-Mn-C alloys were vacuum cast followed by homogenization and hot forging. Scanning electron microscopy including electron backscatter diffraction (EBSD) was utilized for the microstructural characterization. The mechanical behaviour was investigated under uniaxial tensile and compressive load. The corrosion behaviour was analysed by electrochemical methods under hydrodynamic conditions with a rotating disc electrode (RDE) and by using HEPES-buffered saline solution (HBS) with pH 7.4 at 37 °C. The investigation aimed at mimicking physiological conditions for vascular applications.

RESULTS: The microstructural investigation revealed an anisotropic microstructure in the as-cast state. This was homogenised and refined to a mean grain size of 70 µm by the annealing and hot forging treatments, as shown in Figure 1. In both states the microstructure was fully austenitic. The refinement of the microstructure lead to an improved mechanical performance (see Table 1), highlighting the tensile strength and ductility of the twinning induced plasticity (TWIP) Fe-Mn-C-alloys, especially in comparison to the benchmark steel AISI 316 L [2].

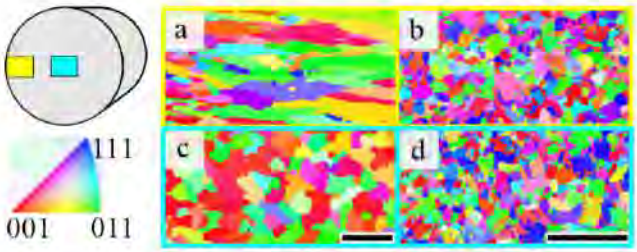

Fig. 1: Inverse pole figure EBSD maps of an Fe-Mn-C alloy. The microstructure is shown in the as-cast (a,c) and hot forged (b,d) state, at the (a,b) outer and (c,d) core region of the sample rods cross section. The scaling bars indicate 500 µm.

The analysis of initial corrosion in HBS revealed for both processing conditions high corrosion current densities in the range of 400 µA/cm² and Lepidocrocite (γ-FeOOH) as the main solid degradation constituent on the surface.

Table 1. Comparison of tensile test values of a high manganese Fe-Mn-C alloy in as-cast and hot forged processing state.

	$R_{p0,2}$/MPa	R_m/MPa	ε_t/%
As-cast	302 ± 3	563 ± 19	27 ± 2
Hot forged	341 ± 11	938 ± 60	71 ± 13

DISCUSSION & CONCLUSIONS:

Significant increases in tensile strength as well as ductility were obtained by solution annealing and hot forging through a homogenized and refined microstructure. The short-term degradation rate under hydrodynamic conditions in a simulated body fluid was high for both processing conditions. Investigations by systematically increasing the complexity of the electrolyte composition are ongoing.

REFERENCES:

[1] H.-S. Han, S. Loffredo, I. Jun et al. (2019) Mater. Today 23:57-71. [2] P. Poncin, J. Proft, (2004) Med. Device Mater. Proc. Mater. Process. Med. Devices Conf. Mater. Park. OH ASM Int. 253–259.

ACKNOWLEDGEMENTS: Funding is thankfully acknowledged by the Leibniz Institute for Solid State and Materials Research Dresden.

Local oxygen concentration above Mg alloys exposed to Hanks' Balanced Salt Solution at 37°C differs significantly from that at room temperature

Cheng Wang[1], Mikhail Zheludkevich[1,2], Sviatlana Lamaka[1]

[1] *Institute of Surface Science, Helmholtz-Zentrum Hereon, Geesthacht, 21502, Germany*

[2] *Institute for Materials Science, Kiel University, 24103 Kiel, Germany*

INTRODUCTION: Oxygen consumption has been found typical during the degradation process of the biodegradable Fe- and Zn-based alloys, where oxygen reduction reaction (ORR) is considered the major cathodic reaction. The strong oxygen consumption at the metal/fluid interface *in vivo* could induce hypoxia, which affects the partial pressure of oxygen and may cause inflammation. Recent studies have demonstrated ORR as an important secondary reaction during the degradation of Mg alloys in NaCl solution. Thus, studying the role of ORR during the degradation of biodegradable Mg alloys in physiological environment is beneficial to further understand the degradation mechanism.

METHODS: Local oxygen concentration was measured by a fiber-optic oxygen micro-optode with a tip diameter of ca. 50 µm (OXR50-UHS, Pyroscience). The O_2 micro-optode was positioned at 50 ± 3 µm above the specimen surface, *in situ* recording the evolution of local oxygen concentration at the interface of Mg alloys (commercial pure Mg (CP-Mg), ultra-high-purity Mg (UHP-Mg), Mg-4wt.%Ag (Mg-4Ag), Mg-1wt.%Y(Mg-1Y)) exposed to Hanks' Balanced Salt Solution (HBSS) at either room temperature (RT) or 37 °C under hydrodynamic conditions.

RESULTS, DISSCUSION & CONCLUSION: At room temperature, a relatively stronger oxygen consumption was observed on CP-Mg and UHP-Mg in the first hour of immersion, compared to that on Mg-4Ag and Mg-1Y, where the oxygen concentration could be quickly supplied by the oxygen diffused from the bulk electrolyte due to their smaller sample size than that of CP-Mg and UHP-Mg. As the immersion time increase to 12 hours, oxygen consumption was barely observed on all the Mg alloys due to the accumulation and stabilization of the Ca-P-containing products layer precipitated on the surface of the specimen. However, at 37 °C, a slightly higher concentration of oxygen was unexpectedly detected above the surface of Mg alloys than the surrounding bulk electrolyte. This slight difference was maintained with the immersion time up to 12 hours. This interesting experimental phenomenon indicates a possible oxygen evolution reaction (OER) occurring on the surface of degrading Mg alloys in HBSS at 37 °C under hydrodynamic conditions.

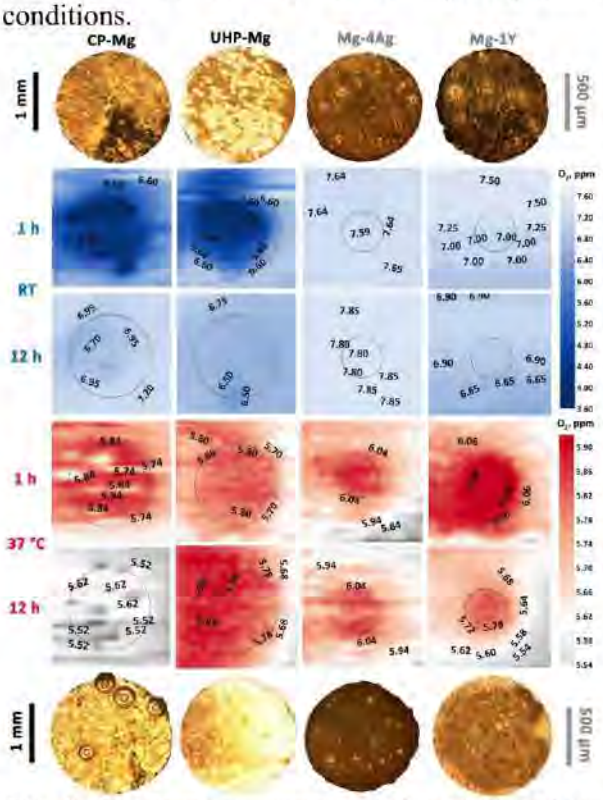

Fig. 1: *The visual appearances (after 12 h) and the distributions of local oxygen concentration at the interface of Mg alloys in HBSS at RT or 37 °C under hydrodynamic condition (flow rate 1.0 mL min^{-1}). The black dot line indicated the position of actual metallic sample embedded in epoxy holder.*

REFERENCES: [1] C. Wang, C. Tonna, D. Mei, J. Buhagiar, M. L. Zheludkevich, S. V. Lamaka. Biodegradation behaviour of Fe-based alloys in Hanks' Balanced Salt Solutions: Part II. The evolution of local pH and dissolved oxygen concentration at metal interface, Bioactive Materials 7 (2022) 412–425. [2] C. Wang, X. Liu, D. Mei, M. Deng, Y. Zheng, M. L. Zheludkevich, S. V. Lamaka. Local pH and oxygen concentration at the interface of Zn alloys in Tris-HCl or HEPES buffered Hanks' balanced salt solution, Corrosion Science 197 (2022) 110061. [3] C. Wang, D. Mei, G. Wiese, L. Wang, M. Deng, S. V. Lamaka, M. L. Zheludkevich. High rate oxygen reduction reaction during corrosion of ultra-high-purity magnesium, npj Materials Degradation 4 (2020) 42. [4] M. G. Strebl, M. P. Bruns, G. Schulze, S. Virtanen. Respirometric In Situ Methods for Real-Time Monitoring of Corrosion Rates: Part II. Immersion, Journal of The Electrochemical Society, 168 (2021) 011502

ACKNOWLEDGEMENTS: Cheng Wang thanks the China Scholarship Council for the award of fellowships (No. 201806310128).

Strain distribution in deformed and degraded Mg10Gd using synchrotron radiation based 2D XRD

B Hindenlang[1], F Wieland[1], D Tolnai[1], J Bohlen[2], R Willumeit-Römer[1]

[1] *Institute of Metallic Biomaterials, Helmholtz-Zentrum Hereon, Geesthacht, DE,*
[2] *Institute of Material and Process Design, Helmholtz-Zentrum Hereon, Geesthacht, DE*

INTRODUCTION: Mg-based alloys are promising biomaterials due to their biocompatibility and biodegradability.[1] Nevertheless, some aspects such as the influence of mechanical stresses on the degradation are not yet fully understood. However, this plays a major role in the application for bone healing since the supporting properties of the implant have to be preserved.[2, 3] To investigate how an applied load influences the degradation, a 2D X-ray Diffraction (XRD) experiment was performed. In combination with Micro-tomography (µCT) scans of the samples, a correlation between preferential degradation sites and the stress distribution in the material is obtained.

METHODS: For this experiment, C-shaped samples of an extruded Mg alloy with 10 wt% Gd were used. The samples have a diameter of 10 mm and were compressed by 1 mm and 2 mm, respectively using PEEK screws. Prior to the 2D XRD experiment, 2 samples for each condition were degraded in simulated body fluid (SBF) for 1 week and 2 weeks. The degradation was performed under near physiological conditions at 37 °C and 5 % CO_2. The 2D XRD experiment was performed at the P07B beamline at the PETRA III storage ring, Deutsches Elektronen-Synchrotron (DESY), with a photon energy of 87.5 keV with a field of view of 100×200 µm². Additionally, µCT scans were performed using a laboratory µCT (Phoenix Nanotom GE) at an operating voltage of 110 kV at 40 µA current.

RESULTS: The 2D XRD scans of the individual degradation steps show that for the (10.0) plane, there is a concentration of compressive strain on the inner curve of the C-shaped sample and a concentration of tensile strain on the outer curve of the sample. These concentrations are reduced but still prominent for advanced degradation, whereas the tensile strain is nearly relieved after 2 weeks degradation. A similar trend is observed for the (00.2) plane, where the compressive and tensile strains are less localized. Nevertheless, the tensile strain is reduced after 2 weeks degradation both in localization and magnitude. In contrast, the µCT scans of the samples (see Fig.1) show no homogeneous degradation but rather localized pitting after one week degradation. This effect is also visible after two weeks of degradation, however the pitting is more pronounced. Additionally, slightly more pits can be seen on the outer curve of the material than on the inner curve.

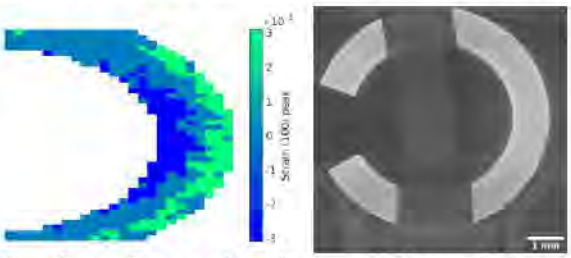

Fig. 1: a) Strain distribution in 1 week degraded and deformed Mg10Gd along (10.0). b) µCT slice of the same sample.

DISCUSSION & CONCLUSIONS: The strain distributions show that in the sample both tensile and compressive strains exist that are locally concentrated for the (10.0) plane but less concentrated for the (00.2) plane. Since the relaxation is occurring in the material and is not influenced by outside parameters, the twinning due to the deformation is one possible reason for the reduced strain. However, by comparing the strain distribution and the µCT scans it can be observed that after 2 weeks of degradation, high pitting corrosion takes place especially on the outer curve of the sample. This leads to a nearly relaxed tensile strain on the outer surface while in the material, residual tensile strains can remain. Moreover, the pitting corrosion on the inner curve leads to a reduction in compressive strain, only less pronounced. Overall this experiment shows how the strain is distributed in a Mg10Gd sample during degradation and how it varies over time as the degradation proceeds.

REFERENCES: [1]Willumeit-Römer, R. et al. in TMS 2018 147th Annual Meeting & Exhibition Supplemental Proceedings (ed. & Materials Society, T. M., Metals) 275–284 [2]Zeller-Plumhoff, B. et al. Adv. Eng. Mater. n/a, 2100197 (2021) [3]Krüger, D. et al. Journal of Magnesium an Alloys 9.6 (2021), pp. 2207-2222

The *in vitro* biodegradation behaviour of as extruded pure Zn, Zn-1.89Mg and PMMA coated Zn-1.89Mg

Alia A. Diaa[1,2], N. El-Mahallawy[1,2], M. Shoeib[3], N. Lallemand[4], P. Masson[4], A. Carradò[4]

[1]Design and Production Engineering Department, Fac. of Eng., Ain Shams University, Cairo, Egypt.
[2]Department of Design and Production Engineering, Fac. of Eng. and Materials Sc., GUC, Cairo, Egypt.
[3]Central Metallurgical Research and Development Institute, El Tebbin, Cairo, Egypt.
[4] Université de Strasbourg, Institut de Physique et Chimie de Strasbourg, Strasbourg, France.

INTRODUCTION: Zinc (Zn) is one of the most promising biodegradable elements. However, in its pure state it is not fulfilling the demands for orthopaedic applications concerning its mechanical properties and degradation behaviour.

The current research aims studying the microstructure and corrosion of pure Zn and Zn-1.89 Mg in an extruded state as well as after being coated with poly(methyl methacrylate) (PMMA). PMMA coating was done by using the *grafting from* technique providing covalent bonds between the PMMA and the metal interface.

METHODS: Zn was cast at 500 °C then heat treated at 350 °C for 8 h. Hot extrusion was carried out at (320 ± 5) °C with a speed of 4 mm/s and an extrusion ratio of approx. 16:1.

The metals were activated by alkali treatment (NaOH) 5M for 1h at 80 °C. They were functionalised afterward with the initiator $C_{15}H_{30}O_5PBr$, finally coated with PMMA using the *grafting from* technique via atomic transfer radical polymerization.[1].

Corrosion tests were carried out at 37 °C in a simulated body fluid (SBF) with a pH of 7.4. The potentiodynamic polarization and electrochemical impedance (EIS) were carried out according to ASTM G5-87 while immersion measurements were following ASTM-G31-72 [2].

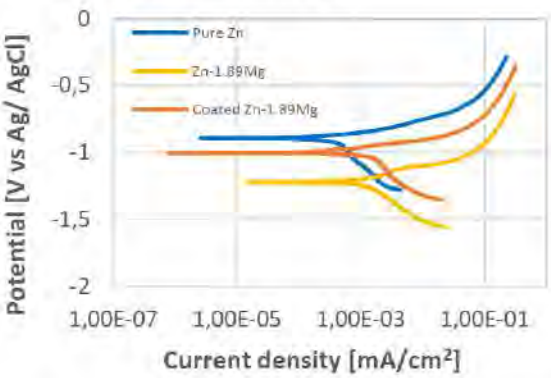

Fig. 1: Potential-dynamic polarization curves of pure Zn, Zn-1.89Mg and PMMA coated Zn-1.89Mg in a simulated body fluid at 37 °C.

RESULTS: According to Tafel fitting of the potentio-dynamic curves, *Figure 1*, alloying increased the corrosion rate from 0.116525 mm/y to 0.366092 mm/y. However, coating decreased the corrosion rate of Zn-1.89Mg by 40.5 %. And, the static immersion test showed that the corrosion behaviour of the as coated Zn-1.89Mg for 120 h is lower than that one of pure Zn.

Figure 2 exhibits the roughness and morphology of the corrosion layer. The roughness of the Zn-1.89Mg is lower than that one of pure Zn and with no base metal constituent.

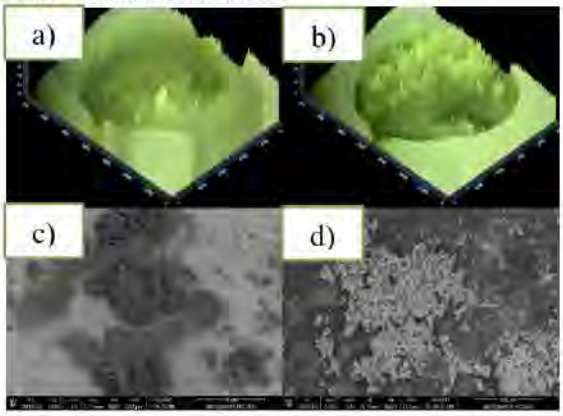

Fig. 2: Stereoscopy and SEM of a) and c) pure Zn and b) and d) coated Zn-1.89Mg after immersion in SBF for 120 h, respectively.

DISCUSSION & CONCLUSIONS: A dense protective PMMA coat using the *grafting from* technique was successfully applied on the eutectic multi-phase surface of the Zn-1.89Mg [3] resulting in a noticeable change in the corrosion behaviour.

REFERENCES:

[1] M. Reggente *et al.*, *ACS Appl. Mater. Interfaces*, vol. 10, no. 6, pp. 5967–5977, Feb. 2018.
[2] Xiao M, Chen YM, et al (2017) Mater Sci Eng C (70):1057–70.
[3] Pachla W, et al (2021) Bioact Mater. 6(1):26–44.

ACKNOWLEDGEMENTS: PHC IMHOTEP 2019- Code Projet: 41847QJ.

Linking geometrical degradation phenomena with the mechanical integrity of rare earth magnesium alloy for implant use

K. van Gaalen[1,2], C. Quinn[1], F. Benn[2,3], P. E. McHugh[1], A. Kopp[2], T. J. Vaughan[1]

[1] National University of Ireland Galway, IE, [2] Meotec GmbH, Aachen, DE [3] School of Mechanical and Aerospace Engineering, Queens University Belfast, Belfast, UK

INTRODUCTION: Magnesium and its alloys are widely discussed biodegradable alternatives to permanent metallic orthopaedic implants (Titanium or Stainless Steel). However, they tend to undergo localised corrosion while implanted in the body which results in challenges in predicting the mechanical stability of an implant during fracture healing and degradation [1]. Still, there is a lack of understanding the relationship between the spatial phenomenology of the surface as corrosion progress and the belonging mechanical integrity of specimens. The objective here is to evaluate the influence of the manner of localised corrosion on the mechanical response.

METHODS: To generate a wide data set for different manners of corrosion formations a numerical approach was used with an adapted phenomenological degradation model [1]. A cylindrical geometry was taken (r=1.5 mm, l=18.95 mm) which underwent degradation. Eight different corrosion profiles, from uniform to severe pitting corrosion were established (Figure 1). The final FE models with six predefined mass losses (5 – 50 %) were simulated under uniaxial tensile test conditions. Geometrical features were calculated, with cross-sectional images by PitScan [3]. Relations were established between the mechanical integrity and key corrosion features. Experimental in-vitro test data was incorporated to evaluate in what extend the numerical model can replicate real corrosion profiles. Here tensile test specimens underwent immersion testing over 4 weeks with weekly time points (n=3 per week, in c-SBF) manufactured from WE43MEO alloy rods (Meotec GmbH, Aachen, Germany). Subsequently, µCT-scans of all samples were conducted for a full spatial reconstruction of the gauge section with PitScan [3]. Following scanning, uniaxial tensile tests were performed.

RESULTS: Figure 1 shows examples of three different corrosion profiles (from uniform to severe localised) at 50 % mass loss. With the implemented adaptations of the numerical degradation code, it is possible to control not only the occurrence of pitting corrosion, it is also possible to control the average pit depth and area. Data evaluation shows that the max. cross-sectional area loss is independent of the manner of corrosion in predicting the maximum specimen strength (σ_{max}) and a linear trend is visible. Features like the av. radius loss also depend on the profiles. Strain at σ_{max} on the other hand strongly depends on the manner of corrosion. Further, a set of input parameters can be identified fitting the experimental one.

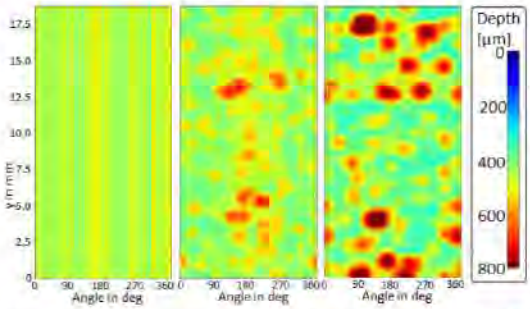

Fig. 1: Surface profiles of gauge section of three different degradation models at 50 % mass loss.

DISCUSSION & CONCLUSIONS: With the FE degradation code, it is possible to control the manner of the corrosion in terms of localised corrosion formation. Correlations were drawn to identify the influence of geometrical features to the mechanical response. Further, it is possible to identify a set of input parameters of the degradation code to achieve similar phenomenological features as well as the mechanical integrity of in-vitro tested samples. However, further experimental testing is necessary to establish a calibrated degradation model.

REFERENCES: [1] J.A. Grogan, B.J. O'Brien, S.B. Leen, et al. (2011) *Acta Biomater*, 7(9): 3523-3533. [2] A.Krause, N. von der Höh, D. Bormann, et al. (2010) *J Mater Sci*, 45:624–632. [3] K. van Gaalen, F. Gremse, F.Benn, et al. (2022), *Bioactive Materials*, 8: 545-558

ACKNOWLEDGEMENTS: This project has received funding from the European Union's Horizon 2020 research and innovation programme under grant agreement No 813869. This publication reflects only the author's view and the REA is not responsible for any use that may be made of the information it contains

Investigation of the biodegradation of Mg-based alloys using *in situ* SRnanoCT

J Reimers[1,2], H C Trinh[1], S Flenner[3], J Hagemann[4], H Cwieka[1], B Hindenlang[1], I Greving[3], R Willumeit-Römer[1], B Zeller-Plumhoff[1]

[1] Helmholtz-Zentrum Hereon, Institute of Metallic Biomaterials, Geesthacht, DE. [2] Forschungszentrum Jülich, Ernst-Ruska Centre, Jülich, DE. [3]Helmholtz-Zentrum Hereon, Institute of Materials Physics, Geesthacht, DE. [4]Center for X-ray and Nano Science, DESY, Hamburg, DE.

INTRODUCTION: Magnesium based alloys are gaining high interest as biodegradable materials for implant applications due to their biocompatibility and biodegradability.[1] Alloying materials like silver (Ag) or gadolinium (Gd) are used due to their antibacterial properties, and improved mechanical properties and degradation resistance.[2,3] Understanding the underlying degradation processes and their interdependencies during the biodegradation of Mg alloys is necessary to control and tailor them. In this regard we have developed a bioreactor-coupled flow-cell setup allowing for *in situ* 3D imaging at the nanoscale using synchrotron radiation. Firstly, we have compared which nanotomographic imaging method yields the best image contrast. Secondly, in order to investigate the influence of alloy composition and precipitates on the degradation process, Mg-xAg and Mg-xGd wires have been degraded under physiological conditions and we have quantified the respective degradation rates (DR) over time.

METHODS: Two generations of a custom flow-cell setup have been developed for *in situ* nanoCT at the P05 beamline at PETRA III, DESY (Hamburg, Germany). The second generation has an integrated heater ensuring a medium temperature of 37 °C during degradation. The setup is connected to a bioreactor and a control unit which autoregulate the pH to 7.4 and a peristaltic pump is used to set a flow rate of 1 ml/min. Using this setup Mg-4Ag, Mg-2Ag and Mg-2Gd wires (80µm diameter) have been degraded for several hours in simulated body fluid (SBF). Transmission X-ray microscopy (TXM) and near-field X-ray holotomography (NFHT) have been compared. Tomographic scans were obtained every 13-30 minutes at an energy of 11 keV and a (binned) voxel size of approx. 90 nm.

RESULTS: While NFHT shows a better image quality than TXM, it has a slightly lower feature resolution and longer processing time. Due to the higher image contrast (see Fig. 1), a more time-efficient segmentation of the images was possible.

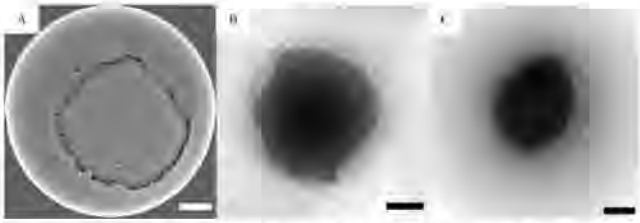

Fig. 1: Tomographic slices of Mg-4Ag degraded in SBF for 6.5 hours. A) TXM, B) NFHT images obtained with the first-generation flow-cell setup. C) NFHT images with the second generation. The scale bars are 20 µm.

Tab. 1 presents first results of the calculated DR of Mg-4Ag samples degraded for 6.5 hours in SBF, corresponding to the data in Fig 1. As previously shown there can be a high variability of the degradation behaviour within the same material.[4]

Table 1: DR of Mg-4Ag wires after 6.5h degradation time. (A), (B) degraded at 22°C, (C) degraded at 37°C.

TXM (A)	NFHT (B)	NFHT (C)
2.2 mm/year	4.87 mm/year	8.29 mm/year

DISCUSSION & CONCLUSIONS: First results show different degradation behaviour when comparing results from both generations of flow-cell setups. This might mainly originate from the elevated temperatures during biodegradation (room temperature to 37°C) thus closer to physiological conditions. Additionally, we will compare the DR of Mg-2Ag and Mg-2Gd, which will yield valuable insight on the influence of the alloying composition on the degradation process. In the future, in combination with transmission electron microscopy techniques, multi-scale imaging of biodegraded Mg alloy wire at the nanoscale can be achieved for a deeper understanding of the microstructure formation and its chemical composition.

REFERENCES: [1]M. P. Staiger, et al. (2006), Biomaterials 27.9 (2006), pp. 1728–1734. [2]S. Silver, et al, Journal of Industrial Microbiology & Biotechnology 33.7 (2006), pp. 627–634. [3]N. Hort, et al (2010), Acta Biomater., 6 (5): 1714-1725. [4]S. Meyer, et al (2021), Metals 11.9, p.1422.

ACKNOWLEDGEMENTS: This project has received funding from the Helmholtz Association.

Local conditions at Zn alloy interface in buffered Hank's Balanced Salt Solution

C. Wang[1], X. Liu[2], D. Mei[1,3], M. Deng[1], Y. Zheng[2], M.L. Zheludkevich[1,4], S.V. Lamaka[1]

[1] *Institute of Surface Science, Helmholtz-Zentrum Hereon, Geesthacht 21502, German;*
[2] *School of Materials Science and Engineering, Peking University, Beijing 100871, China*
[3] *School of Materials Science and Engineering & Henan Key Laboratory of Advanced Magnesium Alloy, Zhengzhou University, Zhengzhou 450001, China;*
[4] *Institute for Materials Science, Faculty of Engineering, Kiel University, Kiel 24103, Germany*

INTRODUCTION: Being one of very few physiologically acceptable bioabsorbable metals, zinc demonstrates optimal degradation rate and mechanical properties for a number of implantable devices. In the search for reliable *in vitro* methodology for understanding Zn degradation, the local interface conditions of Zn alloys were examined in electrolytes containing synthetic pH buffers, such as TRIS and HEPES.

METHODS: Extruded rods of pure Zn, Zn-0.8Mg and Zn-0.8Ca were machined into ∅ 2 mm pins, embedded in epoxy resin and polished. The local pH was recorded by a glass-type pH microelectrode with a tip diameter of 10 µm and length of 50 µm (Unisense, pH-10). The local concentration of dissolved oxygen was monitored by a fiber-optic oxygen micro-optode with a tip diameter of 50 µm (OXR50-UHS, Pyroscience). Finally, the concentration of dissolved H_2 generated during Zn degradation was measured using H_2 micro-sensor with a tip orifice diameter of 10 µm (Unisense, H_2-10). The probes were installed on a dual head stage and positioned 50±3 µm above the specimen surface. The micro-probes were integrated into a commercial SVET-SIET system (Applicable Electronics™) for probe movement and data synchronization. Hanks' Balanced Salt Solution (HBSS) was modified by adding Ca^{2+} ions, HEPES or TRIS. The electrochemical measurements were performed at 37 °C under hydrodynamic conditions, flow rate 1 ml/min. The measurements lasted for 12 to 72 hours. More experimental details can be found elsewhere [1].

RESULTS: As was previously shown for Mg alloys, Ca^{2+} is an important electrolyte constituent also for immersion and degradation of Zn alloys. Its presence significantly stabilises the local pH due to formation of Ca-P corrosion products that also decreases the corrosion rate, Figure 1. The corrosion rate in HBSS for Zn-0.8Ca and Zn-0.8Mg was 1.4 mm/y on average, while it decreased to average 0.38 mm/y in Ca-HBSS. The synthetic pH buffers, TRIS and HEPES also stabilise the pH of HBSS, including the local pH at the alloy interface. In Ca-HBSS, the local pH varied in the range of 6.7 to 7.9, while in presence of TRIS or HEPES this range is much narrower, 7.2 to 7.6. Cathodic oxygen reduction reaction decreases the concentration of dissolved oxygen to 4.5-1.5 ppm, compared to 6.0 ppm in bulk electrolytes. Additionally, low rate concurrent water reduction reaction was detected, generating gaseous hydrogen in the range of 0.5 to 1.5 microM/L.

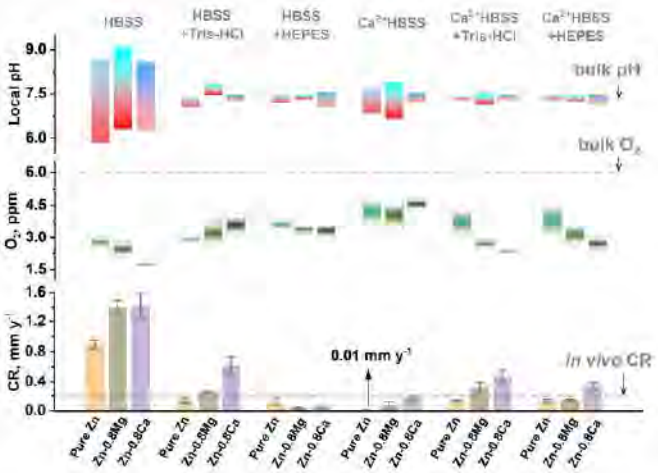

Figure 1: An overview of experimentally measured local pH, concentration of dissolved oxygen and corrosion rate of three Zn-based materials.

DISCUSSION & CONCLUSIONS: In contrast to inability of TRIS and HEPES to buffer local pH at the interface of Mg alloys, and in line with previous work showing reliability of TRIS- and HEPES-containing electrolytes for *in vitro* studies of Zn alloys[2], this work supports the pH buffering by the synthetic compounds for understanding the initial stages of Zn alloys degradation.

REFERENCES: [1] C. Wang, X. Liu, D. Mei, M. Deng, Y. Zheng, M.L. Zheludkevich, S.V. Lamaka, Local pH and oxygen concentration at the interface of Zn alloys in Tris-HCl or HEPES buffered Hanks' balanced salt solution, Corrosion Science (2022) 110061.
[2] X. Liu, H. Yang, P. Xiong, W. Li, H.-H. Huang, Y. Zheng, Comparative studies of Tris-HCl, HEPES and $NaHCO_3/CO_2$ buffer systems on the biodegradation behaviour of pure Zn in NaCl and SBF solutions, Corrosion Science157 (2019) 205-219.

ACKNOWLEDGEMENTS: Cheng Wang thanks the China Scholarship Council for the fellowship (No. 201806310128). Prof. Yufeng Zheng acknowledges the support of key project, National Natural Science Foundation of China (Grant No. 51931001).

Degradation behavior of biodegradable Fe-based alloys in albumin-enriched pseudo-physiological solutions

Quang Nguyen Cao[1], Abdelhakim Cherqaoui[1], Paolo Mengucci[2], Carlo Paternoster[1], Diego Mantovani[1*]
[1]Laboratory for Biomaterials and Bioengineering, Department of Min-Met-Materials Engineering, Research Center of CHU de Quebec, Division of Regenerative Medicine, Laval University, Quebec City, QC, G1V 0A6, Canada; [2]: Department of Materials, Environmental Sciences and Urban Planning, Università Politecnica delle Marche, via Brecce Bianche 12, 60131, Ancona, Italy

INTRODUCTION: Fe-based alloys are potential candidates for biodegradable stent applications for their excellent mechanical properties and biocompatibility [1]. Mn and C are added elements increasing mechanical properties and tuning the degradation rate of Fe-based alloys [2]. Their corrosion assessment in most of previous research works was carried out in pseudo-physiological solutions (PPS) without proteins [3-5], both with static immersion degradation tests and via electrochemical methods. Therefore, the present work aims to investigate the degradation behavior of biodegradable Fe-based alloys in albumin supplemented pseudo physiological solutions, to study the effect of this protein on te corrosion behaviour of the alloys. Two newly developed Fe-5Mn-0.4C (Fe-5Mn), and Fe-20Mn-1.2C (Fe-20Mn) alloys, and Fe-C 1018 commercial (FeC) alloy were used in the present work.

METHODS: The two Fe-Mn alloys were fabricated with a vacuum arc furnace at Québec Metallurgy Centre (Trois Rivières, QC, CA). Samples of the size 10 mm x 10 mm x 1 mm were produced and mechanically polished for following use. Modified Hank's solution (MH), phosphate buffered saline (PBS), and NaCl (9 g/L) solutions with 2 g/L of bovine serum albumin were used for the test. The static degradation tests were carried out accordingly to ASTM G31 standard in an incubator at = 37.0 ± 1 °C, CO_2 = 5 vol%, 90% humidity for a duration of 14 days. After 14 days of immersion, all specimens were retrieved from the solutions for further analysis. All the below-mentioned characterization technique were applied to material before and after degradation tests. The microstructure of the three alloys was characterized by optical microscopy and x-ray diffraction (XRD). Fourier transform infrared spectroscopy (FTIR), scanning electron microscopy (SEM) and energy dispersive X-ray spectroscopy (EDX) were carried out. Potentiodynamic and EIS tests were carried out according respectively to ASTM G106 and ASTM G5-14(2021) standards.

RESULTS: *Figs.* 1a-c show optical microscopy images of the three alloys used for degradation tests. A homogeneous microstructure was obtained for FeC specimen, with an average grain size in the range 5 to10 µm and with a homogeneous distribution of C in the α-Fe matrix. In spite of the small amount of Mn, only α-Fe was found in Fe-5Mn. As the Fe-20Mn specimen showed a fully austenitic structure, with a not uniform grain size, in the average diameter range 10 to 50 µm. All the three alloys showed the highest degradation rate (CR) in NaCl solution, while PBS induced the lowest CRs. The static degradation tests were responsible for the formation of a degradation product multilayer, especially for Hanks' modified solution and for Fe-20Mn. The immersion of specimen in PBS solution determined the formation of a phosphate layer adherent to the surface, showing some crystallization features. In general, Fe-5Mn presented the highest degradation rates for all three considered media.

Fig. 1: Optical microscopy images of: a. FeC alloy, b. Fe-5Mn alloy, and c. Fe-20Mn alloy.

All three alloys showed very low degradation rates in albumin supplemented PBS solution at around 0.03 - 0.04 mm/year. In contrast, the highest degradation rates were obtained in NaCl solution of 0.22 ± 0.02 mm/year for FeC, 0.27 ± 0.01 for Fe-5Mn, and 0.22 ± 0.02 for Fe-20Mn, respectively. FTIR showed the formation of carbonates and phosphates, that were likely in an amorphous form. Electrochemical tests confirmed the findings of the other characterization techniques.

DISCUSSION & CONCLUSIONS: This work investigated the degradation behavior of three Fe-based alloys in three albumin enriched-simulated body fluids. Fe-5Mn showed the highest CR for all three considered media, while CR for Fe-20Mn-1.2C and Fe-C was comparable for the all the considered media. The highest corrosion rates were obtained, for NaCl, while PBS-albumin caused the formation of an inhomogeneous degradation layer.

REFERENCES: [1] P.K. Bowen, et al (2016) *Adv Health Mater* **5:** 1121–40. [2] M Peuster, et al (2006) *Biomaterials* **27:**4955–62. [3] S. Loffredo, et al (2021) *ACS Biomater Sci* Eng **7:**3669–82. [4] B. Wegener, et al (2011) *Mater Sci Eng B* **176:**1789–1796. [5] D. Carluccio, at el (2020) *Acta Biomater* **103**:346–60.

ACKNOWLEDGEMENTS: NSERC-Canada and the Canada Research Chair Program.

High resolution X-ray imaging of degradation and osseointegration of Mg-5Gd and Mg-10Gd screws implanted in rat tibia.

H. Ćwieka[1], B. Zeller-Plumhoff[1], I. Baltruschat[2], J. Moosmann[3], R. Willumeit-Römer[1]

[1] Institute of Metallic Biomaterials, Helmholtz-Zentrum Hereon GmbH, 21502, Geesthacht, Germany. [2] Deutsches Elektronen-Synchrotron DESY, Notkestr. 85, 22607, Hamburg, Germany, [3] Institute of Materials Physics, Helmholtz-Zentrum Hereon GmbH, 21502, Geesthacht, Germany

INTRODUCTION: Magnesium (Mg)-based alloys are becoming an attractive material choice for temporary orthopaedic or dental implants due to their biocompatibility and biodegradability. They indicate sufficient strength for load-bearing applications, reduce stress shielding effect and do not require removal after the fracture healing.[1] High resolution X-ray imaging can be used to investigate detailed insight into the implant degradation and bone regeneration. The aim of presented study is to investigate the degradation and osseointegration of screws made of Mg-5Gd and Mg-10Gd implanted into the rat tibia for 2, 4 and 8 months. The major challenge was to perform highly accurate segmentation on numerous samples, required for quantitative and statistical characterization. Therefore, we developed a trainable and automated segmentation framework.[2] Based on segmented data sets parameters describing metal degradation, osseointegration and implant stability were quantified with respect to implant material and healing time.

METHODS: High resolution synchrotron micro computed tomography (SRμCT) was performed at the p05 imaging beamline at PETRA III at the Deutsches Elekronen Synchrotron (DESY) and at the Diamond Manchester Imaging Branchline I13-2 at the Diamond Light Source. All data sets were pre-processed to a fixed voxel size of 5μm. Quantitative analysis was performed on data segmented with the use of machine learning (ML) algorithms.

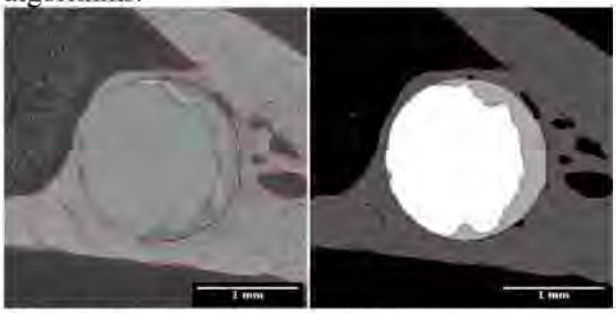

Fig. 1. Cross section of Mg-5Gd screw after 4 months of implantation in rat's tibia. Colorful outlines in the left gray scale image show the quality of ML segmentation. The right image depicts segmented labels where white is the residual metal, gray is the degradation layer and dark grey is the bone.

RESULTS: The visual inspection of ML segmentation shows satisfactory results to perform quantitative analysis (see Fig. 1). As an example of quantitative values, we show the DR results for Mg-5Gd and Mg-10Gd after implantation for 2, 4 and 8 months (see Fig. 2).

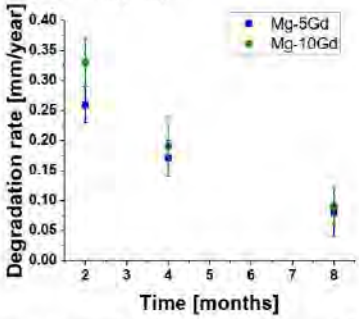

Fig. 2. Comparison of the mean values with standard deviations of degradation rates for Mg-5Gd and Mg-10Gd depending on healing time.

DISCUSSION & CONCLUSIONS: Both Mg-based alloys indicate slowing down of the metal degradation over the time. Mg-10Gd degrades slightly faster than Mg-5Gd which was also observer by Krüger *et al.* but for earlier time points[1]. Both materials create coherent connection with the bone which for Mg-5Gd is depicted in the Fig 1. As reference materials, suitable for osseointegration comparison we used implants made of Ti and PEEK.

REFERENCES: [1] D. Krüger, *et al.*, Bioactive Materials (2022), [2] I. M. Baltruschat, *et al.*, Scientific Reports (2021)

ACKNOWLEDGEMENTS: The research was carried out within the project MgBone (BMBF project number 05K16CGB). The analysis was supported through the Maxwell computational resources operated at DESY. Authors HC and RWR acknowledge funding from the European Union's Horizon 2020 research and innovation programme under the Marie Sklodowska-Curie grant agreement No 811226.

Effect of Zn/Ca Ratio on Corrosion and Mechanical Properties of Mg-Zn-Ca-Mn Biodegradable Alloys

Thomas Avey[1], Dae Hyun Cho[1], David Dean[1,2], Alan A. Luo[1,3]

[1] Department of Materials Science and Engineering, The Ohio State University, Columbus, OH, 43210, USA, [2] Department of Plastic and Reconstructive Surgery, The Ohio State University, Columbus, OH, 43210, USA, [3] Department of Integrated Systems Engineering, The Ohio State University, Columbus, OH 43210, USA

INTRODUCTION: Among all biodegradable metals, magnesium has an advantage in weight, biocompatibility, and a bone-like modulus.[1] Mg-Zn-Ca alloys, specifically, have demonstrated a good balance of mechanical and corrosion properties. Mg alloys are subjected to micro galvanic corrosion initiation between the matrix and secondary phases. Mg_2Ca, $Ca_2Mg_6Zn_3$, and Mg_2Zn are reported to have stable second phases in the Mg-Zn-Ca system. From a biomedical perspective, a Zn/Ca atomic ratio between 1.2-2.0 has been shown to improve the resulting corrosion and mechanical behaviour. However, exploration of the impact of these phases needs to be better understood to further alloy design and microstructure optimization.

METHODS: Selection of potential alloys was based on CALPHAD calculations performed with Pandat software. Casting of Mg-Zn-Ca-Mn alloys at different Zn/Ca atomic ratios were carried out by SF_6 protected melting of pure Mg and adding master alloys: Mg-25%Ca and Mg-10%Mn with CP-Zn pellets. The resulting composition was measured with OES. Warm rolling was carried out after a solution heat treatment. Microstructure characterization was done by SEM, XRD, and Optical Microscopy. Initial corrosion testing was tracked by weight loss, after immersion in HBSS at 36.5°C. Potentiodynamic testing was also done in HBSS to measure corrosion current. In-depth corrosion measurements were done with Micro-Cell, Scanning Kelvin Probe Force Microscopy (SKPFM), and EIS devices. Mechanical properties were obtained via standard tensile testing.

RESULTS & DISCUSSION: Increasing Zn/Ca atomic ratio shows an expected trend for mechanical properties. The as-rolled samples with higher Zn content exhibited a near-linear increase in yield and ultimate strengths. This is a result of the widely reported solid solution strengthening of Zn in Mg alloys.[1] However, the corrosion rate (Figure 1) shows an initial decrease at 1.5 Zn/Ca and then a sharp increase after 2 Zn/Ca. The total secondary phase fraction increases with Zn/Ca ratio. However, over the investigated range, 1-5 Zn/Ca, there is a transition in the phases that forms with Mg in the eutectic region: Mg_2Ca to $Ca_2Mg_6Zn_3$ to MgZn. However, both Zn and Ca have been shown to modify the formation and protective capability of the corrosion film.[2] Local corrosion testing techniques like SKPFM, and Micro-Capillary Cell with EIS is used here to reveal phase-level corrosion behaviour of Mg-Zn-Ca alloys.

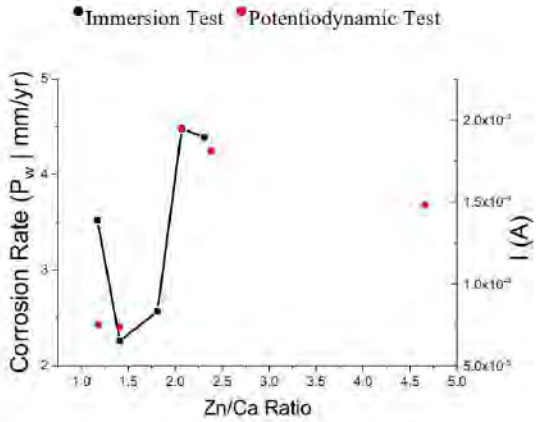

Fig. 1: Corrosion rate measured by weight loss and corrosion current from potentiodynamic testing as a function of Zn/Ca ratio

CONCLUSIONS: Increasing Zn/Ca atomic ratio improves the mechanical properties of Mg-Ca-Zn-Mn alloys but has a more complex effect on the corrosion rate, with the lowest corrosion rate measured between a Zn/Ca ratio of 1.5 to 2. Current micro-scale corrosion tests are being done to understand the mechanism behind this effect.

REFERENCES: [1]H. Ibrahim, A. D. Klarner, et. al: J. Mech. Behav. Biomed. Mater. 69, 203 (2017). [2]M. Deng, L. Wang, et. al:. Mater. Horizons 8(2), 589 (2021).

ACKNOWLEDGEMENTS: Partial support has been provided by the Accelerator Award program at The Ohio State University (OSU) and the Department of Materials Science and Engineering (MSE) at OSU. The authors are grateful to the Fontana Corrosion Center at OSU for providing access to the corrosion testing facility.

In Vitro

Sunday, August 28th 2022

Cellular biocompatibility of different calcium phosphate coatings formed on ZK60 magnesium alloy

Le Thi Trang[1*], Nguyen Quang Cao[2], Sachiko Hiromoto[3], O Minho[1], Equo Kobayashi[1]

[1]: Department of Materials Science and Engineering, Tokyo Institute of Technology, 2-12-1 Ookayama, Meguro, Tokyo, Japan; [2]: Laboratory for Biomaterials and Bioengineering, Université Laval, 2325 Quebec, G1V 0A6 Canada; [3]: Research Center for Structural Materials, National Institute for Materials Science, 1-2-1 Sengen, Tsukuba, Ibaraki, Japan.

INTRODUCTION: Mg-6mass% Zn-0.5mass% Zr (ZK60) alloy has been attracted as a potential candidate for load-bearing applications because of its high biocompatibility, small mismatch of elastic modulus with human bone and biocompatibility [1]. However, ZK60 alloy exhibits a high degradation rate which limits its application. Calcium phosphate (Ca-P) surface coating is a simple but effective method to reduce corrosion rate while enhancing the biocompatibility of the alloy. Cell response to a Ca-P coated material depends on its surface properties [2]. In our previous work, several Ca-P coatings with different types, morphology and corrosion protection were deposited on ZK60 by changing pH coating condition [3]. Hence, in this study, we investigated the cellular biocompatibility on different Ca-P coatings formed on ZK60 alloy.

METHODS: Extruded ZK60 alloy samples (Osaka Fuji Industry, Japan) with 20 mm in diameter and 2 mm in thickness were ground with SiC papers, cleaned with ethanol. In the chemical conversion method, the samples were coated in a solution containing 0.5 mol/L Ca-EDTA ($C_{10}H_{12}CaN_2Na_2O_8$), 0.5 mol/L KH_2PO_4 and 1 mol/L NaOH solutions at 90^{0}C for 2h and at three different pH conditions of 6.5, 7.8 and 10.2. In the cell culture test, mouse MC3T3-E1 pre-osteoblasts were prepared through thawing and passaged 4 to 5 times. The culture medium was α-minimum essential medium (α-MEM) supplemented with 10% fetal bovine serum (FBS) and 1% penicillin/streptomycin solution (P/S). The pre-osteoblasts were seeded on the samples (n=3) at a density of 20x10^3 cells/cm^2 in 3 ml of the culture medium and incubated at 37^{0}C with 5% CO_2 for 24h and 72h. After the incubation, the cells were stained by Giemsa solution for cell counting and observation. The samples were characterized by optical microscopy (OM), x-ray diffraction (XRD), scanning electron microscopy (SEM) and energy dispersive X-ray spectroscopy (EDS).

RESULTS: The type, surface morphology and corrosion protectiveness of the Ca-P coatings governed the cell morphology, mortality and proliferation. Cell proliferation was the highest on the samples coated at pH 6.5 and 7.8, while showed a decreasing trend on the sample coated at pH 10.2, as shown in Fig. 1. Additionally, the cells showed more elongated morphology with a bigger nucleus on the sample coated at pH 7.8 than on that coated at pH 6.5 but shrunk to death on that coated at pH 10.2.

DISCUSSION & CONCLUSIONS: The cell density on the samples coated at pH 6.5 and 7.8 increased significantly because Ca-P coatings enhanced the absorption protein layer which benefits cell adhesion. The cells showed better morphology on the pH 7.8 coating than the pH 6.5 coating because of both the dense distribution of the outer HAp crystals (which is beneficial for the formation of focal contact) and the higher corrosion protection. The decrease in the cell density on the sample coated at pH 10.2 is attributed to the quick initial corrosion caused by the micro-sized defects of the coating and the nanotopography of the outer dense HAp crystals. Generally, ZK60 coated at pH 7.8 showed the best cellular biocompatibility, suggesting that this sample is the most suitable material to be applied in clinical use.

REFERENCES: [1] M. Niinomi, et al. (2012) *Acta Biomater.* **8**:3888-3903. [2] S. Hiromoto, et al. (2017) *Sci. Technol. Adv. Mater.* **18**:96-109. [3] L.T. Trang, et al. (2022) *Surf. Coat. Technol.* **444**:128639.

ACKNOWLEDGEMENTS: This work is partly supported by NIMS Joint Research Hub Program (ID No. 2020-029) of the National Institute for Materials Science, Ibaraki, Japan.

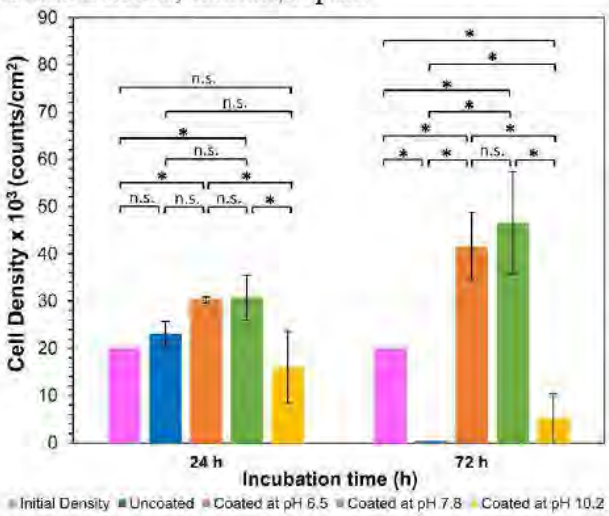

*Fig. 1: Cell proliferation on different types of the cultured samples. n.s.: not significant, *: p≤0.05.*

Towards the development of a biodegradable metallic ureteral stent: Characterizing the corrosion and encrustation tendency of Mg alloys under *in vitro* urinary tract conditions

M Pacheco[1,2], IM Aroso[1,2], JM Silva[1,2], SV Lamaka[3], M Zheludkevich[3], J Bohlen[4], M Nienaber[4], D Letzig[4], CJ Hassila[5], C Persson[5], E Lima[6], AA Barros[1,2], RL Reis[1,2]

[1]3B's Research Group—Research Institute on Biomaterials, Biodegradables and Biomimetics, University of Minho, Guimarães, Portugal. [2]ICVS/3B's-PT Government Associate Laboratory, Braga/Guimarães, Portugal. [3]Institute of Surface Science, Helmholtz-Zentrum hereon GmbH, Germany. [4]Institute of Material and Process Design, Helmholtz-Zentrum hereon GmbH, Germany [5]Division of Biomedical Engineering, Department of Materials Science and Engineering, Uppsala University, Uppsala, Sweden [6]School of Health Sciences, Life and Health Sciences Research Institute (ICVS), University of Minho, Braga, Portugal

INTRODUCTION: A biodegradable metallic ureteral stent (BMUS) is expected to have unique properties, such as slower degradation and improved radial strength (compared with the biodegradable polymers), which will be a novel concept in endourology[1]. The aim of this work was to access the behaviour of different Mg alloys under ureteral stent environment in terms of corrosion and propensity to encrustation.

METHODS: AZ31, Mg1Zn, Mg1Y, Mg4Ag and pure Mg wires -1mm diameter- were produced by direct extrusion (350 ºC, 0.2mm/s). WE43 powder was used for additive manufacturing (AM) assays. Through AM, wires of 1 mm diameter were produced with a hatch distance of 0.05 and 0.06 mm (WE43-0.05_W and WE43-0.06_W, respectively) as well as tubes with an external diameter of 2.34 mm and internal diameter of 1.56 using hatch distances of 0.04, 0.05 and 0.06 mm (WE43-0.04_T, WE43-0.05_T and WE43-0.06_T, respectively). The produced samples were studied under *in vitro* dynamic conditions with artificial urine (AU) –ASTM F 1828-97 (2006). SEM-EDS, ICP-OES, XPS, profilometry, Raman and weight loss were performed for characterization.

RESULTS: All samples were covered by a corrosion layer (Fig.1). Mg4Ag showed a corrosion layer distinguished by the presence of various spots of agglomeration of encrustation along the wire's surface. AZ31 and Mg1Zn showed a similar pattern but a significant lower amount of corrosion products, while a more homogeneous corrosion layer was formed on Mg1Y and pure Mg. As indicated by the chemical analysis, P, O, C and Mg were the most abundant elements and struvite was detected in some samples. Mg1Y presented an even corrosion, which is an important property since it can lead to a homogeneous degradation.

The other alloys, on the other hand, showed to be prone to heavy localized corrosion. The samples produced by AM are still under study, but it is visible clear differences between the different producing parameters used (Fig.1).

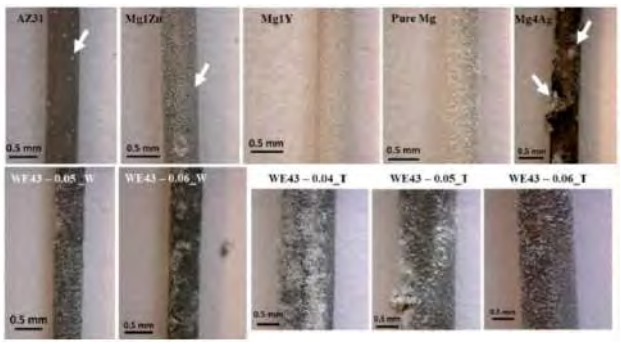

Fig. 1: Macroscopic images of the alloys after 24h in contact with AU under dynamic conditions (the arrows indicate the points of higher accumulation of corrosion products).

DISCUSSION & CONCLUSIONS: Mg1Y showed an homogeneous corrosion – crucial for a biodegradable ureteral stent. The samples produced by AM require further analysis to reach precise conclusions, but this seems to be a promising technique for the development of ureteral stents with innovative designing features. This study revealed important preliminary results on the behaviour of biodegradable metals under urinary environment, which is a key starting point throughout the development of a BMUS.

REFERENCES: [1]Mei D, Wang C, Nienaber M, Pacheco M, Barros A' Neves S, et al. (2021) *Corrosion behavior of Mg wires for ureteral stent in artificial urine solution*. Corros Sci.

ACKNOWLEDGEMENTS: The authors are grateful for the financial support from FCT, through a PhD Scholarship SFRH/BD/145285/2019, and the project NORTE-01-0247-FEDER-047112 as well as VINNOVA through Competence Centre AM4Life (2019-00029).

In vitro and in vivo degradation and biocompatibility of Mg-based intermetallic particles

H.Y. Tang[1], W.T. Lin[1], Y. Zhao[1], X.N. Gu[1,*], Y.B. Fan[1,*]

[1] *Key Laboratory for Biomechanics and Mechanobiology of Ministry of Education, School of Biological Science and Medical Engineering, Beihang University, Beijing, 100083, China*

INTRODUCTION: Mg alloys are widely investigated as candidates for orthopedic implants and vascular stents. However, due to the electrode potential difference, Mg alloys tend to leave high potential intermetallic compounds particles after degradation. In this study, Mg-based intermetallic particles have been prepared and their degradation and associated biocompatibility was systematically investigated *in vitro* and *in vivo*.

METHODS: The Mg-based intermetallic particles were prepared by atomization. The degradation behaviour was studied by immersion in saline and cell culture media, respectively. The effect of Mg-based intermetallic particles on RAW 264.7, MC3T3-E1, HUVEC and HAVSMC were measured with respect to cell viability, inflammatory factor secretion, osteogenic and endothelial cell differentiation. Moreover, the *in vivo* degradation and biosafety of the intermetallic particles were verified by subcutaneous implantation in SD-rats.

RESULTS: The Mg-based intermetallic particles could gradually degrade with the degradation rate ranking order $Mg_{17}Al_{12}$ < $Mg_{12}Nd$ < $Mg_{12}La$ < $Mg_{12}Ce$. As shown in *Fig.1*, viability of all the cell types was decreased concentration-dependently by intermetallic particles. HUVEC and HAVSMC exhibited > 75% cell viability when the concentration of the intermetallic was lower than 0.001 g/ml. In contrast, the cell viability was significantly more affected in MC3T3-E1 and RAW 264.7. Obvious cytotoxicity of MC3T3-E1 was observed for $Mg_{12}Ce$ even the particle concentration is reduced to 0.0002 g/ml. Significantly decreased viability of RAW264.7 was also shown for $Mg_{12}La$ > 0.005 g/ml. Q-PCR results indicated that intermetallic and Mg particles up-regulated the expression of Col-1 in MC3T3-E1 except for $Mg_{12}Ce$, and all intermetallic particles down-regulated the expression of Runx2 and OCN. For HUVEC, up-regulation of eNOs was seen for all the intermetallic and Mg particles except for $Mg_{12}Ce$. Mg particles down- and up-regulated VEGF and VCAM-1 expression, respectively, whereas all intermetallic particles up-regulated VEGF and VCAM-1 expression. Intermetallic particles induced the secretion of inflammatory factors in macrophages similar to that of Mg particle, exhibiting lower IL-1 and IL-6 and higher TNF-α than the control. *In vivo* experiments suggested that, similar to pure Mg, the intermetallic particle caused an infiltration of inflammatory cells at the implantation site, with the inflammatory response decreasing over time. Al and REs were accumulated in the heart, liver, spleen, lung and kidney, while, 4 weeks post-implantation, the element concentrations in each organ were decreased obviously.

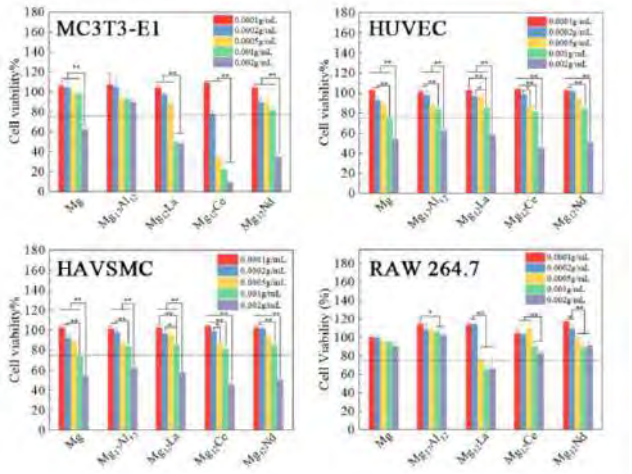

Fig. 1: Cell viability of cells cultured in different concentrations of pure Mg, $Mg_{17}Al_{12}$, $Mg_{12}La$, $Mg_{12}Ce$ and $Mg_{12}Nd$ for 2 days.

DISCUSSION & CONCLUSIONS: The results demonstrated the degradability of Mg-based intermetallic particles. It may be due to the faster degradation of $Mg_{12}La$, $Mg_{12}Ce$, which resulted in cytotoxicity to MC3T3-E1 and RAW 264.7 cells. However, low concentrations of intermetallic particles did not adversely affect the cellular activity. The intermetallic particles had an upregulation effect on eNOs and VEGF expression in HUVEC. Similar to pure magnesium, intermetallic particles induced inflammatory responses at the implantation site due to foreign body reactions. Al and REs, although accumulating significantly in the organ, decreased in elemental concentration over time.

ACKNOWLEDGEMENTS: This work was supported by the National Key R&D Program of China (2018YFC1106600), the National Natural Science Foundation of China (52071008).

Bovine serum albumin additions in Hanks' solutions: Effect on the corrosion mechanism of powder-processed FeMn alloys

C Tonna[1], J Buhagiar[1]

[1] *Department of Metallurgy and Materials Engineering, University of Malta, Msida, Malta.*

INTRODUCTION: The use of Fe-based alloys for biodegradable implant applications has attracted considerable interest over the last couple of decades. Whereas the corrosion mechanisms of the more popular Mg-based alloys have been studied in detail in various *in vitro* scenarios, the influence of testing electrolyte variations on the corrosion behaviour of Fe-based alloys is less clear. In particular, the authors have studied the influence of Ca^{2+} ions in HBSS on the corrosion of Fe-based alloys [1-2]. However, the effect of protein additions to typical testing electrolytes, especially on the widely studied FeMn alloys, has so far not been investigated. When tested with other biodegradable metals like Mg and Zn, protein has been known to chelate positive ions, adsorb to surfaces creating barrier layers and buffer pH [3].

METHODS: Fe35Mn coupons were prepared through the powder metallurgical route. 10 g of mixed Fe35Mn powder was pressed at 520 MPa using a hydraulic press and sintered for 3 hours at 1120°C under 100 l/hr N2-5H2 flow. Electrochemical Impedance Spectroscopy (EIS) tests were performed on an exposed area of 1 cm^2 over the course of 24 hours at 37°C in HBSS (ThermoFisher Scientific, 14025) and in HBSS with 20.6 g/L Bovine Serum Albumin (BSA) (Sigma Aldrich, 07006) and with 8 ml/L Pen Strep (Gibco, 15140) to prevent microbial growth.

RESULTS: Observation of the Bode plots for FeMn tested in HBSS+BSA, compared to Bode plots for tests in HBSS presented in previous work [1], indicates that the total impedance across all frequencies is significantly lower in the former over the 24-hr period. Modelling of the EIS spectra using an adequate equivalent circuit model also indicates that this observation translates to the material's charge transfer resistance, R_{CT}, which loosely represents the corrosion resistance of the material. Moreover, whereas in protein-free electrolyte a very noticeable high-frequency time constant is observed upon immersion, there is a significant delay in the appearance of the same time constant when testing in HBSS+BSA. SEM-EDS analysis of the tested surfaces following the tests also shows visible differences in the surface morphology of FeMn coupons tested in BSA-containing electrolyte exhibited localised pits underneath Ca/P-rich clusters, as seen in *Figure 1*.

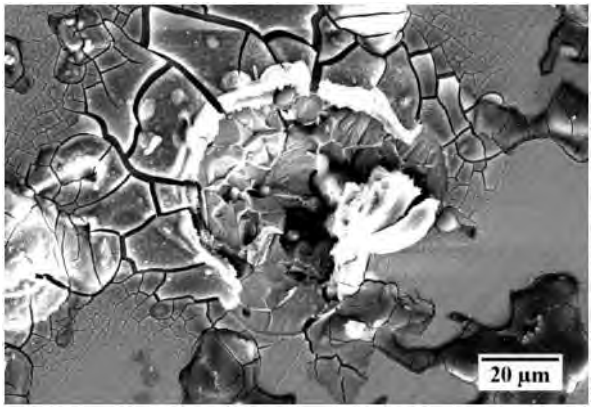

Fig. 1: Cracked Ca/P-rich products revealing localised pit on FeMn alloy tested in HBSS+BSA.

DISCUSSION & CONCLUSIONS: The presence of albumin in HBSS led to a significantly reduced corrosion resistance of the tested FeMn alloys compared to protein-free HBSS, as shown using EIS. The delayed increase in corrosion product resistance, typically observed as a high frequency time constant in Ca^{2+}-containing HBSS, is indicative of the chelating effect protein molecules have on Ca^{2+} ions, reducing the availability of such ions for the precipitation of protective Ca/P products. With time, the chelating capacity is reduced and Ca/P clusters precipitate, underneath which conditions are favourable for pitting to take place. This contrasts with the rather uniform corrosion observed in BSA-free HBSS. The thin oxide layer visible all over the sample surface through dehydration cracks does not provide enough resistance to increase R_{CT} above that measured in BSA-free HBSS. This study indicates that corrosion of FeMn *in vivo* should not be hindered by the presence of proteins alone.

REFERENCES: [1] C. Tonna, C. Wang, D. Mei, et al (2022) *Bioact Mater* **7**:426-440. [2] C. Wang, C. Tonna, D. Mei, et al (2022) *Bioact Mater* **7**:412-425. [3] D. Mei, C. Wang, S. V. Lamaka, et al (2021) *J Magnes Alloy* **9**:805-817.

ACKNOWLEDGEMENTS: The authors would like to thank the Malta Council for Science and Technology, for funding BioSA (R&I-2017-037-T) through FUSION: R&I Technology Development Programme.

In Vivo

Sunday, August 28th 2022

In vitro and *in vivo* corrosion behavior and biocompatibility of biodegradable HA coated ZK60 alloy

Le Van Hai[1], Do Thi Hong Hanh[2], Le Hanh[3], Vu Nhat Dinh[1], Nguyen Viet Nam[3,*]

[1] 103 Military Hospital, Military Medical University, Hanoi, Vietnam
[2] School of Materials Science and Engineering, Hanoi University of Science and Technology, Hanoi, Vietnam
[3] Institute of Traumatology and Orthopaedics, 108 Military Central Hospital, Hanoi, Vietnam

INTRODUCTION: Mg alloys demonstrated their great advantages for applications in biomedical devices including good mechanical properties, biodegradability, and biocompatibility [1]. Although these advantages of Mg alloys make their become potential candidates for use as bioabsorbable and biodegradable materials, their clinical application has been hindered due to their fast biodegradation in the physiological environment [2,3]. The aim of this research is to improve the corrosion resistance of Mg ZK60 alloy by Hydroxyapatite (HA) surface coating. The *in vitro* and *in vivo* biological response of the HA coated ZK60 alloy were investigated intensively as well.

METHODS: HA coatings was prepared from ethylenediaminetetraacetic acid calcium disodium salt hydrate ($C_{10}H_{12}CaN_2Na_2O_8$, Ca-EDTA) solution with the concentration of 0.5 mol/L and potassium dihydrogen phosphate (KH_2PO_4) solution with the concentration of 0.5 mol/L. The pH of the treatment solution was adjusted to 7.5 by NaOH. The ZK60 alloy discs were immersed in the treatment solution at 90 °C for 2 h for HA coating. The *in vitro* cell culture tests were carried out using mouse osteoblastic cell line MC3T3-E1 in α-MEM medium supplemented with 10 vol.% fetal bovine serum (α-MEM+FBS) at 37 ± 0.5 °C under a 5% CO_2 atmosphere for 24 h. After the incubation for 24h the samples were retrieved from the medium, and the cells were stained with Giemsa for the observation of cell proliferation and morphology. *In vivo* experiments were carried out on rabbit for 3 months.

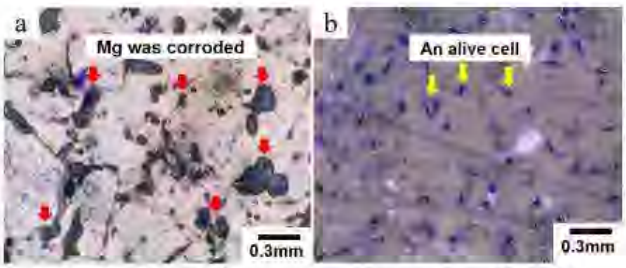

Fig. 1: Optical microscopy images of a: HA coated, and b: non-coated ZK60 specimen after cell culture test for 24 h.

Fig. 2: X-ray images of HA coated ZK60 after implanted on rabbit for a: 1 week, b: 1 month, and c: 3 months.

RESULTS & DISCUSSION: *Fig.1* shows optical microscopy images of HA coated and non-coated ZK60 alloy specimens after cell culture for 24 h. It could be seen that there was almost no cell alive on the surface of non-coated specimen while cell proliferation was on the positive progress on the surface of HA coated specimen. No corrosion occurred on the HA coated specimen, while corrosion occurred severely on the surface of the non-coated specimen.

Fig. 2 shows X ray images of HA coated ZK60 specimen implanted on rabbit after 1 week, 1 month, and 3 months, respectively. After 1 week, the specimen kept original shape without corrosion. After 1 month, corrosion occurred, the specimen was corroded slightly and there was small amount of hydrogen gas accumulated around the specimen. And after 3 months, the specimen was corroded severely and lost the original shape. There was big volume of hydrogen gas accumulated around the specimen; however, the histopathological analysis results indicated that there was no severe inflammation or negative effect due to hydrogen gas after 3 months.

CONCLUSIONS: This research investigated corrosion behavior and biological response of HA coated ZK60 alloy. HA coating layer was effective in improving the corrosion resistance of ZK60 alloy both *in vitro* and *in vivo*. The *in vivo* test results indicated that HA coated ZK60 alloy would be potential material for medical device applications.

REFERENCES: [1] N. Li, et al (2013) *J Mater Sci Technol* **29**;489-502. [2] F. Witte, et al (2005) *Biomaterials* **26**;3557–63. [3] N.T. Kirkland, et al (2010) *Corros Sci* **52**;287–91.

ACKNOWLEDGEMENTS: Center of animal-Vietnam Military Medical University

Comparative tissue performance of Mg alloys in an atherosclerotic in vivo vascular model using multimodal imaging

Maria Kwesiga, Adam Griebel[2], RJ Guillory II [1]

[1] *Michigan Technological University, Biomedical Engineering Dept, Houghton MI, USA*

[2]*Fort Wayne Metals, Fort Wayne IN, USA*[2]

INTRODUCTION: A major hurdle when investigating the in vivo reaction towards new vascular materials is the healthy arterial environment used in pre-clinical animal studies. It is well known that these healthy preclinical models do not fully mimic the tissue progression seen in the clinic. We will attempt to bridge this preclinical knowledge gap by testing Mg alloy wires in a challenging inflammatory microenvironment by implanting wires made from standard and novel Mg materials (AZ31 and WE22) into the abdominal aorta of APOE-/- transgenic mice. These mice development atherosclerotic lesions and possess higher inflammatory cell infiltrates when compared to wild type controls[1]. We then employed multiple imaging modalities in order to characterize the biological response towards the Mg alloys, including immunofluorescence (IF) and elemental mass spectrometric (MS) imaging.

METHODS: AZ31 and WE22 wire materials were prepared via conventional wire drawing practices to a diameter of 100 µm. Due to the low column strength of the fine wires, a modified in vivo wire implantation scheme was adapted wherein pilot holes were punctured via a stiffer stainless-steel wire followed by the Mg alloy wires (n=3 per alloy). Wire segments were left in place for 30 days. Arterial sections were collected and processed for multiple imaging modalities. Frozen sections were either dehydrated in a series of ethanol baths, formalin fixed, or imaged natively (n >20 sections per sample). We then used a high throughput fluorescent slide scanner (Axioscan.Z1) for imaging autofluorescence and IF labelled sections. Serial colocalization of multiple signals were performed in order to obtain detailed description of the Mg-product-tissue interface. High resolution mass spectrum (MS) imaging was then performed on tissue cross sections in order to visualize the in-situ elemental distribution of implant derived metals.

RESULTS: We characterized the progression of the biological response of Mg materials using multimodal imaging. We observed that WE22 wires resisted complete degradation by the 30-day timepoint, even within atherogenic APOE-/- environments. Inflammatory reactions were investigated by performing CD80 IF stains on tissue cross sections. WE22 wires produced more inflammation in peripheral areas vs AZ31 implanted wires. Considerable ^{56}Fe and ^{31}P was present surrounding WE22 implants, which we speculate is a marker of macrophage-based inflammation. Heightened ^{26}Mg presence is seen within both AZ31 and WE22 neointimas at 30 days.

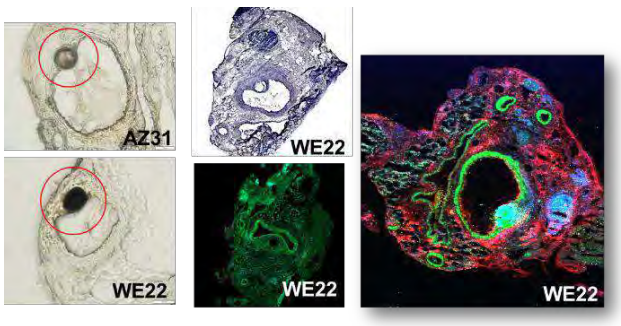

Fig. 1: Cross sections and imaging of AZ31 and WE22 wires implanted in atherogenic APOE-/- mice for 30 days. First column displays brightfield imaging of sections containing the wires, with AZ31 showing substantially more degradation. Second column demonstrates standard H&E and immunofluorescent (CD80) imaging of WE22 implanted within arteries. Third column shows elemental ratios of ^{56}Fe-^{66}Zn and ^{31}P via elemental MS imaging.

DISCUSSION & CONCLUSIONS: Our preliminary results show that WE22 wires may elicit a more robust arterial inflammatory response when compared to AZ31.This could be due to the differences in corrosion rates, with the AZ31 material being nearly completely resorbed in some sections at 30 days. This complete resorption was seen in unstained un fixed tissue sections, and in cross sections observed with elemental imaging, displaying high amounts of Ca and P present throughout the entire wire cross section suggesting complete conversion to corrosion products. Investigating Mg alloys within atherogenic mouse models could allow for more realistic inspection of Mg bio-alloy performance.

REFERENCES: [1] Nakashima, Yutaka, et al. "ApoE-deficient mice develop lesions of all phases of atherosclerosis throughout the arterial tree." *Arteriosclerosis and thrombosis: a journal of vascular biology* 14.1 (1994): 133-140

RF-induced heating of biodegradable magnesium-based implants during MRI

J Espiritu[1], M Berangi[2,3,4], H Cwieka[5], K Iskhakova[5], A Kuehne[2], B Zeller-Plumhoff[5], F Wieland[5], T Niendorf[2,3,4], R Willumeit-Römer[5], JM Seitz[1]

[1] Syntellix AG, Hannover, Germany, [2] MRI.TOOLS GmbH, Berlin, Germany, [3] Charité – Universitätsmedizin, Berlin, Germany, [4] Berlin Ultra-high Field Facility, Max-Delbrueck Center for Molecular Medicine in the Helmholtz Association, Berlin, Germany, [5] Institute for Materials Research, Helmholtz Zentrum Hereon, Geesthacht, Germany

INTRODUCTION: Tracking bone healing post-surgery using medical imaging is essential for appropriate patient care. Magnetic resonance imaging (MRI) provides bone-soft-tissue contrast sans ionising radiation. Radiofrequency (RF) power deposition, required for signal generation, in the presence of conductive implants might induce local temperature increase due to antenna effects. Local tissue/implant heating via induced currents caused by the electromagnetic fields may lead to tissue damage[1]. Previous studies documented heating caused by permanent implants in MRI[2]. The literature does not reveal any study examining RF induced heating of biodegradable implants. To close this gap, it is essential to elucidate the impact of implant degradation shape and degradation layer on RF induced heating. Recognizing this opportunity, this work uses µCT, XRD, SEM, and EDX imaging to characterize the degradation layer of *in vitro* corroded WE43 screws and employs these insights to simulate implant heating scenarios during MRI. *In vitro* MRI was performed to validate the numeric electromagnetic field (EMF) simulations.

METHODS: WE43 screws of diameter 3.2 mm and 40 mm length were degraded following the ASTM F3268 standard. Samples were removed sequentially per week for five weeks. Additionally, a titanium and PEO-coated WE43 equivalent were included for further comparison. The degraded samples underwent further imaging (µCT, XRD, SEM, and EDX) for material characterisation. Subsequently, *in vitro* temperature measurements were conducted according to the ASTM F2182 standard for passive implants. RF transmission field mapping was performed *in vitro* to validate the EMF simulations (Fig. 1) deduced from CST Studio Suite (Simulia, Providence, USA). Findings from initial material characterization were utilized to set up potential implant geometries modeled as a perfect conductor for RF-field simulation at 2 W/kg.

RESULTS: Key results from the material characterisation were considered for simulations: pitting geometries, loss of screw threads, $Mg(OH)_2$ content increasing with time, and discrete change at interface between the degradation layer and base material were incorporated into simulations. The *in vitro* temperature measurements exhibited no significant differences between maximum heating caused by Ti, PEO-coated, and uncoated WE43 material. However, a decrease in maximum temperature was noticed as degradation time persisted (Fig. 1). The simulations revealed that pitting caused by corrosion contributed to no further RF induced heating. However, a decrease in base metallic material (excluding degradation layer) diameter was found to increase implant heating.

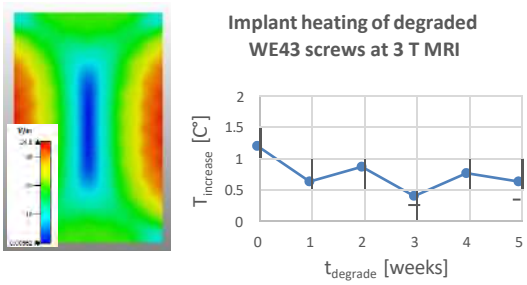

Fig. 1: E-field map obtained from simulations of an ASTM phantom at 3.0 T (left) and in vitro heating results of time-corroded implants (right).

DISCUSSION & CONCLUSIONS: Our simulations showed an increase in RF induced heating with decreasing the base metallic material of the implant. This finding was not confirmed by the *in vitro* temperature measurements which may suggest that the corrosion layer which continuously forms during the degradation process may disrupt potential increases in E-fields surrounding the implant. Our results show most pronounced RF induced heating for the largest amount of base metallic material. Recognizing the increasing incidence of biodegradable implants, our findings also underline the need for guidelines and standards for the assessment of biodegradable implants.

REFERENCES: [1] PL Davis, et al. (1981) *Am J Roentgenol*, 137: 857-860. [2] L Winter, et al. (2021) *J Magn Reson Imaging*, 53: 1646-1665.

ACKNOWLEDGEMENTS: This project has received funding from the European Union's Horizon 2020 research and innovation programme under the Marie Skłodowska-Curie grant agreement No 811226.

ANALYSIS OF THE BONE MICROARCHITECTURE AROUND BIODEGRADABLE MG-10GD IMPLANTS

S Sefa[1], D. C. F. Wieland[1], R Willumeit-Römer[1], J Espiritu[2], H Cwieka[1], I Greving[3], S Flenner[3], B Zeller-Plumhoff[1]

[1] Institute of Metallic Biomaterials, Helmholtz Zentrum Hereon, Geesthacht Germany. [2]Syntellix AG, Hannover, Germany. [3]Institute of Materials Physics Helmholtz Zentrum Hereon, Geesthacht Germany

INTRODUCTION: Mg-10Gd is a biodegradable magnesium (Mg)-based alloy formulated by the addition of 10 wt. % of gadolinium (Gd) to pure Mg to improve its corrosion resistance. Mg-10Gd is known to yield a relatively high bone volume fraction and make good bone-implant contact, similar to titanium (Ti) implants[1]. Bone's adaptive response during implant osseintegration is influenced by its micro porosity. Micro porosity consists of vascular porosity which is associated with blood vessels and the lacuno-canalicular system (LCS), which surrounds the osteocytes and their cell processes. Together, they contribute to the transport phenomena within bone and its remodeling. Given that osteocytes are mechano-sensors, structural parameters associated with the LCS such as the morphology of the lacunar-canalicular network (LCN) and lacuna porosity are key determinants of bone remodeling kinetics, especially during peri-implant bone healing. To attain a comprehensive understanding of the effect of Mg degradation on bone tissue response, it is imperative to study the bone microarchitecture around the implant. The aim of this study is to use hierarchical multiscale 3D imaging including both synchrotron radiation micro computed tomography (SRµCT) and transmission x-ray microscopy (TXM) to study the effect of biodegradable Mg-10Gd implants in comparison to Ti on the vascular and lacuna porosity as well as LCN morphology at the bone-implant interface.

METHODS: To study the lacuna and vascular porosity, Mg-10Gd and Ti screws were implanted into rat tibia for 4, 8 and 12 weeks followed by a SRµCT investigation with a pixel size of 0.5 µm. For the characterization of the morphological changes in the LCN, Mg-10Gd and Ti screws were implanted into rat tibia for 10 weeks and 20 weeks and TXM was performed at 22 nm pixel size. Image analysis was employed to quantify the lacuna porosity and vascular porosity as well as LCN morphology.

RESULTS: Our SRµCT results revealed that the lacuna porosity of Mg-10Gd implant was significantly lower than Ti implant from 4 to 12 weeks of observation period (***Fig. 1***). On the other hand, no significant difference in vascular porosity was found between Mg-10Gd and Ti implants during the investigation period. Also, preliminary results from the morphological characterization of the LCN at 20 weeks show that while the lacunae around both Mg-10Gd and Ti are geometrically round, the lacunae volumes are slightly larger (8 %) in the bone around Ti.

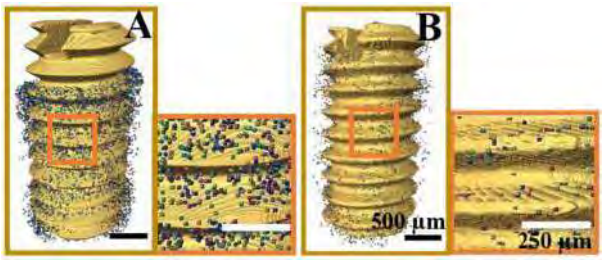

Fig. 1: Exemplary 3D rendering of the differences in lacuna distribution around (A) Ti and (B) Mg-10Gd screws at 8 weeks after implantation obtained using SRµCT. The colored dots represent lacunae.

DISCUSSION & CONCLUSIONS: The similarity in the round lacunae shape around both implants might indicate increased mechanosensation[2] of the osteocytes around both implants. However, the difference in lacuna porosity between both implants and the larger osteocyte volumes around Ti jointly points towards differences in the mechanism of mechanosensation and cellular communication of the osteocytes around both implants. The differences might be an effect of the changes in the chemical environment perceived by the osteocytes due to Mg-10Gd degradation. The LCN morphological analysis is still ongoing and will be presented in detail. The findings of the combined information from several length scales will expedite our understanding on the effect of degradable Mg-10Gd on the bone response.

REFERENCES: [1]D. Krüger, S. Galli, B. Zeller-Plumhoff, et al (2021). *Bioact Mater* 37-52. [2]R. G Bacabac, D. Mizuno, C.F Schmidt et al (2008). *Journal of Biomechanics* 41: 1590 – 1598.

In vitro and in vivo degradation performance of ZX00 screw for bone implants applications

DC Martinez[1], A Dobkowska[1], R Marek[2], J Jaroszewicz[1], T Plocinski[1], H Helmholz[3], R Willumeit[3], W Swieszkowski[1]

[1] *Biomaterials group, Materials Design Division, Faculty of Materials Science and Engineering, Warsaw University of Technology, Poland;* [2] *Department of Orthopaedics and Traumatology, Medical University of Graz, Austria;* [3] *Institute of Metallic Biomaterials, Helmholtz Zentrum Hereon, Germany*

INTRODUCTION: Mg and its alloys, due to their mechanical properties close to the bone, such as elastic modulus and density, are promising biodegradable materials [1]. Although some *in vitro* and *in vivo* research have studied the corrosion behaviour of ZX00 alloys [2,3], there is a lack of information on the kinetic changes in thickness and composition of the corrosion products and the corrosion performance of Mg-0.45Zn-0.45Ca (ZX00) screws. The present study investigates the corrosion behaviour of ZX00 screws under *in vitro* physiological environments and the degradation performance on an *in vivo* sheep model.

METHODS: 30 sterilized Mg-0.45Zn-0.45Ca wt% (ZX00) screws of 3.5 mm diameter and 16 mm length were immersed for 3, 6, 14, 21, and 28 days in α-MEM (Minimum Essential Medium) with 10% FBS (Fetal Bovine Serum) and 1% P/S (Penicillin/Streptomycin). Immersion was done under cell culture conditions (37ºC, 20% O_2, 5% CO_2, 95% rH). The alloy corroded surface of the screws was characterized by scanning electron microscopy (SEM) and energy dispersive X-ray spectroscopy (EDX). For the *in vivo* study, 18 sterilized screws were implanted in the diaphysis of tibiae of sheep. The animals were euthanized at 6,12, and 24 weeks for post evaluation by µCT. Then specimens were embedded in Technovit® 9100 for SEM/EDX and histologic analysis.

RESULTS: After 28 days of immersion, the screws' sharp contours are being lost gradually with substantial dissolution of the threads. EDX results showed that the corroded surfaces after immersion consisted mainly of O, Mg, P, Ca and trace amount of Zn and Cl (Fig 1).

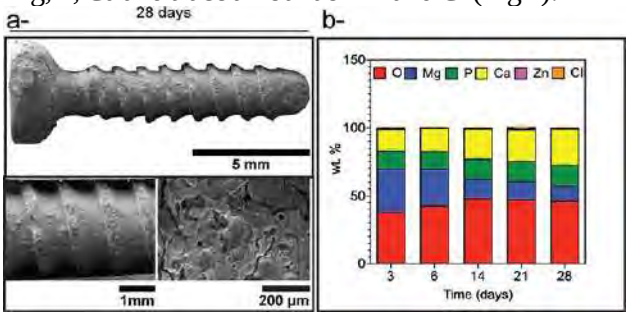

Figure 1: a) Corroded surface of ZX00 screw after 28 days of immersion. b) EDX weight percent of elements composing the corrosion layer of ZX00 screw over 28 days of immersion.

From explanted screws after 24 weeks (Fig 2a.), they maintained their screw shape with an uneven, corroded cracked surface with the threads losing their sharp shape. Some remnants of bone were still attached on the surface of the implant (orange arrows). After 24 weeks, µCT revealed small gas voids in the surrounding tissue (Fig. 2b). From histology, osseointegration, bone in-growth and direct contact between corrosion layer and bone (Fig 2c) was observed. At 24 weeks, Mg, O, and P are steadily distributed within the degradation layer with slightly higher Ca and P content detected at the external part of the corrosion products (Fig 2d-e).

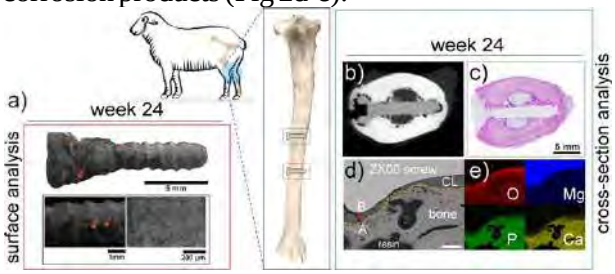

Figure 2 a) SEM image of explanted screw after 24 weeks illustrating the corrosion layer formed on the surface and remnants of bone tissue attached on it (orange arrows). µCT (b) and histological images (c) of ZX00 implant after 24 weeks d) Cross-sectional backscattered electron image illustrating the direct contact between corrosion layer (CL) and bone (orange dotted line), and the corresponding elemental mapping of oxygen (O) (red), magnesium (Mg) (blue), phosphorus (P) (green) and calcium (Ca) (yellow) (Scale bar =100µm).

DISCUSSION & CONCLUSIONS: This study revealed that the screws maintained their shape with an uneven, corroded cracked surface after 24 weeks of implant placement. The thickness, distribution and extent of the corrosion layer formed on the screw during implantation and its chemical composition were implantation-site-dependent. Moreover, osseointegration was observed after 24 weeks of *in vivo* implantation as direct contact between degradation layer-bone, demonstrating that ZX00 screws are promising candidates for use in orthopaedic applications.

REFERENCES: [1]L. Elkaiam, O. Hakimi, G. Yosafovich-Doitch, S. Ovadia, E. Aghion (2020) Ann. Biomed. Eng. **48**: 380-392. [2] P. Holweg, V. Herber, M. Ornig, G. Hohenberger, N. Donohue, P. Puchwein, A. Leithner, F. Seibert (2020) Acta Biomater. **113**: 646-659. [3] N.G. Grün, P. Holweg, S. Tangl, J. Eichler, L. Berger, J.J.J.P. van den Beucken, J.F. Löffler, T. Klestil, A.M. Weinberg (2018) Acta Biomater. **78**: 378-386.

ACKNOWLEDGEMENTS: This work was funded by the European Training Network within the framework of orizon 2020 Marie Skłodowska-Curie Action (MSCA) grant number No 811226.

Long term degradation performance of Mg-Zn-Ca ESIN in a sheep model

R Marek[1], U Kronsteiner[1], U Schwarze[1,2], S Fischerauer[1], A M Weinberg[1]

[1]*Med Uni Graz, Medical University of Graz, Department of Orthopaedics and Trauma, Austria*

[2]*Med Uni Graz, Medical University of Graz, Department of Dental Medicine and Oral Health, Austria*

INTRODUCTION: Magnesium (Mg)-based alloys constitute a promising alternative to overcome drawbacks associated with permanent implant materials, including long-term foreign body effects and removal surgeries [1]. A lot of research has been carried out on the degradation performance and optimization of different Mg alloys [2]. Yet, data on the long-term performance is still sparse. It is known that the degradation rate decreases over time after implantation [3]. Thus, it is difficult to estimate the exact duration, until an implant is fully resorbed. Therefore, the aim of this study was to investigate the degradation performance of bioresorbable Mg-Zn-Ca implants in a sheep model over three years, in order to elaborate the duration to complete resorption more accurately. Elastic stable intramedullary nails (ESIN) were chosen as implant type, as a longer degradation period was expected, due to their large dimensions.

METHODS: A total of four sheep was used for this study. We performed trans-epiphyseal implantation of two ESIN (200 x 3 mm) into the right tibia of all animals. One half of the sheep received ZX10 (Mg-1Zn-0.3Ca; in wt.%) ESIN, the other half ZX00 (Mg;<0.5Zn;<0.5Ca, in wt.%) ESIN. The ESIN were cut to the right length during the operation. We performed *in vivo* clinical computed tomography (cCT) after 2, 6, 12, 24, 52 and 76 weeks, in order to follow the *in vivo* degradation process over time. As each ESIN was cut to the right length during the surgery, we used the first cCT data from 2 weeks after implantation, in order to calculate the initial implant volume. Both ZX10 animals and one ZX00 animal were euthanized after 2 years. One ZX00 animal was euthanized after 3 years. We performed mid- resolution micro computed tomography (µCT) imaging on all extracted tibiae. Implant volume, surface area and degradation rate were calculated for all animals. Histological analysis was performed to evaluate the bone quality around the implants, using Levai Laczko staining.

RESULTS: *In vivo* cCTs and *ex vivo* µCTs revealed homogenous degradation behaviour over time for all animals and both alloying systems (Fig. 1a). The implant volumes of the ZX10 animals were reduced by 85% two years after implantation. In case of the ZX00 animals, the implant volumes were reduced by 91% after two, and 95% after three years. A degradation rate of 0.29 ± 0.00 mm/y was calculated for all animals euthanized after two years, regardless of the alloying system. The degradation rate of the three-year animal was slightly lower with 0.25 mm/y. Histological evaluation revealed direct contact between calcified bone and implant residuals (Fig. 1b).

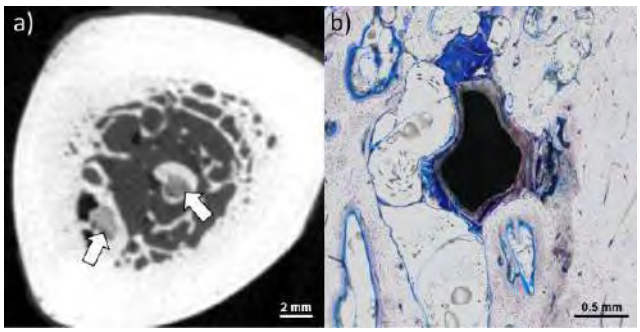

Fig. 1: Ex vivo µCT image of ZX00-ESIN-residuals in the diaphysis, three years after implantation (a). Residuals (white arrows) are surrounded by bone. Histology image of ZX00-ESIN-residual in the same animal (b). There is a direct contact between bone and implant material.

DISCUSSION & CONCLUSIONS: Taken together both alloying systems showed a homogenous degradation behaviour and an appropriate degradation rate over time. Most of the implant material was degraded after three years. Histological analysis showed good bone-to-implant contact on the remaining implant material. We suggest that both, ZX10 and ZX00 are promising implant materials for orthopaedic applications.

REFERENCES: [1] M. Ziegler (1991) *Essentials of Writing Biomedical Research Papers*, McGraw-Hill, Inc. [2] P. Holweg et al. (2020) *Acta Biomaterialia* **113**:646-659. [3]N.G. Grün et al. (2018) *Acta Biomaterialia* **78**:378-386

ACKNOWLEDGEMENTS: This project has received funding from Laura Bassi BRIC under the FFG grant agreement No 840286.

Bone healing around biodegradable Magnesium implants: *Differential response between interfacial and near-implant bone in vivo*

H Ben Amara[1], DC Martinez[2], F A Shah[1],
T Plocinski[2], W Swieszkowski[2], A Palmquist[1], O Omar[1], P Thomsen[1]

[1] *Department of Biomaterials, University of Gothenburg, Sweden;* [2] *Biomaterials group, Materials Design Division, Faculty of Materials Science and Engineering, Warsaw University of Technology, Poland.*

INTRODUCTION: By virtue of their mechanical properties and of their degradation, magnesium (Mg)-based osteosynthesis systems are metallic implants that hold the fractured bones while eliminated in situ, thus offering the promise of reduced complications posed by permanent implants. A growing amount of research validated Mg-based implants for bone fixation by providing robust evidence in support of new bone deposition in contact with the interfacial degradation layer. Whereas Mg-degradation products are known to distribute in the implant environment, less attention has been paid to the bone response at distance from the implant interface. The present study investigated the structural, cellular, and molecular events taking place at the bone-Mg implant interface and at distance from it after *in vivo* implantation in an experimental rat model.

METHODS: Following approval by the Local Ethical Committee at the University of Gothenburg (Dnr: 14790/2019), male Sprague-Dawley rats (n=56) were implanted with miniature screws manufactured from pure magnesium (99.99% - high purity; ***Mg***) or from pure titanium (grade 4; ***Ti***) (herein, serving as a control, enabling osseointegration in this model). In each animal, the metaphysis of the left and right tibiae was drilled prior to the insertion of Ti or Mg screws.
After 3 and 28 days, animals were euthanized, and two types of samples were retrieved (Fig. 1):
1-Implants and peri-implant bone for quantitative polymerase chain reaction (qPCR) (n=8/group/time-point): were separately collected and allocated for molecular gene expression of the implant-adherent cells and of the cells in the peri-implant space.
2-Peri-implant bone with implants en bloc for paraffin or plastic embedding (n=6/group/time-point): enabling radiographical analyses using micro-computed tomography (micro-CT) and histomorphometrical measurements of the bone at the implant interface and at distance from it.
Statistical comparisons were made between experimental groups at each time point and between time-points for each experimental group. (Kruskal-Wallis, Mann-Whitney and Wilcoxon signed-rank tests; $p<0.05$).

RESULTS: While histological observations provided evidence of new bone formation at the vicinity of both Ti and Mg, the bone marrow at distance from the implant-interface featured morphological differences between groups (Fig. 2). At 3 days, the proportion of the interstitial and microvascular area was significantly higher at the expense of the area occupied by the hematopoietic cells in Mg- *vs* Ti-implanted metaphyses. At 28 days, bone marrow around Mg implants showed significantly higher adiposity in comparison to Ti implants. Yet, no differences in the trabecular bone micro-architecture were detected between biomaterials by micro-CT analysis at distance from the implant-interface. The RNA extracted from cells from the implant surface and from the peri-implant bone revealed good quality, allowing detailed molecular analysis.

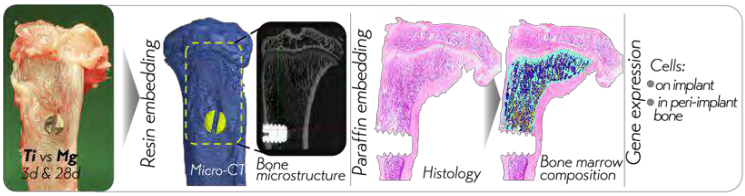

Fig. 1: Experimental design (Histological section stained with hematoxylin and eosin).

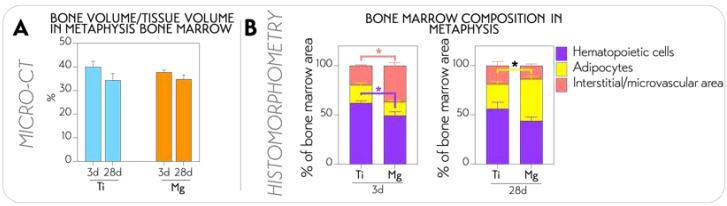

Fig. 2: A- Microstructure of trabecular bone analyzed with micro-CT in the metaphysis at distance from the interface with Ti and Mg implants. B- Bone marrow composition characterized by histomorphometry in the metaphysis at distance from the interface with Ti and Mg implants
(Statistically significant difference between Ti and Mg).*

CONCLUSIONS: In comparison to non-degradable Ti controls, the degradation of Mg implants changes the composition of the peri-implant bone marrow, but yet without alteration of new bone formation at the implant interface.

ACKNOWLEDGEMENTS: Mg rods were generously provided by the Helmholtz-Zentrum Hereon, Geesthacht, Germany. This project is part of the European Training Network within the framework of Horizon 2020 Marie Skłodowska-Curie Action No 811226.

Degradable magnesium alloy suture promotes fibrocartilaginous interface regeneration in a rat rotator cuff transosseous repair mode

Baoxiang[1], Wen Zhang[2], Lili Tan[2]*, Qiang Zhang[1], Ke Yang[2]

[1] *Department of Sports Medicine, the Fourth Medical Centre, Chinese PLA General Hospital, Beijing 100853, China*

[2]*Institute of Metal Research, Chinese Academy of Sciences, Shenyang, 110016, Chinas*

INTRODUCTION: The fibrocartilaginous enthesis regeneration has been a challenge limiting the ability of tendon bone to heal after rotator cuff repair. Although biologically based strategies including the use of growth factors and stem cell therapy and related tissue engineering strategies are employed to augment the healing of tendon-to- bone [1]. The biomaterials used to achieve mechanical stability are indispensable. Magnesium alloys are bioactive materials with good biosafety, mechanical properties and osteogenic activity [2]. In this study, compared with the Vicryl Plus 4-0 absorbable suture for clinical use, magnesium wires were used to tenodesis to assess postoperative biomechanical properties and enthesis regeneration in a rat rotator cuff tear model.

METHODS: Magnesium alloy (Mg-2 wt.% Zn- 0.5 wt.% Nd) wires of 0.23mm diameter and Vicryl Plus 4-0 suture were used to repair the severed supraspinatus tendon in rats. At 4, 8 and 12 weeks postoperatively, the supraspinatus tendon-humerus complex was harvested for uniaxial tensile biomechanical testing and histological analysis of the decalcified section of the tendon bone interface was performed by staining with Safranin O/fast green.

RESULTS: The ultimate load to failure of the magnesium alloy sutures group was greater than that of the Vicryl Plus 4-0 sutures group at 12 weeks postoperatively. The more mature fibrocartilage enthesis regeneration and the obvious tendon bone embedded structure were observed in the magnesium alloy sutures group at 12 weeks postoperatively, as illustrated by the figure 1.

DISCUSSION & CONCLUSIONS: The potential mechanisms for this enhancement are related to magnesium ions regulating the cellular functions involved in osteogenic activity, indirectly stimulate the release of TGF-β1 and the secretion of platelet-derived growth factor [3], and bone marrow mesenchymal cells were recruited at the tendon-bone interface. In addition, magnesium ions promote the differentiation of macrophages to M2 type, upregulating the level of growth factors such as BMP-2, and thus promote the expression of fibrochondrogenic transcription factors such as SOX-9 [4]. Enthesis regeneration close to the native structure improves the bioconjugation of tendon bone.

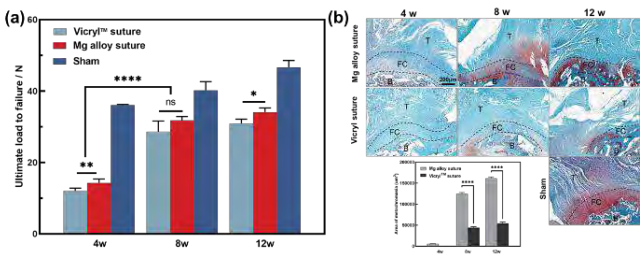

Fig. 1: (a) Biomechanical test of the ultimate load to failure; (b) Safranin O/fast green staining of bone-to-tendon interface. Fibrocartilage is red

REFERENCES: [1] Gulotta LV, Kovacevic D, Ying L, et al (2008) *Am J Sports Med*. **7**: 1290-7. [2] Wang JL, Xu JK, Hopkins C, et al (2020) *Adv. Sci*. **7**: 1902443. [3] Chen Z, Mao X, Tan L, et al (2014) *Biomaterials*. **35**: 8553-8665. [4] Cheng PF, Han P, Zhao CL, et al (2016) *Biomaterials* **81**: 14-26..

ACKNOWLEDGEMENTS: This work was supported by the National Key Research and Development Program of China (No. 2020YFC1107501), the National Natural Science Foundation of China （ No. 51971222, 51801220), the Natural Science Foundation of Liaoning Province of China (No. 2020-MS-001), the DongGuan Innovative Research Team Program (No. 2020607134012) and the DongGuan Science and Technology Service Network Initiative (20201600200042)

Biocompatibility and Degradation Behavior of Molybdenum in an In Vivo Rat Model

C Redlich[1], A Schauer[2], G Poehle[1], V Adams[2], P Quadbeck[3]

[1] Fraunhofer Institute for Manufacturing Technology and Advanced Materials IFAM, Branch Lab Dresden, Germany; [2] Laboratory for Experimental and Molecular Cardiology, Technische Universität Dresden, Germany; [3] Peter-Osypka-Institut für Medizintechnik, Hochschule Offenburg, Germany

INTRODUCTION: Bioresorbable molybdenum (Mo) has great potential as a material for load-bearing implants, e. g. cardiovascular or orthopedic implants, due to its high mechanical strength and very uniform and predictable degradation in vitro [1,2]. In this work, we report on the in vivo biocompatibility and degradation behavior of pure Mo in a rat model.

METHODS: Commercially available pure Mo wire (ø 250 µm) was implanted into the abdominal aorta of Wistar rats for 3, 6 and 12 months. After explantation, Mo levels in serum, urine, aortic vessel wall and organ extracts were investigated via ICP-OES analysis. Histological analyses of the liver, kidneys, spleen, brain and lungs were performed, as well as blood count and differentiation by FACS analysis. Levels of the C-reactive protein were measured in blood plasma of all animals. Microstructure and corrosion behavior of explanted wires in cross-section were analyzed by SEM/EDX and compared to samples from in vitro experiments.

RESULTS: In vitro and in vivo degradation behavior was very similar, with formation of uniform and non-passivating product layers from which Mo slowly dissolves. No localized corrosion is observed. The in vitro degradation rate after 28 days was 102 $g \cdot cm^{-2} \cdot d^{-1}$ (34 $\mu m \cdot y^{-1}$). In vivo degradation rates of 12, 33 and 36 $g \cdot cm^{-2} \cdot d^{-1}$ were observed after 3, 6 and 12 months for samples with good integration into the aortic vessel wall. This corresponds with a degradation rate of 13.5 $\mu m \cdot y^{-1}$ for the 12-month cohort. Degradation of the implanted Mo wire did not lead to increased Mo level in urine, serum, liver, or kidneys compared to the controls. Increased Mo levels were only observed in the immediate vicinity of the implant in the aortic vessel wall. No abnormalities were detected for any of the cohorts in histological and blood analyses compared to the control group. The C-reactive protein levels were similar in all groups, indicating no inflammation processes. Radiographic and CT analyses revealed excellent radiopacity of Mo compared to body tissues.

DISCUSSION & CONCLUSIONS: The findings underscore that pure Mo is a highly promising material for resorbable metallic implants. Degradation in vivo is uniform and predictable while all results point to good biocompatibility. The results also suggest that dissolved Mo does not accumulate in the body and is excreted. In combination with the extraordinary mechanical strength, this makes Mo an interesting alternative to established bioresorbable metallic materials.

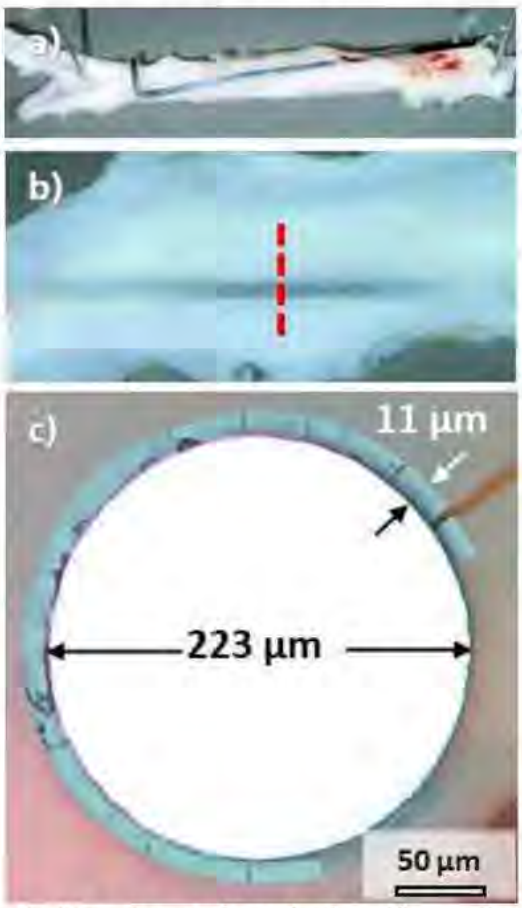

Fig. 1: Mo wire explanted after 12 months from abdominal rat aorta (a), dissected aorta (b) and cross-sectional view of wire (c).

REFERENCES:

[1] C. Redlich, *Acta Biomaterialia*, **2020**, *104 (1)*, 241-251.

[2] C. Redlich, *Metals* **2021**, *11*(5), 761 ff.

ACKNOWLEGDEMENT: This work was financially supported by Saxon Ministry of Science and the Fine Arts SMWK.

In vivo comparison of ultrahigh-purified lean Mg alloys and rare-earth-containing WE43

L Berger[1], S Dolert[2], T Akhmetshina[1], JP Burkhard[5], M Tegelkamp[2], AM Rich[1], W Rubin[1], S Darwiche[2,3], G Kuhn[4], B von Rechenberg[2,3], B Schaller[5], K Nuss[2,3], JF Löffler[1]

[1] Laboratory of Metal Physics and Technology, Department of Materials, ETH Zurich, CH. [2] Musculoskeletal Research Unit, University of Zurich, CH. [3] Center for Applied Biotechnology and Molecular Medicine, University of Zurich, CH. [4] Institute for Biomechanics, ETH Zurich, CH. [5] Inselspital, University Hospital of Bern, CH.

INTRODUCTION: Two magnesium alloy systems have shown particular promise for use as degradable implants: Y- and rare-earth (RE)-containing Mg alloys, the most prominent being WE43, and Mg–Ca-based alloys [1]. While in the case of WE43 the addition of Y supports the goal of reducing the degradation rates to a clinically desired level, in the case of Mg–Zn–Ca alloys a combination of extraordinary purification and a reduction of Zn and Ca has generated similar results [2,3]. However, different study protocols from different research groups make it difficult to compare literature results. Here, we carried out a direct *in vivo* comparison of WE43 with RE-free ultrahigh-purified lean Mg alloys (LMg), as well as LMg treated with plasma electrolytic oxidation (LMgPEO).

METHODS: Plates and screws of extruded WE43, LMg, and LMg subjected to PEO (LMgPEO) were implanted in the pelvis of 6 adult female Swiss alpine sheep (license ZH121/2020). In total, 7 plates and 28 screws were implanted from each group. Fluorescent dyes were injected at two time points to track bone formation and remodelling. After 8 weeks, the animals were sacrificed and microCT scans were performed. The implants were extracted and either examined histologically or used to assess degradation rate by mass loss. Quantitative bone-implant-contact (BIC) and histomorphometry measurements were performed on histological slices.

RESULTS: MicroCT images revealed partly degraded implants with millimetre-sized gas pockets surrounding them (Fig. 1). LMgPEO exhibited a slightly lower degradation rate than LMg and WE43 (0.31 mm/yr, 0.32 mm/yr and 0.37 mm/yr, respectively), with screws showing a significantly higher average degradation rate than plates. The plates, furthermore, showed greater corrosion attack on the side in contact with bone. BIC was found to be significantly higher for LMgPEO (82%) than for LMg (62%) and WE43 (50%). Histomorphometry revealed significantly more new bone formation for LMgPEO compared to the other two groups. Qualitatively, degradation products of WE43 stayed in the original place, whereas in lean Mg alloys only a very thin layer of degradation products was visible (Fig. 1, bottom).

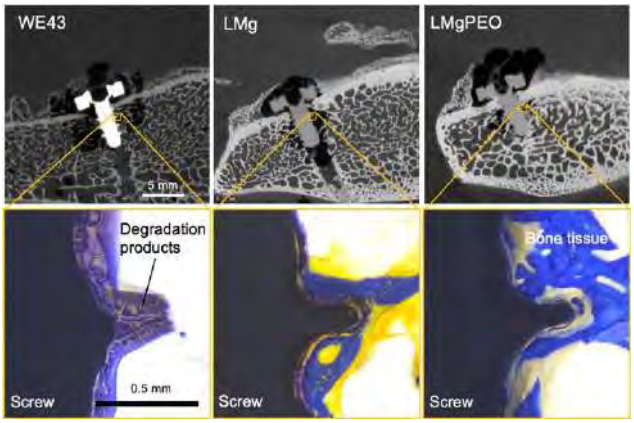

Fig. 1: MicroCT images (top) and enlarged histological slices (bottom) of the three investigated groups 8 weeks after implantation.

DISCUSSION & CONCLUSIONS: The study shows similar degradation rates for coated and uncoated LMg and WE43, although unlike LMg, the degradation products of WE43 stay exactly in the original shape, suggesting a different body response caused by Y and/or RE. The additional PEO surface treatment only minimally reduced the degradation rate over 8 weeks but resulted in significantly better osseointegration. It is expected that this better bone-implant interface will lead to an improved biomechanical response during fracture healing. The cause of the greater degradation of screws and bone-contacting plate surfaces is part of ongoing work.

REFERENCES: [1] H.S. Han, et al. (2019) *Mater Today* **23**:57-71. [2] J. Hofstetter, et al. (2014) *JOM* **66**:566-572. [3] P.L. Holweg, et al. (2020) *Acta Biomater.* **113**:646-659.

ACKNOWLEDGEMENTS: The authors thank ETH Zurich's Lab for Orthopaedic Technology for access to microCT, and Lucia Kölle for assistance. The work was funded by the Swiss National Science Foundation (Sinergia, CRSII5-180367).

In situ reservoir for continuous evolution of H_2 gas to regulate ROS-Warburg Effect Axis for tumor therapy

Qingqing Guan[1], Zhou Yang[2], Jinyun Tan[2], Guangyin Yuan[1], Jia Pei[1,*], Wenjiang Ding[1]

[1] *Center of Hydrogen Science, School of Materials Science and Engineering, Shanghai Jiao Tong University, Shanghai, 200240, China*

[2] *Department of Vascular Surgery, Huashan Hospital, Fudan University, Shanghai, 200040, China*

INTRODUCTION: Hydrogen (H_2) is known to have anti-oxidant effects and serve as an effective strategy in treatment of many diseases. However, the bioavailability of directly administered H_2 is usually poor and uncontrolled. To address the above challenge, a local acid-sensitive sustainable delivery system (Magnesium hydride, MgH_2) that provides high therapeutic concentration of H_2 in tumor tissues is proposed. It is the first time to particularly study the regulation of ROS and Warburg effect axis triggered by the hydrogen in tumor cells.

METHODS: MgH_2 was fabricated as our previous work demonstrated [2].

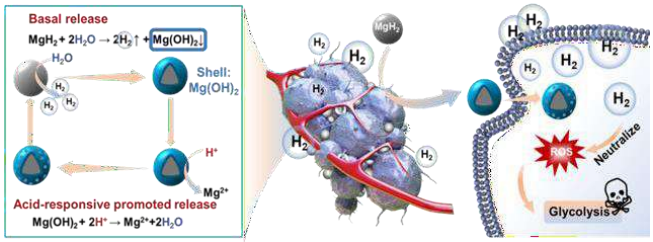

RESULTS and DISCUSSION: TEM image showed that MgH_2 was subsphaeroidal structure and the size was about 1 μm. MgH_2 quickly resolved to form an enormous amount of H_2 bubbles in acid aqueous media. The hydrogen loading capacity of MgH_2 reached 76.9 mmol/g by calculated, which outclass known hydrogen storage materials. In vitro experiments exhibited that MgH_2 significantly suppressed proliferation of tumor cells and much ROS inside cells was eliminated (Fig 1C-D). As demonstrated in Fig 1E, the expression of Warburg effect-associated proteins (HIF-1α, Glut1, HK2 and GAPDH) were all suppressed along with the addition of MgH_2, suggesting the inhibition of the Warburg effect. These results verified that H_2 gas regulated the ROS-Warburg effect axis for tumor therapy. Moreover, distinct inhibition of tumor growth was observed in mice receiving MgH_2 treatment.

CONCLUSIONS: MgH_2 as a local, pH-sensitive hydrogen generator was constructed for the first time for anticancer therapy. Within-depth understanding of its mechanism to tumor therapy, H_2 effectively suppressed proliferation and invasion of tumors by inhibiting Warburg effect via neutralizing ROS and further induced cell apoptosis directly. Our finding brings hydrogen therapy a step closer to practical applications and the methodology presented here opens new pathways for mono-hydrogen treatment.

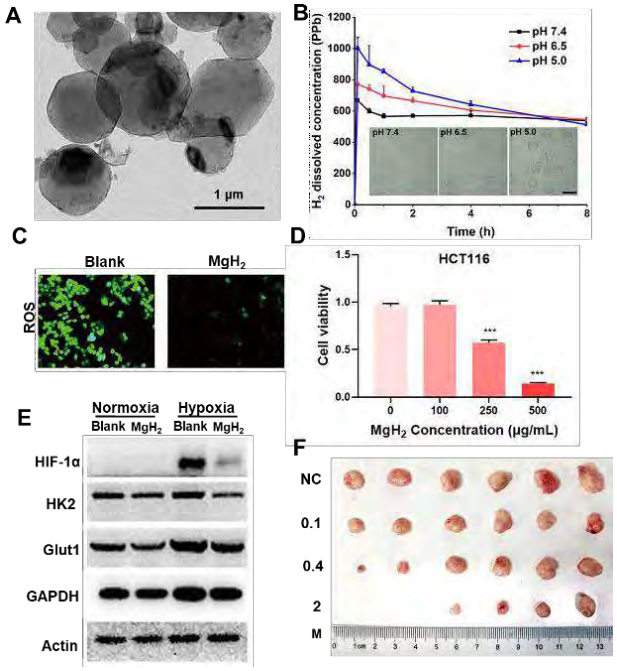

Fig. 1: (A) TEM image of MgH_2. (B) pH-sensitive H_2 release (Insert picture: bright-field images of H_2 bubbles). (C) ROS reduction, (D) cell viability and (E) western blot assay of HCT116 cells treated with MgH_2. (F) Photos of HCT116 tumors in different treatment groups.

REFERENCES:

[1] Shigeo Ohta1, et al, *Nat Med*, 2007, 13, 688.

[2] JX Zou, et al, *INT JHYDROGEN ENERG*, 2015, 40, 1820.

ACKNOWLEDGEMENTS: We would like to thank the National Key Research and Development Program of China (2021YFE0204900) and Natural Science Foundation of Shanghai (22ZR1432000).

BioMg 250 – Results on in vivo animal models

T. Melkent[1], R. Decker[1], S. Lebeau[1]

[1] *nanoMAG,13753 Otterson Ct., Livonia, MI, USA 48150*

Abstract

Results on *in vivo* animal studies of CMF mandible and mid-face models will be presented. These evaluations were undertaken with uncoated plate and screw devices of BioMg 250, a Mg -based alloy microalloyed with Zn, Ca and Mn to generate nanostructures. Data were developed out to 3 years demonstrating healing comparable with Ti and bioabsorbable polymer devices. Clinical observations confirm the positive results of these *in vivo* exposures.

In-vivo results of NOVAMag® membrane performance study

ŽP Kačarević[1,2,3], P Rider[2,3], A Elad[3], D Rothamel[4], G Sauer[4], F Bornert[5], P Windisch[6], D Hangyási[6], B Molnar[6], B Hesse[7], M Assad[8], F Witte[2], S Rogge[9] and D Tadic[3,9]

[1]Department of Anatomy Histology, Embryology, Pathology Anatomy and Pathology Histology, Faculty of Dental Medicine and Health, University of Osijek, Osijek, Croatia; [3]botiss biomaterials GmbH, Berlin, Germany; [2]Department of Prosthodontics, Geriatric Dentistry and Craniomandibular Disorders, Charité Universitätsmedizin Berlin, Berlin, Germany; [4]CMF surgery, Johannes BLA hospital, Germany; [5]Faculté de Chirurgie Dentaire de Strasbourg, Université de Strasbourg, Strasbourg, France; [6]Department of Periodontology, Semmelweis University, Budapest, Hungary; [7] Xploraytion GmbH, Berlin, Germany; [8] Medical Device Preclinical Services, Charles River Laboratories, Quebec, Canada; [9]botiss medical AG, Berlin, Germany

INTRODUCTION: To overcome the limitations of collagen membranes, which are most used membranes for guided bone regeneration (GBR), a synthetic magnesium membranes has been developed as alternatives. [1], [2].

METHODS: Eighteen Beagle dogs were divided into three cohorts of six animals each at different time points (1 week, 8 weeks, 16 weeks), and two animals were assigned to a 52-week cohort. Experimental bone defects were filled with bovine xenograft and covered with either magnesium membrane or collagen membrane. The health status of the animals was regularly monitored and recorded. Following sacrifice, the hemimandibles were prepared for micro-CT (µ-CT) analysis. The following outcomes were observed - the new bone volume/total defect volume (BV/TV), soft tissue volume, void volume and residual magnesium metal and histological evaluation. The surface area and volume of the magnesium metal were also determined.

Fig. 1: The magnesium barrier membrane (NOVAMag® membrane, botiss biomaterials GmbH, Germany).

RESULTS: The µ-CT analysis and histology evaluation showed that the greatest degradation of the magnesium membranes occurred between 1 and 8 weeks and continued until week 16, when only one membrane had visible remnants. Complete degradation of all the magnesium membranes had occurred at a time point of 52 weeks.

Fig. 2: The membrane is fixated from both the buccal and palatial/ lingual sides.

DISCUSSION & CONCLUSIONS: The *in vivo* performance study demonstrated that the magnesium membrane has a comparable healing response and tissue regeneration to that of a resorbable collagen membrane. Overall, the magnesium membrane demonstrated all of the ideal qualities for a barrier membrane used in GBR treatment.

[1] P. Rider *et al.*, "Biodegradable magnesium barrier membrane used for guided bone regeneration in dental surgery," *Bioact. Mater.*, vol. 14, pp. 152–168, Aug. 2022, doi: 10.1016/J.BIOACTMAT.2021.11.018.

[2] P. Rider *et al.*, "Analysis of a Pure Magnesium Membrane Degradation Process and Its Functionality When Used in a Guided Bone Regeneration Model in Beagle Dogs," *Mater. 2022, Vol. 15, Page 3106*, vol. 15, no. 9, p. 3106, Apr. 2022, doi: 10.3390/MA15093106.

FeMn and FeMnAg biodegradable alloys: A biological *in vitro* and *in vivo* investigation

L Saliba[1], K Sammut[1], C Tonna[2], F Pavli[3], V Valdramidis[3], J Buhagiar[2], P Schembri Wismayer[1]

[1] *Department of Anatomy, Faculty of Medicine and Surgery, University of Malta, Msida, Malta*

[2] *Department of Metallurgy and Materials Engineering, University of Malta, Msida, Malta.*

[3] *Department of Food Sciences and Nutrition, Faculty of Health Sciences, University of Malta, Msida, Malta.*

INTRODUCTION: Non-union fractures are a common occurrence and to encourage bone healing surgeons may opt to use bone scaffolds. Magnesium and its alloys are the only biodegradable metals used in the medical industry. Biodegradable zinc- and iron-based alloys, on the other hand, are still in the research phase with the latter showing the biggest promise. In 2007 [1], non-magnetic biodegradable FeMn alloys were considered for orthopaedic applications since they have a better corrosion rate than Fe. Other noble additions were studied in an effort to further enhance the corrosion rate. To date, the work by Dargusch *et al.* [2] is one of the first and latest to report on the *in vivo* behaviour of FeMnAg alloys. In their work both *in vitro* and *in vivo* corrosion studies confirm an increase in corrosion rate in the Fe35Mn alloy after Ag addition, attributed to the occurrence of microgalvanic corrosion. They also conclude that for the Fe35Mn1Ag alloy no chronic toxicity was observed, suggesting acceptable in vivo biocompatibility and hence suitable for orthopaedic applications [2]. This study aims to provide a comprehensive investigation of cytotoxicity and antibacterial behaviour of powder processed Fe-based alloys *in vitro* and *in vivo*.

METHODS: Fe35Mn, Fe35Mn1Ag and Fe35Mn5Ag coupons (*in vitro*) and pins (*in vivo*) were prepared through the powder metallurgical route by uniaxially pressing at 442 MPa and sintering for 3 hours at 1120°C under 100 l/hr N_2-$5H_2$ flow. MnO precipitates were removed by immersing for 5 minutes in 1M HCl and 3.5 g/L of the corrosion inhibitor hexamethylenetetramine. Antimicrobial tests were performed using stock cultures of Staphylococcus aureus, Staphylococcus epidermidis, Streptococcus agalactiae and Escherichia coli. Cytotoxicity tests were performed on freshly ground and pre-corroded coupons using a mouse pre-osteoblasts MC3T3-E1 subclone 4 cell line. The *in vivo* work was done on rats by implanting pins in the tail vertebra for 5 months. Post-mortem ICP-OES of digested organs was performed to evaluate traces of Fe, Mn and Ag.

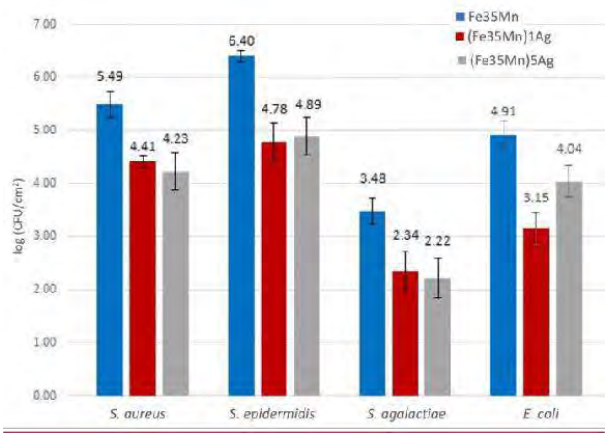

Fig. 1: Cross-species comparison of mean counts per coupon composition. Error bar: SD n=3.

Explant SEM and XRD analysis was performed to evaluate the corrosion attack on the implants.

RESULTS: Addition of silver to Fe35Mn coupons infers an anti-biofilm effect against all the bacteria used in this work with lower biofilm counts observed in each of the biological replicates performed (Figure 1). *In vivo*, the corrosion rate of FeMn and FeMnAg alloys was low and corrosion products accumulated remained at the surface potentially preventing further degradation from taking place.

DISCUSSION & CONCLUSIONS: The *in vivo* degradation rate of the FeMn and FeMnAg alloys used in this work does not reflect the conclusions by Dargusch *et al.* [2]. The materials tested did not elicit a negative cytotoxicity response in *in vivo* tests and the alloys with silver had a positive anti- biofilm effect against all bacteria tested in this work.

REFERENCES: [1]H. Hermawan, D. Dubé, D. Mantovani (2007). *Adv. Mat. Res.* **15-17**:107–112
[2]M. S. Dargusch, J. Venezuela, Dehghan-Manshadi et al. (2021) *Adv. Healthcare Mater.* **10**:2000667

ACKNOWLEDGEMENTS: The authors would like to thank the Malta Council for Science and Technology, for funding Project BioSA (R&I-2017-037-T) through FUSION: R&I Technology Development Programme.

Preclinical biocompatibility assessment of high-strength and corrosion-controlled magnesium-based bone implants

C. Billings[1], M. Abdalla[2], D. Anderson[1], H. Ibrahim[2]

[1] Veterinary College, University of Tennessee at Knoxville, USA [2]College of Engineering and computer science, University of Tennessee at Chattanooga, USA.

INTRODUCTION: Mg and its alloys have a biodegradable nature in aqueous mediums which makes them attractive for various biomedical applications when the material is not recommended to stay permanently in the body [1]. Some of the main challenges that hinder the use of Mg for bone fracture repair are its limited mechanical strength and fast corrosion rates [2]. To this end, we have developed both a biocompatible Mg alloy (Mg-Zn-Ca-Mn alloy) and post-fabrication methods (heat treatment and coating) that deliver a high-strength and corrosion-tailored material that can provide the needed stability during the healing period [3]. In this work, we assessed the biocompatibility of the fabricated Mg alloy before and after the post-fabrication methods, in vitro and in vivo.

METHODS: Mg alloy samples were produced using conventional casting process. The alloy was then heat treated and then coated with ceramic layer (10 µm thick) made by using the micro arc oxidation (MAO) process followed by a thinner layer (1-2 µm thick) of Ca/P-based ceramics created by using the sol-gel technique.

Potentiodynamic polarization test (PDP) was used to measure the relative change in the corrosion rate due to the heat treatment and surface coating. The cytotoxic properties of the samples were determined using an effluent based testing method following the ISO 10993-5 cytotoxicity testing standard.

Six New Zealand White (NZW) rabbits, female, aged 10 – 12 weeks, approximately 3kg were utilized for this study. Animals had two experimental implants (one coated and one uncoated) surgically placed into bone sites. Animals were maintained for either one or two months, at which point they underwent humane euthanasia. Bone samples were collected for histological analysis to evaluate material compatibility.

RESULTS: The sol-gel coating resulted in a significant reduction in corrosion rate, as low as 1.1 µm/year which is 27 times less than that for the MAO-coated alloy alone, see *Table 1*. In vitro and in vivo assessments of our magnesium alloy and fabrication method showed high levels of biocompatibility in terms of cytotoxicity, degradation rates, and osseointegration into bone defects. For instance, bone defect sites did not demonstrate evidence of a significant inflammatory response after 2 months of implantation for all cases, see *Figure 1*. However, an inflammatory response was noted surrounding some uncoated implants. The coated implants were deemed to have superior osseointegration.

Table 1. PDP test corrosion characteristics of the ceramic coated sample.

E_{corr} (V)	i_{corr} (µA/cm^2)	P (µm/year)
-1.63	0.233	2.12

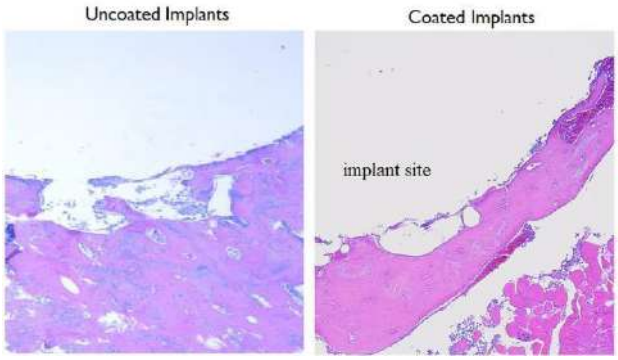

Fig. 1: The proximal bone defect for the uncoated and coated implant at two-month timepoints.

DISCUSSION & CONCLUSIONS: Our animal studies, utilizing a rabbit lateral femoral condyle defect model, showed no negative effects on bone formation, and no evidence of a persistent inflammatory response. The results of this study show that it is possible to produce biocompatible magnesium-based implants with stronger and more corrosion-controlled properties.

REFERENCES: [1] Y. Chen, et al (2014) *Acta biomaterialia* **10:**4561-4573. 2 H. Ibrahim, et al (2017) *Materials Science and Engineering: C* **70:**870-888. [3] H. Ibrahim, et al (2019) *Thin Solid Films* **687**:137456.

ACKNOWLEDGEMENTS: This work was supported by Center of Excellence for Applied Computational Science competition at the University of Tennessee.

Potential clinical scenarios of bioabsorbable zinc as bone implants

Hongtao Yang[1], Yufeng Zheng[2*], Bo Jia[3], Xinhua Qu[3], Kerong Dai[3*]

[1]School of Engineering Medicine, Beihang University, Beijing, 100191, China

[2]Department of Materials Science and Engineering, Peking University, Beijing 100871, China.

[3]Department of Orthopedics, Shanghai Jiaotong University School of Medicine, Shanghai 200011, China

INTRODUCTION: After a decade of endeavour to develop zinc as a novel candidate for biometal, more and more evidence is emerging to support the promising role of zinc and its alloys in clinical applications, especially for bone implants. Here, we build up three distinguished animal models including rabbit shaft fracture model, rat critical bone defect model, and rat femur osteomyelitis prevention model, to explore the potential clinical scenarios of functional bioabsorbable Zn alloy bone implants.

METHODS: Zn-0.4Li alloy screw and plate system was fabricated and used in a load-bearing rabbit shift fracture model, with Ti-6Al-4V counterpart as a control. Zn-0.8Sr alloy porous scaffold was prepared and evaluated in a rat critical bone defect model, with pure Ti implants as a control. Zn-2.0Ag alloy implants were testified in a rat femur osteomyelitis prevention model, a mouse cranial osteolysis model, and a rabbit femoral condyle fracture model with Ti-6Al-4V alloy as a control. In vitro tests include mechanical properties, corrosion behaviour, cellular study, and antibacterial study were carried out as well.

RESULTS: In the rabbit shift fracture model, the Zn-0.4Li based bone plates and screws showed comparable performance in bone fracture fixation compared to the Ti-6Al-4V counterpart. The fracture was healed completely after 6 months. The osteogenic activity of Zn-0.4Li alloy, as a result of biodegradation, was verified in a rat femur model. Furthermore, the underlying mechanism could include activation of the PI3K-AKT pathway and stimulation of metallothionein proteins.

In the critical bone defect model, the scaffold-bone integration and bone ingrowth confirmed the favorable in vivo repair properties of the Zn–Sr alloy, which was verified to offer satisfactory biosafety based on the hematoxylin-eosin (H&E) staining and ion concentration testing of important organs. RNA-sequencing illustrated that the Zn-0.8Sr alloy promoted osteogenesis by activating the wnt/β-catenin, PI3K/Akt, and MAPK/Erk signaling pathways.

The antibacterial activity of the Zn–2Ag alloy was verified in a rat femur osteomyelitis prevention model, while the anti-osteolytic properties were evaluated using a mouse cranial osteolysis model. Moreover, the Zn–2Ag based screws showed similar performance in bone fracture fixation compared to the Ti–6Al–4V counterpart. The fracture healed completely after 3 months in the rabbit femoral condyle fracture model. Furthermore, the underlying antibacterial mechanism may include inhibition of biofilm formation, autolysis-related pathways, and antibiotic resistance pathways. Osseointegration mechanisms may include inhibition of osteoclast-associated protein expression, no effect on osteogenic protein expression, and no activation of related inflammatory protein expression.

DISCUSSION & CONCLUSIONS: The empirical findings here reveal the great potential of Zn alloys implant in clinical applications such as load-bearing fracture fixation, bone defect, and bone infection.

ACKNOWLEDGEMENTS: This work was supported by the National Natural Science Foundation of China (Grant No.5193000081, No 5210010632), and the Fundamental Research Funds for the Central Universities (Grant No. JKF-YG-21-B003).

In-vivo study of additively manufactured Mg lattices in a large animal model

F Benn[1,2], R Smeets[3], S Malinov[1], A Kopp[2]

[1] School of Mechanical and Aerospace Engineering, Queen's University Belfast, Belfast UK. [2] Meotec GmbH, Aachen, Germany. [3] Department of Oral Maxillofacial Surgery, University Medical Center Hamburg-Eppendorf, Hamburg, Germany.

INTRODUCTION: The combination of laser-powder bed fusion (L-PBF) and Magnesium (Mg) enables the fabrication of macroporous structures, similar to that of human trabecular bone [1]. In addition to sufficient mechanical stability, biodegradable implants require a degradation behaviour that matches with the healing bone. A major challenge regarding Mg implants is their fast degradation rate as rapid early-stage degradation may be accompanied by pronounced hydrogen gas release, which can inhibit bone growth [2]. For macroporous structures, the vastly increased surface area leads to even higher degradation rates. Additionally, the process of L-PBF is fundamentally different from conventional manufacturing such as casting, thereby creating novel microstructure which results in altered mechanical and degradation properties [3]. Following successful in-vitro experiments of additively manufactured Mg lattices [4], the next step is to study the in-vivo performance. Therefore, this study investigated the in-vivo performance of PEO modified lattice structures in a large animal model.

METHODS: Macro-porous lattices from the alloy Mg4Y3RE with outer dimension of 9x9x6 mm were additively manufactured and PEO surface modified. After inducing a critical size defects, the lattices were implanted in the mandibular of Miniature pigs. Additionally, state of the art bone graft material (granulate) was implanted in separate but similar sized defects as a reference. CT scans were performed throughout the implanted time period of 32 weeks. At two and thirty-two weeks after surgery, histomorphometric analysis was performed.

RESULTS: Degradation and beginning osteoid formation were observed after two weeks with no significant difference between the two implant materials. At week sixteen, Mg scaffolds showed accumulations of voids together with new calcified bone, while at the same time degraded implant material was detected. For the bone graft granulate, a higher amount of calcified bone was recorded, but the remaining implant material appeared comparable to the scaffolds. After thirty-two weeks, the initial defect was fully filled by calcified newly formed bone, regardless of implant material. The residues of both implant materials were still clearly visible, indicating the incomplete degradation.

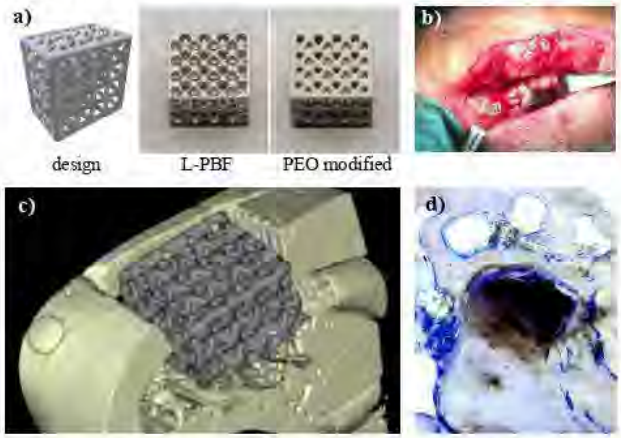

Fig. 1: (a) Design of the Mg lattice and the states during manufacturing, (b) creation of defect in the mandibular and placement of implants, (c) CT reconstruction after surgery and (d) histology after 32 weeks showing the Mg strut (black) and surrounding new bone formation.

DISCUSSION & CONCLUSIONS: The additively manufactured Mg lattices were successfully implanted and showed good osseointegration right after implantation. The fracture healing was accompanied by temporary void generation, possibly due to Mg degradation. Nonetheless, it had no significant effect on the long-term osseointegration and bone healing capacity of the Mg lattices could be rated non-inferior to the reference material.

REFERENCES: [1] Javaid et al. (2018), Journal of Clinical Orthopaedics and Trauma: 9 202–206. [2] Sezer et al. (2018), Journal of Magnesium and Alloys: 6 23–43. [3] Esmaily et al. (2020), Additive Manufacturing: 35 101321. [4] Benn et al. (2021), Material Science and Engineering C: 124 112016.

ACKNOWLEDGEMENTS: This project has received funding from the European Union's Horizon 2020 - Research and Innovation Framework Programme under the H2020 Marie Skłodowska-Curie Actions grant agreement No 813869.

The effect of zinc and calcium on magnesium's biodegradation

B Okutan[1], UY Schwarze[1,2], L Berger[3], V Herber[2], O Suljevic[1], JF Löffler[3], AM Weinberg[1], NG Sommer[1]

[1] *Department of Orthopaedics and Traumatology, Medical University of Graz, Graz, Austria.*
[2] *Department of Dental Medicine and Oral Health, Medical University of Graz, Graz, Austria.*
[3] *Metal Physics and Technology, Department of Materials, ETH Zurich, Zurich, Switzerland.*

INTRODUCTION: Magnesium (Mg)-based implants have become promising candidates for orthopedic interventions over the past years. Besides their biocompatibility and good mechanical features, Mg-based implants have the ability to degrade completely in the body, eliminating the need for removal surgery[1]. However, high corrosion rate and excessive hydrogen gas formation of commercially pure Mg implants are still major concerns in clinical application. Hence, ultra-high purity Mg (XHP-Mg) and, especially, Mg alloys might overcome these disadvantages. It is therefore important to understand the degradation behavior of Mg-based implants and their effect on bone remodeling.

METHODS: In this study, we investigated (i) the degradation behavior of ZX00 (Mg<0.5Zn<0.5Ca; in wt%) and XHP-Mg (>99.999 wt% Mg) implants, and (ii) their safety and impact on bone in-growth in Sprague Dawley rats compared to state-of-the-art titanium (Ti) implants. Five rats per group underwent bilateral, transcortical implantation of cylindrical pins (ZX00 and XHP-Mg: *d*=1.6mm, *l*=8 mm; Ti: *d*=1.5 mm, *l*=8mm) into the diaphysis of both femurs. Sequential fluorochrome markers were administered in rats to evaluate new bone- tissue formation. Serum ALP, Ca, and Mg levels were measured to elucidate the systemic effect of the degrading Mg implants. Material degradation was observed via *in vivo* low-medium resolution and *ex vivo* high-resolution micro-computed tomography. Degradation behavior evaluations were followed by investigations of bone response and in-growth via histological and gene expression analysis.

RESULTS: Biochemical analysis showed that the *in vivo* degradation of both implant types had no impacts on ALP, Ca, and Mg serum level. ZX00 homogenously degraded with an increased hydrogen gas formation 12 and 24 weeks after implantation, whereas XHP-Mg exhibited a higher gas formation at 2 weeks of implantation. Degradation rates were computed as 0.18±0.12 µm/day and 0.23±0.18 µm/day for ZX00 and XHP-Mg, respectively. Histologically, the Mg-based implants are superior with respect to new bone-tissue formation and in-growth compared to the Ti implants. Gene expression analysis showed a positive effect on the up-regulation of the chondrogenic gene markers for ZX00 and XHP-Mg compared to the Ti group at 6 weeks of implantation.

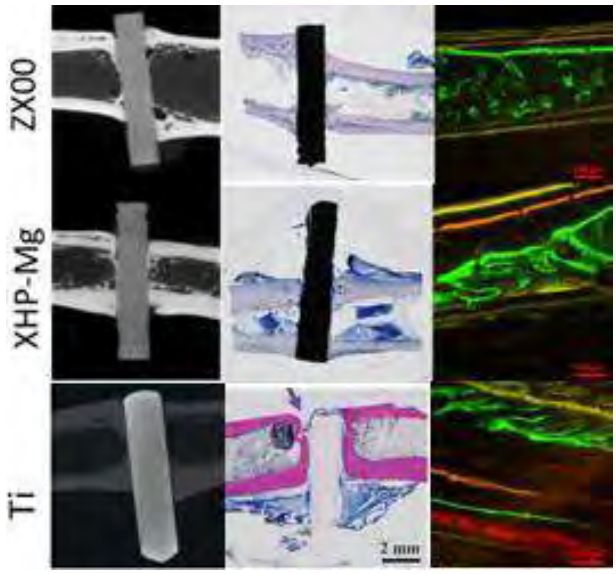

Fig. 1: Representative ex vivo high-resolution µCT images (pixel size=10.1 µm), Levai-Laczko stained bone sections, and fluorochrome images (scale bar=100µm) of ZX00 and XHP-Mg samples after 24 weeks of implantation

DISCUSSION & CONCLUSIONS: We demonstrated safe *in vivo* degradation of two different Mg-based implants and the corresponding bone response in a healthy juvenile growing rat model. Our findings suggest that (i) ZX00 and XHP-Mg support bone formation and remodelling, (ii) both Mg-based implants are superior to Ti implants in terms of new bone-tissue formation and osseointegration, and (iii) ZX00 is more favorable due to its lower degradation rate and moderate gas formation.

REFERENCES: [1]F. Witte, V. Kaese, H. Haferkamp, et al. (2005), *Biomaterials* **26**(17):3557-63.

ACKNOWLEDGEMENTS: This work was supported by the European Marie Curie Program.

Influence of ZX00 implants on the sheep bone ultrastructure

K. Iskhakova[1], D.C.F. Wieland[1], H. Ćwieka[1], T Albaraghtheh[1], B. Zeller-Plumhoff[1], R. Willumeit-Römer[1]

[1] *Institute of Metallic Biomaterials, Helmholtz-Zentrum Hereon, Geesthacht, Germany.*

INTRODUCTION: Biodegradable magnesium (Mg) implants are becoming a promising material for bone fracture treatment due to high biocompatibility and good mechanical properties similar to the bone itself. Furthermore, the degradation rate of Mg alloys can be tailored by the choice of alloying material[1]. Alloying elements such as calcium (Ca) and zinc (Zn) are highly favoured for bone implant materials, as Mg-Ca-Zn alloys show increased biocompatibility and improved mechanical properties[2]. ZX00 is a Mg-0.45Zn-0.45Ca (in wt%) alloy which demonstrates a slow and homogeneous degradation *in vivo*[3]. During the healing process, the ultrastructure of the newly formed bone can be affected by implant degradation, e.g. through ionic substitution or change in crystal parameters. Thus, the mechanical properties of the bone matrix might change resulting in worse performance and, thus, reduced performance of the implant. This study is focused on determining such an effect of the ZX00 implant on the sheep bone ultrastructure.

METHODS: Ti and ZX00 screws (3.5 mm in diameter, 29 mm in length) were implanted into the sheep femur. After 6, 12, and 24 weeks, sheep were sacrificed and the metal implants with the surrounding bone were explanted. The explants were embedded into Technovit 9100, sliced into 15 µm thin sections, and fixated onto the Kapton tape. Synchrotron scanning small-angle/wide-angle scattering (SAXS/WAXS) study was performed at a photon energy of 12 keV at the P03 microfocus endstation at PETRA III (DESY, DE) with the beamsize of 31×22 µm. Analysis was performed using a custom-made MATLAB R2022a (The MathWorks, Inc., Natick, US) script. We determined the T-parameter, d-spacing, and crystallite size of the newly formed bone and investigated their dependence on the distance from the implant, healing time, and the material.

RESULTS: On the basis of the SAXS analysis we calculated the median hydroxyapatite (Hap) platelet thickness (T-parameter). The T-parameter did not show a significant difference between ZX00 and Ti and did not depend on the healing period. Similar behaviour was observed while studying the d-spacing and the crystallite size of Hap averaged over a 1×0.3 mm region. However, a closer look at the interface between bone and the implant (up to 0.2 mm distance from the implant) showed a slight decrease in all 3 parameters for the ZX00 after 6, 12, and 24 weeks (Fig. 1) in contrast to the Ti samples.

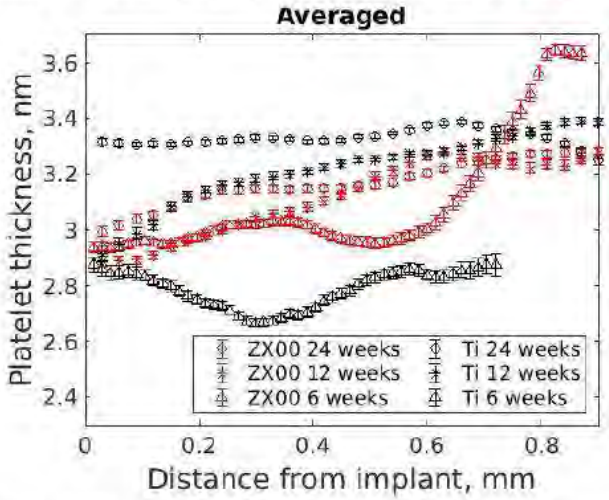

Fig. 1: The T-parameter of the newly formed bone as a function of the distance from the implant for ZX00 and Ti implants after 6, 12, and 24 weeks of healing.

DISCUSSION & CONCLUSIONS: The study shows that the d-spacing, T-parameter, and the crystallite size of Hap, and therefore, bone ultrastructure near the ZX00 biodegradable implant differed from the Ti at a short distance of 0.2 mm from the bone/implant interface. By contrast, at larger distances of up to 1 cm, the ultrastructure remained unaffected. Such an alteration could be explained by the possible ionic incorporation, when the Mg^{2+} ions released from the implant bulk replaced Ca^{2+} in the Hap lattice.

REFERENCES: [1]F. Witte, et al. (2008), Solid State Mater. Sci., 12 (5–6): 63–72. [2]J. Hofstetter, et al. (2014), JOM 66: 566-572. [3]N.G. Grün, et al. (2018), Acta. Biomater 78: 379-386.

ACKNOWLEDGEMENTS This project has received funding from the European Union's Horizon 2020 research and innovation program under the Marie Skłodowska-Curie grant agreement No. 811226. The authors acknowledge funding from the German Federal Ministry of Education and Research for project MgBone (BMBF project number 05K16CGB). The authors thank Romy Marek and Prof. Dr. Annelie-Martina Weinberg (MUG, Austria) for providing the samples.